

Joint Programme with Abstracts Programme Conjoint avec Résumés

18th Annual Congress/
18^e Congrès Annuel

Canadian Meteorological
and Oceanographic
Society/
La Société Canadienne
de Météorologie et
d'Océanographie

11th Annual Meeting/
11^e Réunion Annuelle

Canadian
Geophysical Union/
L'Union Canadienne
de Géophysique



Canadian Meteorological
and Oceanographic
Society

La Société Canadienne
de Météorologie et
d'Océanographie



CANADIAN
GEOPHYSICAL
UNION

UNION
CANADIENNE
DE GÉOPHYSIQUE

Dalhousie University, Halifax, Nova Scotia
29 May - 1 June 1984 / 29 mai - 1^{er} juin 1984

Programme - Abstracts

18th Annual CMOS Congress/18^e Congrès annuel de la SCMO

11th Annual CGU Meeting/11^e Assemblée annuelle de l'UCG

Contents/Table des matières

Summary of Sessions 3

Résumé des sessions 4

Programme 7

Abstracts 29

Communiqué 132

Announcements 132

Editor / Rédacteur en chef -
E.J. Truhlar

Technical Editor / Rédaction technique -
I. Savdie

Eighteenth Annual Congress Canadian Meteorological and Oceanographic Society Eleventh Annual Meeting Canadian Geophysical Union

The Eighteenth Annual Congress and Annual General Meeting of the Canadian Meteorological and Oceanographic Society and the Eleventh Annual Meeting of the Canadian Geophysical Union will be held at Dalhousie University, Halifax, Nova Scotia, May 29 - June 1, 1984. The scientific programme is fully integrated with the theme *The Marine Environment: Atmosphere, Ocean and Lithosphere*. An opening plenary session and a number of theme sessions will be of common interest to meteorologists, oceanographers and geophysicists. The other sessions comprise papers on topics of special interest announced in the Call for Papers, and on other topics in the fields of meteorology, oceanography and geophysics.

The Scientific Programme and the local arrangements were organized by:

SCIENTIFIC PROGRAMME COMMITTEE

H.R. Jackson, Co-Chairman	A.J. Bowen
S.D. Smith, Co-Chairman	R. Nelis
G.J. Boer	C. Quon

LOCAL ARRANGEMENTS COMMITTEE

J.W. Loder (replacing R.W. Shaw), Co-Chairman
P.J.C. Ryall, Co-Chairman
J.M. Woodside, Secretary/Social (CGU)
R.F. MacNab, Treasurer
P.W. Galbraith, Accommodations
E.B. Bennett (replacing J. Brooke), Exhibits
D.A. Huntley, Facilities
B.D. Loncarevic, Publicity
W.G. Richards, Registration
J.R.N. Lazier, Social (CMOS)

INVITED SPEAKERS

E.A. Boyle, Massachusetts Institute of Technology
K.H. Brink, Woods Hole Oceanographic Institution
R. Peltier, University of Toronto
W.F. Ruddiman, Lamont-Doherty Geological Observatory
I. Rutherford, Atmospheric Environment Service
D.W. Simpson, Lamont-Doherty Geological Observatory
W.M. Washington, National Center for Atmospheric Research

Dix-Huitième Congrès Annuel Société Canadienne de Météorologie et d'Océanographie Onzième Assemblée Annuelle Union Canadienne de Géophysique

Les dix-huitièmes congrès annuel et assemblée générale annuelle de la Société Canadienne de météorologie et d'océanographie ainsi que l'onzième assemblée annuelle de l'Union Canadienne de Géophysique se tiendront du 29 mai au 1^{er} juin 1984 à l'université Dalhousie, à Halifax en Nouvelle-Écosse. L'intégration totale du programme scientifique est reflétée par le thème: *L'Environnement Marin: Atmosphère, Océan et Lithosphère*. La série d'ouverture plénière ainsi qu'un nombre de sessions à thème central seront d'intérêt aussi bien pour le météorologiste que pour les océanographes et géophysiciens. D'autres sessions comprenant d'études sur des sujets d'intérêt particulier tel qu'annoncé dans la demande d'articles ainsi que de sujets portant sur le domaine de la météorologie, océanographie et géophysique seront comprises.

Le programme scientifique et les arrangements locaux ont été organisés par:

LE COMITÉ DU PROGRAMME SCIENTIFIQUE

H.R. Jackson, Co-Président	A.J. Bowen
S.D. Smith, Co-Président	R. Nelis
G.J. Boer	C. Quon

LE COMITÉ DES ARRANGEMENTS LOCAUX

J.W. Loder (le remplaçant de R.W. Shaw), Co-Président
P.J.C. Ryall, Co-Président
J.M. Woodside, Secrétaire / Chargé des activités sociales (UCG)
R.F. MacNab, Trésorier
P.W. Galbraith, chargé du logement
E.B. Bennett (le remplaçant de J. Brooke), chargé des expositions
D.A. Huntley, chargé de la location des lieux
B.D. Loncarevic, chargé de la publicité
W.G. Richards, chargé des inscriptions
J.R.N. Lazier, chargé des activités sociales (SCMO)

CONFÉRENCIERS INVITÉS

E.A. Boyle, Massachusetts Institute of Technology
K.H. Brink, Woods Hole Oceanographic Institution
R. Peltier, université de Toronto
W.F. Ruddiman, Lamont-Doherty Geological Observatory
I. Rutherford, Service de l'environnement atmosphérique
D.W. Simpson, Lamont-Doherty Geological Observatory
W.M. Washington, National Center for Atmospheric Research

Summary of Sessions

		Room
Monday, May 28		
0900 - 1200		CMOS Editorial Committee A&A 21B
0900 - 1645		CMOS Education Committee A&A 21F
1300 - 1645		CMOS Scientific Committee A&A 21A
1400 - 1645		CMOS Sea Ice Special Interest Group A&A 201
1400 - 1645		CMOS Centre Chairpersons A&A 21B
		SUB:
1700 - 1800		CMOS National Council (Session I) Council Chambers
1900 - 2100		CMOS National Council (Session II) Council Chambers
1900 - 2130		Registration and Information Green Room
2000 - 2230		Ice Breaker Reception Green Room
Tuesday, May 29		
0800 - 1130		Registration and Information Lobby, Arts Centre
0900 - 1220	I	Plenary Theme Session: The Marine Environment Rebecca Cohn Auditorium
1230 - 1800		Registration and Information A&A 225
1230 - 1800		Commercial Exhibits A&A 202, 225, 228
1400 - 1730	2A	Theme Session: Geophysical Fluid Dynamics I LS 2840
1400 - 1730	2B	Sea Level, Tides and Storm Surges LS 2805
1400 - 1730	2C	Operational Meteorology LS 2815
1400 - 1710	2D	Marine Chemistry A&A 201
1400 - 1740	2E	Lithospheric Stress I A&A 234
1930 - 2200		CMOS Annual General Meeting A&A 234
1930		Arctic Science Symposium A&A 201
Wednesday, May 30		
0830 - 1400		Registration and Information A&A 225
0830 - 1400		Commercial Exhibits A&A 202, 225, 228
0900 - 1220	3A	Geophysical Fluid Dynamics II LS 2840
0900 - 1230	3B	Scientific Services to the Offshore Industry LS 2805
0900 - 1020	3C	Agricultural and Forest Meteorology LS 2815
1050 - 1230	3CC	Air Pollution Meteorology LS 2815
0900 - 1240	3D	Paleoclimate A&A 201
0900 - 1240	3E	Lithospheric Stress II A&A 234
1400 - 1700		Tour: Bedford Institute of Oceanography Open House
1900 - 2100		CMOS Agriculture and Forest Meteorology Special Interest Group Meeting A&A 234
1900 - 2100		CMOS Committee on Professionalism A&A 201
Evening		CGU Banquet Shore Club, Hubbards
Thursday, May 31		
0830 - 1800		Registration and Information A&A 225
0830 - 1800		Commercial Exhibits A&A 202, 225, 228
0900 - 1020	4A	Numerical Weather Prediction LS 2840
1050 - 1230	4AA	Climate Change and Variation LS 2840
0900 - 1230	4B	Theme Session: Coastal Oceanography I: Circulation Driven by Winds and Tides LS 2805
0900 - 1230	4C	Theme Session: Boundary-Layer Processes LS 2815

Résumé des sessions

Lundi le 28 mai

		Salle
0900 - 1200	Comité de rédaction de la SCMO	A&A 21B
0900 - 1645	Comité de l'éducation de la SCMO	A&A 21F
1300 - 1645	Comité scientifique de la SCMO	A&A 21A
1400 - 1645	Réunion du Groupe d'études de sujets particuliers en glace de mer	A&A 201
1400 - 1645	Comité des présidents des centres de la SCMO	A&A 21B SUB: Council Chambers
1700 - 1800	Conseil national de la SCMO (session I)	Council Chambers
1900 - 2100	Conseil national de la SCMO (session II)	Council Chambers
1900 - 2130	Inscriptions et renseignements	Green Room
2000 - 2230	Réception pour briser la glace	Green Room

Mardi le 29 mai

0800 - 1130	Inscriptions et renseignements	Lobby, Arts Centre
0900 - 1220	1 Session plénière, thème central: L'environnement marin	Auditorium, Rebecca Cohn
1230 - 1800	Inscriptions et renseignements	A&A 225
1230 - 1800	Expositions commerciales	A&A 202, 225, 228
1400 - 1730	2A Thème central de session: Dynamique géophysique des fluides I	LS 2840
1400 - 1730	2B Niveau de mer, marées et marées de tempêtes	LS 2805
1400 - 1730	2C Météorologie opérationnelle	LS 2815
1400 - 1710	2D Chimie marine	A&A 201
1400 - 1740	2E Tension de la lithosphère I	A&A 234
1930 - 2200	Assemblée générale annuelle de la SCMO	A&A 234
1930	Symposium de la science de l'arctique	A&A 201

Mercredi le 30 mai

0830 - 1400	Inscriptions et renseignements	A&A 225
0830 - 1400	Expositions commerciales	A&A 202, 225, 228
0900 - 1220	3A Dynamique géophysique des fluides II	LS 2840
0900 - 1230	3B Services scientifiques aux industries aux explorations côtières	LS 2805
0900 - 1020	3C Agrométéorologie et météorologie forestière	LS 2815
1050 - 1230	3CC Météorologie de la pollution de l'air	LS 2815
0900 - 1240	3D Paléoclimat	A&A 201
0900 - 1240	3E Tension de la lithosphère II	A&A 234
1400 - 1700	Visite: Institut océanographique de Bedford	
1900 - 2100	Réunion des groupe d'étude de sujets particuliers de la SCMO: Agrométéorologie et météorologie forestière	A&A 234
1900 - 2100	Comité sur le professionnalisme de la SCMO	A&A 201
Soir	Banquet de la UCG	Shore Club, Hubbards

Jeudi le 31 mai

0830 - 1800	Inscriptions et renseignements	A&A 225
0830 - 1800	Expositions commerciales	A&A 202, 225, 228
0900 - 1020	4A Prévisions météorologiques numériques	LS 2840
1050 - 1230	4AA Changements et variations du climat	LS 2840

0900 – 1230	4D	Remote Sensing and Meteorological Instrumentation	A&A 201
0900 – 1230	4E	Theme Session: Arctic Expeditions, CESAR, LOREX and FRAM: I	A&A 234
1230 – 1400		Patterson Medal Award Luncheon	SUB
1400 – 1540	5A	Large-Scale Dynamic Meteorology	LS 2840
1610 – 1730	5AA	Cloud Physics	LS 2840
1400 – 1520	5B	Coastal Oceanography II: Inlets and Fjords	LS 2805
1550 – 1730	5BB	Coastal Oceanography III: Strait Talk	LS 2805
1400 – 1650	5C	Synoptic Meteorology and Climatology	LS 2815
1340 – 1520	5D	Continental Margin Studies	A&A 201
1550 – 1730	5DD	Seismology and Deep Crustal Structure	A&A 201
1400 – 1730	5E	Arctic Expeditions, CESAR, LOREX and FRAM: II	A&A 234
1730 – 1830		CGU Annual Meeting	LS 2805
Evening		CMOS Banquet	

Friday, June 1

0830 – 1630		Registration and Information	A&A 225
0830 – 1330		Commercial Exhibits	A&A 202, 225, 228
0900 – 1230	6A	Sea Ice and Icebergs	LS 2840
0900 – 1020	6B	Coastal Oceanography IV: Stratification and Mixing	LS 2805
1050 – 1230	6BB	Deep-Sea Oceanography I	LS 2805
0900 – 1210	6C	Mesoscale Meteorology	LS 2815
0900 – 1230	6D	Marine Sediment Geochemistry and Paleo-Oceanography	A&A 201
0900 – 1230	6E	Theory, Modelling, General Geophysics and Navigation	A&A 234
1330 – 1610	7AB	Deep-Sea Oceanography II	LS 2805
1330 – 1530	7C	Panel Discussion: Nuclear Winter Scenario	LS 2815
1330 – 1550	7D	Geophysical Heat Flow	A&A 201
1330 – 1630	7E	Magnetics	LS 2805

0900 - 1230	4B	Thème central de session: Océanographie côtière I: Circulation provoquée par les vents et les marées	LS 2805
0900 - 1230	4C	Thème central de session: Processus de la couche limite	LS 2815
0900 - 1230	4D	Téledétection et instruments météorologiques	A&A 201
0900 - 1230	4E	Thème central de session: Expéditions arctiques, CESAR, LOREX et FRAM: I	A&A 234
1230 - 1400		Repas à l'occasion de la remise de la médaille Patterson	SUB
1400 - 1540	5A	Météorologie dynamique à grande échelle	LS 2840
1610 - 1730	5AA	Physique des nuages	LS 2840
1400 - 1520	5B	Océanographie côtière II: Bras de mer et fjords	LS 2805
1550 - 1730	5BB	Océanographie côtière III: Discussion sur les détroits	LS 2805
1400 - 1650	5C	Météorologie synoptique et climatologie	LS 2815
1340 - 1520	5D	Études sur la marge continentale	A&A 201
1550 - 1730	5DD	Seismologie et zone inférieure de l'écorce terrestre	A&A 201
1400 - 1730	5E	Expéditions arctiques, CESAR, LOREX et FRAM: II	A&A 234
1730 - 1830		Réunion annuelle de l'UCG	LS 2805
Soir		Banquet de la SCMO	

Vendredi le 1^{er} juin

0830 - 1630		Inscriptions et renseignements	A&A 225
0830 - 1330		Expositions commerciales	A&A 202, 225, 228
0900 - 1230	6A	Icebergs et glace de mer	LS 2840
0900 - 1020	6B	Océanographie côtière IV: Stratification et mélange	LS 2805
1050 - 1230	6BB	Océanographie des eaux profondes I	LS 2805
0900 - 1210	6C	Météorologie à l'échelle moyenne	LS 2815
0900 - 1230	6D	Géochimie des sédiments marins et paléocéanographie	A&A 201
0900 - 1230	6E	Théorie, modélisation, géophysique générale et navigation	A&A 234
1330 - 1610	7AB	Océanographie des eaux profondes II	LS 2805
1330 - 1530	7C	Réunion-débat: Scénario de l'hiver nucléaire	LS 2815
1330 - 1550	7D	Écoulement géophysique de la chaleur	A&A 201
1330 - 1630	7E	Magnétisme	LS 2805

Programme

Tuesday morning, 29 May 1984

**Session 1: Plenary Theme Session:
The Marine Environment**

Chairman: G.T. Needler

Tuesday 0900 - 1220.
Rebecca Cohn Auditorium
*Director, Atlantic Oceanographic Laboratory,
Bedford Institute of Oceanography*

Welcoming remarks (0900)

R.O. Ramseier, President, Canadian Meteorological and Oceanographic Society
Zoli Hajnal, President, Canadian Geophysical Union
Hon. George Moody, Minister of the Environment, Province of Nova Scotia
A.M. Sinclair, Vice-President (Academic), Dalhousie University

Invitation to Bedford Institute of Oceanography Open House (0925)

A.R. Longhurst, Director General

Invited Speaker: The Halifax Explosion - December 6, 1917 (0930)

D.W. Simpson, Lamont-Doherty Geological Observatory, Columbia University, Palisades, New York
Alan Ruffman, Geomarine Associates, Halifax, N.S.

Invited Speaker: The East vs West Coasts of North America: Differences in the response of coastal waters to wind driving (1005)

K.H. Brink, Woods Hole Oceanographic Institution, Woods Hole, Massachusetts

Coffee (1040 - 1110)

Invited Speaker: Critical problems in Quaternary Paleo-Oceanography (1110)

E.A. Boyle, Department of Earth, Atmospheric and Planetary Sciences, Massachusetts Institute of Technology, Cambridge, Massachusetts

Invited Speaker: The AES Vector Computer: Opportunities for the future (1145)

I.D. Rutherford, Atmospheric Environment Service, Downsview, Ont.

Lunch (1220 - 1400)

Tuesday afternoon, 29 May 1984

**Theme Session 2A:
Geophysical Fluid Dynamics I**
Chairman: C. Quon

Tuesday 1400 - 1730, LS 2840

Invited Speaker: The transition to turbulence in finite-amplitude Kelvin-Helmholtz billows (1400)

W.R. Peltier, Department of Physics, University of Toronto, Toronto, Ont.

Barotropic instability in a slowly varying easterly jet (1440)

M.S. Peng, R.T. Williams, and C.-P. Chang, U.S. Naval Postgraduate School, Monterey, California

Barotropic stability of finite-amplitude, topographically-forced flows (1500)	<i>John Fyfe and Jacques Derome, Department of Meteorology, McGill University, Montréal (Qué.)</i>
Coffee (1520 – 1550)	
A barotropic study of waves and turbulence in a stationary zonal jet (1550)	<i>Theodore G. Shepherd, Department of Earth, Atmospheric, and Planetary Sciences, Massachusetts Institute of Technology, Cambridge, Massachusetts</i>
Barotropic instability of the Gaspé Current (1610)	<i>Yves Gratton, Département d'océanographie, Université du Québec à Rimouski, Rimouski (Qué.)</i>
Non-linear meridional scale interaction in baroclinic instability (1630)	<i>Charles A. Lin, Department of Physics, University of Toronto, Toronto, Ont.</i>
Momentum transport in thermohaline staircases (1650)	<i>Barry R. Ruddick, Department of Oceanography, Dalhousie University, Halifax, N.S.</i>
Parameterizing double-diffusion (1710)	<i>Dan Kelley, Department of Oceanography, Dalhousie University, Halifax, N.S.</i>
Session 2B: Sea Level, Tides and Storm Surges	Tuesday 1400 – 1730, LS 2805
<i>Chairman: S. T. Grant</i>	
Practical Problems of computing tidal residuals (1400)	<i>J. Nasr and P.A. Bolduc, Marine Environmental Data Services Branch, Department of Fisheries and Oceans, Ottawa, Ont.</i>
Preprocessing of water-level data for tidal analysis (1420)	<i>Bryan F. White, Canadian Hydrographic Service, Burlington, Ont.</i>
Geodetic applications of tide gauge observations (1440)	<i>G. Carrera and P. Vanicek, University of New Brunswick, Fredericton, N.B.</i>
Analysis of tide data collected during the Arctic winter of 1848 (1500)	<i>P.A. Bolduc and F. Barber, Marine Environment Data Services Branch, Department of Fisheries and Oceans, Ottawa, Ont.</i>
Coffee (1520 – 1550)	
The modulation of tides (1550)	<i>Lung-fa Ku, Canadian Hydrographic Service, Ottawa, Ont.</i>
Sea level of Atlantic Canada (1610)	<i>Keith R. Thompson, Department of Oceanography, Dalhousie University, Halifax, N.S.</i>
Sea-level response to atmospheric pressure and wind at Katakolon, Greece and Nain, Labrador (1630)	<i>Chris Garrett, Fouad Majaess and Bechara Toulany, Department of Oceanography, Dalhousie University, Halifax, N.S.</i>
Impacts of the Caniapiscou cutoff on the Koksoak River Estuary (1650)	<i>Danielle Messier, Société d'Énergie de la baie James, Montréal (Qué.)</i>
An approach to benefit/cost analysis of storm surge forecasting (1710)	<i>Eldon J. Oja, Atmospheric Environment Service, Bedford, N.S.</i>

Session 2C: Operational Meteorology

Tuesday 1400 - 1730, LS 2815

Chairman: R. Nelis

The doubtful value of snow survey data for run-off forecasting (1400)*R.F. Hopkinson, Atmospheric Environment Service, Regina, Sask.*

The development of a new method for generating wind streamline charts from scattered station data (1420)*Robert R. Dickinson, H.G. Engineering Ltd, Don Mills, Ont.
Art Leganchuk, Atmospheric Environment Service, Downsview, Ont.*

Tests of three objective analysis schemes (1440)*E.J. Goldberg, Atmospheric Environment Service, Downsview, Ont.*

Computer-assisted, site-specific enhancement of digital PIXEL data (1500)*Philip R.J. Chadwick, Maritimes Weather Office, Atmospheric Environment Service, Halifax, N.S.*

Coffee (1520 - 1540)

Determining boundaries between areas of rain, snow and freezing rain in Ontario using TOVS data (1540)*T.C. Yip and B. Greaves, Atmospheric Environment Service, Downsview, Ont.
M. Leduc, Ontario Weather Centre, Toronto, Ont.*

Weather element prediction at CMC (1555)*N. Brunet and N. Yacowar, Canadian Meteorological Centre, Dorval (Qué.)*

Automated worded forecasts for days 3 to 5 (1610)*D. Soucy and N. Yacowar, Canadian Meteorological Centre, Dorval (Qué.)*

Experiments in the development of marine weather forecasting techniques off the East Coast (1630)*J.I. Walker, Acres Consulting Services Ltd, Niagara Falls, Ont.
L.J. Wilson, Atmospheric Environment Service, Downsview, Ont.*

Software design for the development of marine weather forecast techniques (1650)*J.I. Walker, R.A. Gauthier and S. Martin-McGinty, Acres Consulting Services Ltd, Niagara Falls, Ont.*

Development and testing of MOS wind forecasts in Canada (1710)*W.R. Burrows, Atmospheric Environment Service, Downsview, Ont.*

Winnipeg Radar Data Base Management System (Poster)*G. Machnee, Prairie Weather Centre, Winnipeg, Man.*

A biometeorological model of an encephalitis vector (Poster)*R.L. Raddatz, Atmospheric Environment Service, Winnipeg, Man.*

Session 2D: Marine Chemistry

Tuesday 1400 - 1710, A&A 201

Chairman: E.P. Jones

Surface coagulation in sea water (1400)*Bruce D. Johnson, Department of Oceanography, Dalhousie University, Halifax, N.S.*

Isotopic profile of a 32-m ice core from the Ward Hunt Ice Shelf (1420)*Martin O. Jeffries, Department of Geography and H. Roy Krouse, Department of Physics, The University of Calgary, Calgary, Alta*

Chemical changes in a light crude oil on a sandy beach (1440)	<i>Peter M. Strain, Atlantic Oceanographic Laboratory, Bedford Institute of Oceanography, Dartmouth, N.S.</i>
Reactive mercury in the central North Atlantic Ocean (1500)	<i>J.A. Dalziel and P.A. Yeats, Atlantic Oceanographic Laboratory, Bedford Institute of Oceanography, Dartmouth, N.S.</i>
Coffee (1520 - 1550)	
Heavy metal levels of commercially valuable seaweeds near point sources of pollution (1550)	<i>G.J. Sharp, Halifax Fisheries Research Laboratory, Department of Fisheries and Oceans, Halifax, N.S. H.S. Samant and O.C. Vaidya, Environmental Protection Service, Bedford Institute of Oceanography, Dartmouth, N.S.</i>
Simultaneous determination of nitrate, nitrite and ammonia in water by HPLC (1610)	<i>R.M. Gershey, National Research Council, Halifax, N.S. E.C.V. Butler, Division of Chemical and Physical Sciences, Deakin University, Victoria, Australia</i>
Development of an <i>in situ</i> water sampler (1630)	<i>David Green, Seakem Oceanography Ltd, Sidney, B.C.</i>
Disposal of PCB-contaminated dredged sediments from Petit-de-Grat, Nova Scotia (1650)	<i>S. MacKnight, OceanChem. Ltd, Dartmouth, N.S.</i>
Session 2E: Lithospheric Stress I <i>Chairman: J.A. Adams</i>	Tuesday 1400 - 1740, A&A 234
Introduction (1400)	<i>J.A. Adams, Earth Physics Branch, DEMR, Ottawa, Ont.</i>
Invited Speaker: Intra- vs inter-plate tectonics in Soviet Central Asia (1405)	<i>D.W. Simpson, Lamont-Doherty Geological Observatory, Columbia University, Palisades, New York</i>
Long axis orientation in elongated boreholes and its correlation with rock stress data (1435)	<i>John W. Cox, Schlumberger of Canada, Calgary, Alta</i>
Stress orientations from breakouts and their application in the Western Canadian Basin and Rocky Mountain Foothills (1455)	<i>J.S. Bell, Atlantic Geoscience Centre, Bedford Institute of Oceanography, Dartmouth, N.S., D.I. Gough, C.K. Fordjor and E.A. Babcock</i>
Stress orientations in the North American plate (1515)	<i>D.I. Gough, Institute of Earth and Planetary Physics, University of Alberta, Edmonton, Alta, J.S. Bell and C.K. Fordjor</i>
Stress orientations in North America and mantle dynamics (1535)	<i>D.I. Gough, Institute of Earth and Planetary Physics, University of Alberta, Edmonton, Alta</i>
Coffee (1545 - 1605)	

Ground stress gradients in the Canadian Shield (1605)	<i>G. Herget, CANMET, Ottawa, Ont.</i>
Rock stresses at the north shore of Lake Ontario (1625)	<i>K. Y. Lo, University of Western Ontario, London, Ont. B. Lukajic and C. F. Lee</i>
Stress relief bed slip in the Canadian Rocky Mountains (1645)	<i>J.S. Bell, Atlantic Geoscience Centre, Bedford Institute of Oceanography, Dartmouth, N.S.</i>
Finite-element models of lithospheric flexure during thrusting (1705)	<i>Paul Lloyd, Department of Geology, Dalhousie University, Halifax, N.S.</i>
Lithospheric stress and seismic ground motions (1725)	<i>H.W. Asmis, Ontario Hydro, Toronto, Ont.</i>

Arctic Science Symposium

Chairman: A. Judge

Tuesday 1930, A&A 201

An informal discussion of Arctic science will be held, sponsored by the Canadian Committee on the Lithosphere. A special invitation is extended to university personnel. Topics to be covered include what experiments are going on, what needs to be done and how to get involved.

Cold refreshments will be served.

Wednesday morning, 30 May 1984

Theme Session 3A:

Geophysical Fluid Dynamics II

Chairman: C. Quon

Wednesday 0900 - 1220, LS 2840

Topographic generation of the Sitka Eddy (0900)	<i>Gordon E. Swaters and Lawrence A. Mysak, Department of Mathematics and Department of Oceanography, University of British Columbia, Vancouver, B.C.</i>
On tidally-generated internal hydraulic jumps and solitary waves (0920)	<i>H. Sandstrom and J.A. Elliott, Atlantic Oceanographic Laboratory, Bedford Institute of Oceanography, Dartmouth, N.S.</i>
Forced finite-amplitude local baroclinic waves of constant form (0940)	<i>William Perrie, Atlantic Oceanographic Laboratory, Bedford Institute of Oceanography, Dartmouth, N.S.</i>
Coastal flows driven by a local density flux (1000)	<i>Motoyoshi Ikeda, Atlantic Oceanographic Laboratory, Bedford Institute of Oceanography, Dartmouth, N.S.</i>
Coffee (1020 - 1050)	
A solution-scheme for the convective-diffusion equation (1050)	<i>P.J. Sullivan and H. Yip, Department of Applied Mathematics, University of Western Ontario, London, Ont.</i>
Ringdown of inertial waves in a spheroidal shell of rotating fluid (1110)	<i>S. Stergiopoulos and K.D. Aldridge, Department of Earth and Atmospheric Science, York University, Downsview, Ont.</i>

Transient multiple vertical wave number convective instability in a rotating fluid (1130)	<i>C. Quon, Atlantic Oceanographic Laboratory, Bedford Institute of Oceanography, Dartmouth, N.S.</i>
30-Minute Film (1150)	<i>C. Quon</i>
Theme Session 3B: Scientific Services to the Offshore Industry <i>Chairman: A.D.J. O'Neill</i>	Wednesday 0900 - 1230, LS 2805
Calculation of extreme design parameters for offshore drilling units (0900)	<i>Langley R. Muir, Canada Oil and Gas Lands Administration, Ottawa, Ont.</i>
Marine climate information systems for offshore engineering (0920)	<i>A. Saulesleja, V. Swail, T. Agnew and L. Moritsch, Canadian Climate Centre, Downsview, Ont. T. Mathews, Canada Systems Group, Don Mills, Ont.</i>
Searching for long-distance wave group correlations at Hibernia (0940)	<i>P.H. LeBlond, D. Cumming and G. Staples, Department of Oceanography, University of British Columbia, Vancouver, B.C.</i>
Sable Island wind comparison (1000)	<i>William Richards, Atmospheric Environment Service; Erik Banke, Maritime Offshore Services; Bedford, N.S.</i>
Coffee (1020 - 1050)	
Oil spill tracking buoy research and applications (1050)	<i>Douglas White, MacLaren Plansearch Ltd, Halifax, N.S.</i>
Initial stabilization of man-made islands in Grande-Entrée Lagoon, Îles-de-la-Madeleine (1110)	<i>Georges Drapeau and Mario Gagnon, INRS-Océanologie, Université du Québec à Rimouski, Rimouski (Qué.)</i>
A simple summary wave-hindcast model (1130)	<i>David P. Krauel, Royal Roads Military College, Victoria, B.C.</i>
Real-time operation of spectral ocean wave models (SOWM) (1150)	<i>Simon G.P. Skey and Bassem M. Eid, MacLaren Plansearch Ltd, Halifax, N.S.</i>
On the development of an operational spectral wave model for the Canadian East Coast offshore (1210)	<i>M.L. Khandekar, Atmospheric Environment Service, Downsview, Ont.</i>
Session 3C: Agricultural and Forest Meteorology <i>Chairman: Roger B. Street</i>	Wednesday 0900 - 1020, LS 2815
The effects of terrain and moisture on lightning activity over southern British Columbia (0900)	<i>Larry Funk, Pacific Weather Centre, Atmospheric Environment Service, Vancouver, B.C.</i>
Airflow measurements above a forest canopy during spray trials in New Brunswick (0920)	<i>R.E. Mickle, Atmospheric Environment Service, Downsview, Ont.</i>
A climatology of historical drought on the Canadian Prairies (0940)	<i>Roger B. Street, Canadian Climate Centre, Atmospheric Environment Service, Downsview, Ont.</i>

An on-line drought index for forest fire management purposes (1000)	<i>Monique Loiselle, Ontario Region, Atmospheric Environment Service, Toronto, Ont.</i>
A comparison between climate parameters in an open site and a farmed forest site (Poster)	<i>Philip J. Sajecki and Roger B. Street, Canadian Climate Centre, Atmospheric Environment Service, Downsview, Ont.</i>
Session 3CC: Air Pollution Meteorology <i>Chairman: R.W. Shaw</i>	Wednesday 1050 - 1230, LS 2815
A preliminary assessment of wood smoke emission levels from residential sources in Canadian urban centres (1050)	<i>Ambury Stuart, INTERA Technologies Ltd, Calgary, Alta</i> <i>William Lowe, Dept. of Energy, Mines and Resources, Ottawa, Ont.</i>
Meteorology, long range transport of pollutants and health: An integrated study (1110)	<i>F. Fanaki, Atmospheric Environment Service, Downsview, Ont.</i> <i>M. Raizenne, Department of Health and Welfare, Ottawa, Ont.</i>
Further investigation of local wet sulphur deposition patterns around Halifax and Dartmouth, N.S. (1130)	<i>R.W. Shaw, Atmospheric Environment Service, Downsview, Ont.</i>
The detectability of trends in wet deposition data (1150)	<i>R.E. Munn, Institute for Environmental Studies, University of Toronto, Toronto, Ont.</i> <i>D.M. Whelpdale, Atmospheric Environment Service, Downsview, Ont.</i>
Automated minitube air sampling system (1210)	<i>Don Barnett, Terry Locke and Orville Olm, Canadian Centre for Advanced Instrumentation, Saskatchewan Research Council, Saskatoon, Sask.</i>
Session 3D: Paleoclimate <i>Chairman: R. Fillon</i>	Wednesday 0900 - 1240, A&A 201
Invited Speaker: A model of the Ice-Age cycle (0900)	<i>W.R. Peltier, Department of Physics, University of Toronto, Toronto, Ont.</i>
Invited Speaker: Orbital periods in climate records of the Ice-Age North Atlantic (0930)	<i>W.F. Ruddiman, Lamont-Doherty Geological Observatory, Columbia University, Palisades, New York</i>
Deglacial melt water plumes in the North Atlantic: Isotopic evidence (1000)	<i>Richard H. Fillon and Douglas F. Williams, Department of Geology, University of South Carolina, Columbia, South Carolina</i>
Coffee (1020 - 1040)	
Planktonic foraminiferal, palynological and oxygen isotopic stratigraphy of CESAR 83-102 and 83-103: A 1-Ma record of Arctic Ocean climate (1040)	<i>A.E. Aksu, Department of Geology, Dalhousie University, Halifax, N.S.</i> <i>P.J. Mudie, Geological Survey of Canada, Dartmouth, N.S.</i>
Patterns of sedimentation in the Arctic Ocean: Key to a high latitude Late Cenozoic chronology? (1100)	<i>David L. Clark, Department of Geology and Geophysics, University of Wisconsin, Madison, Wisconsin</i>

Foraminifera from the Lomonosov Ridge and adjacent basins, Central Arctic Ocean (1120)	<i>G. Vilks, Atlantic Geoscience Centre, Dartmouth, N.S., and Ali Aksu</i>
Paleoclimate reconstruction from deep ground temperatures, Canadian Arctic Archipelago (1140)	<i>Alan Taylor, Earth Physics Branch, Ottawa, Ont., and Alan Judge</i>
Late glacial to recent stratigraphy and sedimentary processes: Newfoundland Continental Slope and Rise (1200)	<i>C.T. Schafer, Atlantic Geoscience Centre, Dartmouth, N.S., and F.C. Tan, D.F. Williams and J.N. Smith</i>
The influence of sea level rise on the Bay of Fundy-Gulf of Maine tidal ranges from 7500 B.P. (1220)	<i>David B. Scott, Dalhousie University, Halifax, N.S., and David A. Greenberg</i>
Session 3E: Lithospheric Stress II <i>Chairmen: J.A. Adams and G. Quinlan</i>	Wednesday 0900 - 1240, A&A 234
The Miramichi earthquake sequence of 1982-1984 and its relation to regional crustal stresses in New Brunswick (0900)	<i>John Adams, Earth Physics Branch, Ottawa, Ont. and R.J. Wetmiller</i>
Stress-drops of aftershocks of the Miramichi earthquake recorded in July 1983 (0920)	<i>E. Cranswick, United States Geological Survey, Menlo Park, California</i>
Recent and historic seismicity of southeastern Maine (0940)	<i>John E. Foley, John E. Ebel and Alan L. Kafka, Boston College, Weston, Massachusetts</i>
Grenville structure and the Central Adirondack seismic zone including the October 7, 1983 main shock-aftershock sequence (1000)	<i>L. Seeber, Lamont-Doherty Geological Observatory, Columbia University, Palisades, New York; N. Barstow, E. Cranswick, J.G. Armbruster, G. Suarez, K. Coles and C. Aviles</i>
Coffee (1020-1040)	
A large intraplate stress-strain event from seismicity changes associated with the 1886 South Carolina earthquake (1040)	<i>L. Seeber, Lamont-Doherty Geological Observatory, Columbia University, Palisades, New York; and J.G. Armbruster</i>
Historical seismicity, 1983 OBS Experiment and seismic hazard along the southeastern Canadian Margin (1100)	<i>John Adams, Earth Physics Branch, DEMR, Ottawa, Ont.; I. Reid and P.W. Basham</i>
Post-glacial rebound and the focal mechanisms of Eastern Canadian earthquakes (1120)	<i>Garry Quinlan, Department of Earth Sciences, Memorial University of Newfoundland, St John's, Nfld</i>
Tilt observations from three inland stations in Western Canada (1140)	<i>P. Rouleau, Department of Physics, University of Alberta, Edmonton, Alta, J.S. Rogers, F.W. Jones, K. Hutchence and L.W. Vigrass</i>
Tidal tilt observations around the Bay of Fundy and Gulf of Maine: Implications for crustal structure and ocean tides (1155)	<i>P. Rouleau, Department of Geology, Dalhousie University, Halifax, N.S.</i>

Analysis of tidal tilt and gravity measurements at the Fredericton earth tides station (1210)

Spiros Pagiatakis, University of New Brunswick, Fredericton, N.B., and Peter Vanicek

Tidal tilt in the Charlevoix seismic zone (1225)

J.A. Peters, Department of Oceanography, Dalhousie University, Halifax, N.S.

Thursday morning, 31 May 1984

Session 4A: Numerical Weather Prediction

Thursday 0900-1020, LS 2840

Chairman: Ian Rutherford

Eliminating the interpolation associated with the semi-Lagrangian scheme (0900)

Harold Ritchie, Service de l'environnement atmosphérique, Dorval (Qué.)

The representation of the boundary layer in atmospheric circulation models: A choice? (0920)

Yves Delage, Service de l'environnement atmosphérique, Dorval (Qué.)

Impact of turbulent energy modelling in an NWP model (0940)

Robert Benoit and Jean Coté, Service de l'environnement atmosphérique, Dorval (Qué.)

A spectral analysis of error in the CMC forecast system (1000)

G.J. Boer, Canadian Climate Centre, Atmospheric Environment Service, Downsview, Ont.

Theme Session 4AA: Climate Change and Variation

Thursday 1050-1230, LS 2840

Chairman: P.E. Merilees

Some questions associated with assessing carbon dioxide buildup in the oceans (1050)

E.P. Jones, Atlantic Oceanographic Laboratory, Bedford Institute of Oceanography, Dartmouth, N.S.

Invited Speaker: Computer experiments on the climate sensitivity to a doubling of CO₂ with an atmospheric general circulation model coupled to a simple mixed-layer ocean model (1110)

Warren M. Washington, National Center for Atmospheric Research, Boulder, Colorado

The effect of ozone photochemistry on atmospheric and surface temperature changes due to increased CO₂ and volcanic aerosols in the atmosphere (1150)

R.K.R. Vupputuri, Canadian Climate Centre, Atmospheric Environment Service, Downsview, Ont.

Positive and negative El Niños - Modelling the atmospheric response (1210)

G.J. Boer, Canadian Climate Centre, Atmospheric Environment Service, Downsview, Ont.

Theme Session 4B:
Coastal Oceanography I -
Circulation Driven by Winds and Tides
Chairmen: Peter C. Smith and A.J. Bowen

Thursday 0900 - 1230, LS 2805

Dynamical balances of the mean barotropic circulation of the Gulf of Maine (0900)

D.A. Greenberg, J.W. Loder, P.C. Smith and D.G. Wright, Atlantic Oceanographic Laboratory, Bedford Institute of Oceanography, Dartmouth, N.S.

Gulf of Maine response to wind stress (0920)

Daniel G. Wright, David A. Greenberg, John W. Loder and Peter C. Smith, Atlantic Oceanographic Laboratory, Bedford Institute of Oceanography, Dartmouth, N.S.

Wind-driven circulation on the Northwest Shelf of Australia (0940)

Ian Webster, Department of Physics, Memorial University of Newfoundland, St John's, Nfld

Wind-driven circulation models of Lake Melville (1000)

T.E. Keliher and A.S. Bhogal, Department of Physics, Memorial University of Newfoundland, St John's, Nfld

Coffee (1020 - 1050)

Tidally-induced residual upwelling and downwelling on the sides of Georges Bank (1050)

Kim-Tai Tee, Atlantic Oceanographic Laboratory, Bedford Institute of Oceanography, Dartmouth, N.S.

Tidal rectification off southwest Nova Scotia (1110)

Peter C. Smith, Atlantic Oceanographic Laboratory, Bedford Institute of Oceanography, Dartmouth, N.S.

Current-meter measurements near Sable Island: Their features and dynamics in conjunction with local boundary conditions (1130)

Bassem M. Eid and Simon G.P. Skey, MacLaren Plansearch Ltd, Halifax, N.S.

Evaluation of the direct influence of the freshwater run-off on the coastal zone of the northern part of the Gulf of St Lawrence (1150)

Denis Lefavre, Champlain Centre for Marine Science and Surveys, Department of Fisheries and Oceans, Québec (Qué.)

The Beaufort Current on the Continental Slope (1210)

Paul Greisman, Dobrocky Seatech Ltd, Sidney, B.C.

Theme Session 4C:
Boundary-Layer Processes
Chairman: Peter A. Taylor

Thursday 0900 - 1230, LS 2815

Boundary-layer flow over a low hill - The Askervein Experiments (0900)

Peter Taylor, Hans Teunissen, Bob Mickle Atmospheric Environment Service, Downsview, Ont.; Jim Salmon

MS3DJH/3R – The incorporation of variable surface roughness in a simple model of boundary-layer flow over low hills, with application to a barchan sand dune (0920)	<i>John L. Walmsley and Peter A. Taylor, Atmospheric Environment Service, Downsview, Ont. Alan D. Howard, Department of Environmental Sciences, University of Virginia, Charlottesville, Virginia Tim Keith, Department of Mathematics, University of Wisconsin, Madison, Wisconsin</i>
A control-volume-based, finite-difference technique applied to the planetary boundary layer over homogeneous surfaces (0940)	<i>D. Rooney and G.D. Stubbley, Mechanical Engineering Department, University of Waterloo, Waterloo, Ont.</i>
Vertical structure in the nearshore zone (1000)	<i>John W. Haines, Department of Oceanography, Dalhousie University, Halifax, N.S.</i>
Coffee (1020 – 1050)	
Saturation-point analysis of S i REX boundary-layer/cloud-layer data (1050)	<i>Gordon A. McBean, Atmospheric Environment Service, Institute of Ocean Sciences, Sidney, B.C.</i>
The profile structure of wind over sea ice (1110)	<i>K. Shirasawa, Newfoundland Institute for Cold Ocean Science, Memorial University of Newfoundland, St John's, Nfld</i>
Studies on the variability in space and time of boundary-layer fluxes (1130)	<i>P.H. Schuepp, Macdonald College, McGill University, Ste-Anne-de-Bellevue (Qué.) P. Alvo, University of Guelph, Ont., R.L. Désjardins, Agriculture Canada, and J.I. MacPherson, National Aeronautical Establishment, Ottawa, Ont.</i>
Eddy correlation measurements of CO ₂ flux over the sea near Sable Island (1150)	<i>Stuart D. Smith and E. Peter Jones, Atlantic Oceanographic Laboratory, Bedford Institute of Oceanography, Dartmouth, N.S.</i>
CO ₂ exchange on a regional scale (1210)	<i>R.L. Désjardins, P. Alvo, J.I. MacPherson and P.H. Schuepp</i>
Session 4D: Remote Sensing and Meteorological Instrumentation	
<i>Chairman: B.J. Topliss</i>	
The use of ocean colour data to map surface dynamic features (0900)	<i>Jim Gower, Gary Borstad and Dawson Truax, Institute of Ocean Sciences, Sidney, B.C.</i>
Freshwater-driven eastern boundary current in the Pacific (0920)	<i>Mikio Miyake, Gary Borstad and Jim Gower, Institute of Ocean Sciences, Sidney, B.C.</i>
Satellite remote sensing of the spatial and temporal variations of coastal phytoplankton patches (0940)	<i>Soon T. Kim, Department of Earth and Space Sciences, Indiana University-Purdue University, Fort Wayne, Indiana</i>
Sediment mapping by remote multispectral techniques (1000)	<i>B.J. Topliss, Atlantic Oceanographic Laboratory; and C.L. Amos, Atlantic Geoscience Centre; Bedford Institute of Oceanography, Dartmouth, N.S.</i>

Coffee (1020 - 1050)

- | | |
|---|---|
| Analysis of time-lapse radar imagery of the ocean's surface (1050) | <i>M.J. Press and H.J. Duffus, Royal Roads Military College, Victoria, B.C.</i> |
| Winds over ocean surfaces determined from satellite measurements of passive microwave brightness temperatures (1110) | <i>I. Rubinstein, Ph.D. Associates Inc., Rexdale, Ont.</i> |
| Atmospheric icing of some wind speed sensors (1130) | <i>E.M. Gates, Department of Mechanical Engineering, University of Alberta, Edmonton, Alta</i>
<i>W.C. Thompson, Petro-Canada Resources, Calgary, Alta</i> |
| An application of automated Data Collection Platforms on ships (1150) | <i>John Elliott, Atmospheric Environment Service, Bedford, N.S.</i>
<i>R. Vockeroth, Atmospheric Environment Service, Downsview, Ont.</i> |
| Acoustic measurements of wind speed, precipitation and near-surface bubbles over a continental shelf (1210) | <i>David D. Lemon, Arctic Sciences Ltd;</i>
<i>David M. Farmer, Institute of Ocean Sciences, Sidney, B.C.</i> |
| Sea-ice and sea-surface wind mapping: Now operational from satellite measurements of passive microwave thermal emissions (Poster) | <i>Frank W. Thirkettle, Ph.D. Associates Inc., Rexdale, Ont.</i> |
| The University of Toronto balloon radiometer (Poster) | <i>J.R. Drummond, D. Turner and A. Ashton, Department of Physics, University of Toronto, Toronto, Ont.</i> |

**Theme Session 4E:
Arctic Expeditions, CESAR, LOREX
and FRAM: I**

Chairman: J.R. Weber

Thursday 0900 - 1230, A&A 234

- | | |
|--|---|
| Bathymetry and gravity of the Alpha Ridge (0900) | <i>J.R. Weber, Earth Physics Branch, DEMR, Ottawa, Ont. and D.W. Halliday</i> |
| CESAR cores: Lithostratigraphic correlation and paleoenvironmental interpretation of Alpha Ridge Cretaceous and Late Cenozoic sediments (0920) | <i>Peta J. Mudie, Atlantic Geoscience Centre, Dartmouth, N.S. and Ali E. Aksu</i> |
| Geothermal measurements on the Alpha Ridge during CESAR (0940) | <i>Alan Judge, Earth Physics Branch, DEMR, Ottawa, Ont., Vic Allen, and Alan Taylor</i> |
| Seismic reflection profiles across the Lomonosov Ridge and on the Alpha Ridge, Arctic Ocean Basin (1000) | <i>A. Overton, Geological Survey of Canada, Ottawa, Ont.</i> |

Coffee (1020 - 1050)

- | | |
|--|--|
| Magnetotelluric measurements over the Alpha Ridge (1050) | <i>E.R. Niblett, Earth Physics Branch, DEMR, Ottawa, Ont., C. Michaud and R.D. Kurtz</i> |
| Alpha and Lomonosov Ridge crustal structures (1110) | <i>D.A. Forsyth, Earth Physics Branch, DEMR, Ottawa, Ont., and R. Jackson</i> |

Petrography and geochemistry of the CESAR "Hard Rock": Possible implications for the origin of the Alpha Ridge (1130)

Nancy A. Van Wagoner, Acadia University, Wolfville, N.S. and Paul T. Robinson

Constraints on the tectonic origin of the Alpha Ridge (1210)

H. R. Jackson, Atlantic Geoscience Centre, Dartmouth, N.S.; D.A. Forsyth, P. Mudie and C. Amos

Lunch (1230 -)

Thursday afternoon, 31 May 1984

Session 5A: Large-Scale Dynamic Meteorology

Thursday 1400 - 1540, LS 2840

Chairman: G.J. Boer

Effects of stratospheric mean wind variations on the solar semidiurnal barometric oscillation (1400)

Kevin Hamilton, Department of Oceanography, University of British Columbia, Vancouver, B.C.

Stratospheric "prehistory" revealed by observations of the solar semidiurnal barometric oscillation (1420)

*Kevin Hamilton, Department of Oceanography, University of British Columbia, Vancouver, B.C.
Rolando R. Garcia, National Center for Atmospheric Research, Boulder, Colorado*

Mean wind evolution in the tropical lower stratosphere (1440)

Kevin Hamilton

An interesting Southern Hemisphere wave-number two (1500)

Steven Lambert, Canadian Climate Centre, Atmospheric Environment Service, Downsview, Ont.

The effect of gravity wave drag on simulations of the lower stratospheric general circulation (1520)

N.A. McFarlane, Atmospheric Environment Service, Downsview, Ont.

Session 5AA: Cloud Physics

Thursday 1610 - 1730, LS 2840

Chairman: E. P. Lozowski

Numerical simulation of the chemistry of convective clouds (1610)

André Tremblay and Henry Leighton, Department of Meteorology, McGill University, Montréal (Qué.)

A simple estimator of collision efficiency for ice accretion models (1630)

K.J. Finstad and E.P. Lozowski, Department of Geography, University of Alberta, Edmonton, Alta

Utilisation de spectres de gouttes de pluie pour évaluer les performances des radars à polarisation multiple (1650)

Gilles Boulet et Enrico Tortolasci, Université du Québec à Montréal, Montréal (Qué.)

On the retrieval of the wind field in storms from single Doppler radar measurements (1710)

I. Zawadzki and R. Hogue, Université du Québec à Montréal, Montréal (Qué.)

Session 5B: Coastal Oceanography II – Inlets and Fjords

Thursday 1400 – 1520, LS 2805

Chairman: C.J.R. Garrett

A numerical model of Burrard Inlet and Indian Arm, B.C. (1400)

Donald S. Dunbar, Department of Oceanography, University of British Columbia, Vancouver, B.C.

Tidally-generated internal waves at the sill of a deep, tidally-energetic inlet (1420)

Michael W. Stacey, Institute of Ocean Sciences, Sidney, B.C.

Observations of an internal resonance in a fjord (1440)

J.R. Keeley, Marine Environmental Data Services, Department of Fisheries and Oceans, Ottawa, Ont.

Exchange of deep water in Fortune Bay, Newfoundland (1500)

Brad de Young, Department of Oceanography, University of British Columbia, Vancouver, B.C.
Alex E. Hay, Department of Physics, Memorial University of Newfoundland, St. John's, Nfld

Session 5BB: Coastal Oceanography III – Strait Talk

Thursday 1550 – 1730, LS 2805

Chairman: J.W. Loder

A model of low-frequency flow in the Canadian Arctic Archipelago (1550)

Sherman R. Waddell, Department of Oceanography, Dalhousie University, Halifax, N.S.

Seasonal variations in surface transport through the Strait of Gibraltar (1610)

Myriam Bormans, Chris Garrett and Keith Thompson, Department of Oceanography, Dalhousie University, Halifax, N.S.

The Strait of Belle Isle: Theory vs observations (1630)

Bechara Toulany and Chris Garrett, Department of Oceanography, Dalhousie University, Halifax, N.S.
Brian Petrie, Atlantic Oceanographic Laboratory, Bedford Institute of Oceanography

Surface current measurements in southeast Dixon Entrance (1650)

J.R. Buckley and W.J. Robson, Petro-Canada Inc., Calgary, Alta

The cross-channel flow at the entrance of Lancaster Sound (1710)

B.G. Sanderson and P.H. Le Blond, Department of Oceanography, University of British Columbia, Vancouver, B.C.

Session 5C: Synoptic Meteorology and Climatology

Thursday 1400 – 1650, LS 2815

Chairman: C. Fraser MacNeil

Arctic meteorology and climatology: Present problems and potential directions (1400)

Claude Labine, Campbell Scientific Canada Corp., Edmonton, Alta

On the motion and shape of migrant Arctic Highs (1420)

E.R. Reinelt, Department of Geography, University of Alberta, Edmonton, Alta

Variability of the North Pacific Ocean-atmosphere heat exchanges (1440)	<i>Gordon A. McBean, Atmospheric Environment Service, Institute of Ocean Sciences, Sidney, B.C.</i>
Estimating incoming solar radiation at sea (1500)	<i>F.W. Dobson and S.D. Smith, Atlantic Oceanographic Laboratory, Bedford Institute of Oceanography, Dartmouth, N.S.</i>
Coffee (1520 - 1550)	
Sea surface temperature distribution in the tropics and its relationship to the incidence of tropical storms in oceans around the Americas (1550)	<i>M.R. Morgan, Dartmouth, N.S.</i>
Sea surface temperature distribution and its relationship to monsoon rainfall and line squall activity in SE Asian waters (1610)	<i>M.R. Morgan, Dartmouth, N.S.</i>
El Niño Southern Oscillation (ENSO) and the Indian monsoon rainfall - A brief update (1630)	<i>M.L. Khandekar and V.R. Neralla, Atmospheric Environment Service, Downsview, Ont.</i>
Canada's National Climate Data Archive (Poster)	<i>Mike Webb, Canadian Climate Centre, Atmospheric Environment Service, Downsview, Ont.</i>
Session 5D: Continental Margin Studies	
<i>Chairman: A.C. Grant</i>	
Time-series analysis of gravity anomalies and topography across the Nova Scotian continental margin (1340)	<i>K.E. Loudon, Department of Oceanography, Dalhousie University, Halifax, N.S.</i>
A seismic base-event map for the Continental Margin around Newfoundland (1400)	<i>A.C. Grant, Atlantic Geoscience Centre, Dartmouth, N.S.</i>
An investigation of the thermal and subsidence history of the Labrador Margin (1420)	<i>Dale Issler, Dalhousie University, Halifax, N.S.</i>
Geophysical crustal studies off the southwest Greenland margin (1440)	<i>Apostolos B. Stergiopoulos, Dalhousie University, Halifax, N.S.</i>
Iceberg scouring on Saglek Bank, Northern Labrador Shelf (1500)	<i>B.J. Todd, Dalhousie University, Halifax, N.S., C.F.M. Lewis and S.J. d'Appollonia</i>
Session 5DD: Seismology and Deep Crustal Structure	
<i>Chairman: G. Quinlan</i>	
Preliminary gravity, magnetic, and refraction seismic results from the Abitibi greenstone belt, Québec (1550)	<i>E.J. Schwarz, Geological Survey of Canada, Ottawa, Ont., L. Laverdure, L. Losier, M. Bilkington, B. Keating and B.J. Crossley</i>
Interpretation of seismic refraction data from the Abitibi region of the Canadian Shield (1610)	<i>D. Crossley, Laboratory in Applied Geophysics, McGill University, Montréal (Qué.), C. Parker, E. Poterlot, and E.J. Schwarz</i>

The crust under the Canadian portion of the Williston Basin (1630)	<i>Z. Hajnal, Department of Geological Sciences, University of Saskatchewan, Saskatoon, Sask.</i>
Update on Lithoprobe - A coordinated national geoscience project (1650)	<i>Gordon F. West, Department of Physics, University of Toronto, Ont., M.J. Berry, R.M. Clowes, W.S. Fyfe, R.D. Hyndman, E.R. Kanasewich, J.C. McGlynn and C.J. Yorath</i>
Crustal electrical conductivity in the region of the Wopmay Orogen, N.W.T. (1710)	<i>P.A. Camfield, Earth Physics Branch, DEMR, Ottawa, Ont., D.H. Krentz, Queen's University, Kingston Ont., J.C. Gupta and J.A. Ostrowski</i>
Theme Session 5E: Arctic Expeditions, CESAR, LOREX and FRAM: II <i>Chairman: J.R. Weber</i>	Thursday 1400 - 1710, A&A 234
Office of Naval Research programs: Present and future (1400)	<i>G. Leonard Johnson, Office of Naval Research, Arlington, Virginia</i>
Scientific activity in Arctic Canada (1420)	<i>George Hobson, Polar Continental Shelf Project, Ottawa, Ont.</i>
Biological sampling program: CESAR Expedition (1440)	<i>N.J. Prouse, Marine Ecology Laboratory, Bedford Institute of Oceanography, Dartmouth, N.S.</i>
The origin of the nutrient maximum in the Arctic Ocean (1500)	<i>E.P. Jones, Bedford Institute of Oceanography, Dartmouth, N.S. and L. Anderson</i>
<i>Coffee</i> (1520 - 1550)	
F-11 and F-12 distributions in Polar Oceans (1550)	<i>D.W.R. Wallace, Department of Oceanography, Dalhousie University, Halifax, N.S., and R.M. Moore</i>
Sellafield (Windscale) tracers in the Arctic Ocean (1610)	<i>J.N. Smith, Bedford Institute of Oceanography, Dartmouth, N.S., K.M. Ellis and P. Jones</i>
Radiocarbon and water isotopes at CESAR (1630)	<i>H. Gote Ostlund, University of Miami, Miami, Florida, and Valery Lee</i>
Regional oceanography around Fram III (1650)	<i>R. Perkin, Institute of Ocean Science, Sidney, B.C.</i>
CESAR radiopositioning evaluation (1710)	<i>J.R. Weber, Earth Physics Branch, DEMR, Ottawa, Ont., and D.E. Wells</i>
Annual General Meeting of the Canadian Geophysical Union	Thursday 1730, Arts & Administration 201

Friday morning, 1 June 1984

Session 6A: Sea Ice and Icebergs

Friday 0900 - 1230, LS 2840

Chairmen: R.O. Ramseier and F.J. Eley

Ice forecasting requirements of the Gulf Beaufort Sea drilling system (0900)

F.J. Eley, Gulf Canada Resources Inc., Calgary, Alta

Labrador sea-ice dynamics as determined by Nimbus-7 SMMR data, March 1982 (0920)

R.W. Gorman and M.A. Cameron, Ph.D. Associates Inc., Rexdale, Ont.

Comparison of sea-ice algorithms using Nimbus-7 SMMR data (0940)

Anne E. Owens, Ph.D. Associates Inc., Rexdale, Ont.

A digital SLAR analysis of Mould Bay second-year ice (1000)

*M.A. Cameron and R.W. Gorman, Ph.D. Associates Inc., Rexdale, Ont.
R.G. Onstott, Remote Sensing Laboratory, University of Kansas, Center for Research Inc., Lawrence, Kansas*

Coffee (1020 - 1050)

Upwelling under a fast-ice cover (1050)

Edward B. Bennett, Atlantic Oceanographic Laboratory, Bedford Institute of Oceanography, Dartmouth, N.S.

Iceberg drift and dispersion at the junction of Lancaster Sound and Baffin Bay (1110)

B.G. Sanderson and P.H. LeBlond, Department of Oceanography, University of British Columbia, Vancouver, B.C.

Eddies and tides from iceberg trajectories (1130)

Chris Garrett, Mark Hazen, Fouad Majaess and John Middleton, Department of Oceanography, Dalhousie University, Halifax, N.S.

On damping inertial oscillations in time-dependent free-ice drift without employing empirical damping (1150)

Gordon E. Swaters, Department of Mathematics and Department of Oceanography, University of British Columbia, Vancouver, B.C.

An experimental study to investigate the drift of a number of idealized iceberg models (1210)

*K. Shirasawa, Newfoundland Institute for Cold Ocean Science;
D. B. Muggeridge, Faculty of Engineering and Applied Science; Memorial University of Newfoundland, St John's, Nfld*

Session 6B: Coastal Oceanography IV: Stratification and Mixing

Friday 0900 - 1020, LS 2805

Chairman: P.C. Smith

Predictions of the summertime extent of vertically well-mixed areas in the Gulf of Maine (0900)

John W. Loder and David A. Greenberg, Atlantic Oceanographic Laboratory, Bedford Institute of Oceanography, Dartmouth, N.S.

The influence of lake morphometry upon thermal stratification and the depth of the summer thermocline (0920)	<i>E. Gorham, Department of Ecology and Behavioral Biology, University of Minnesota, Minneapolis, Minn. F.M. Boyce, National Water Research Institute, Burlington, Ont.</i>
Internal waves on Georges Bank (0940)	<i>R.F. Marsden, Department of Physics, Royal Roads Military College, Victoria, B.C.</i>
Optimal sampling and stratification in the Gulf of St Lawrence (1000)	<i>J.-P. Chanut, Département d'océanographie, Université du Québec à Rimouski, Rimouski (Qué.)</i>
Physical oceanography of the St Lawrence Estuary (Poster)	<i>Mohammed I. El-Sabh, Département d'océanographie, Université du Québec à Rimouski, Rimouski (Qué.)</i>
Session 6BB: Deep-Sea Oceanography I <i>Chairman: R.M. Hendry</i>	Friday 1050 - 1230, LS 2805
Drifter spectra and diffusivities (1050)	<i>John F. Middleton, Department of Oceanography, Dalhousie University, Halifax, N.S.</i>
Observations and a model of turbulence in an internal wave field (1110)	<i>Jim Moum, Department of Oceanography, University of British Columbia, Vancouver, B.C.</i>
Horizontal coherence of mixed-layer turbulence (1130)	<i>N.S. Oakey, Atlantic Oceanographic Laboratory, Bedford Institute of Oceanography, Dartmouth, N.S.</i>
Observations of internal oscillations and mixed-layer deepening in the Western Mediterranean (1150)	<i>J. Moen, SACLANT ASW Research Centre, La Spezia, Italy</i>
Eddies in the Pacific North Equatorial Current (1210)	<i>K.A. Thomson and W.J. Emery, Department of Oceanography, University of British Columbia, Vancouver, B.C. D. Krauel, Department of Physics, Royal Roads Military College, Victoria, B.C.</i>
Session 6C: Mesoscale Meteorology <i>Chairman: G. Isaac</i>	Friday 0900 - 1210, LS 2815
Diurnal variation of valley flows in the Alberta Foothills (0900)	<i>P. Gourlay, R.P. Angle and S.K. Sakiyama, Alberta Environment, Edmonton, Alta</i>
Vertical structure of mountain valley flows in Alberta (0920)	<i>S.K. Sakiyama, R.P. Angle, and P. Gourlay, Alberta Environment, Edmonton, Alta</i>
The usefulness of supplemental upper-air sites to increase spatial and temporal resolutions (0940)	<i>G.S. Strong and R.K.W. Wong, Alberta Research Council, Edmonton, Alta</i>
Observational studies of sea breezes in the Lower Fraser Valley, B.C.: Preliminary results (1000)	<i>Douw G. Steyn, Department of Geography, University of British Columbia, Vancouver, B.C.</i>
Coffee (1020 - 1050)	

Field-dependent estimation: A key to meso-scale prediction (1050)	<i>H. Jean Thiébaux, Department of Mathematics, Dalhousie University, Halifax, N.S. Paul R. Julian, National Center for Atmospheric Research, Boulder, Colorado</i>
Mesoscale forecasting with the RPN finite-element model (1110)	<i>Robert Benoit and Pierre Koclas, Service de l'environnement atmosphérique, Dorval (Qué.)</i>
The formation of multiple frontal structures as a forcing mechanism for rain bands in extratropical cyclones (1130)	<i>Han-Ru Cho, Department of Physics, University of Toronto, Toronto, Ont.</i>
On the dynamics of mid-latitude synoptic systems with strong cumulus convection (1150)	<i>J. Mailhot and M.K. Yau, Department of Meteorology, McGill University, Montréal (Qué.)</i>
Session 6D: Marine Sediment Geochemistry and Paleo-Oceanography	
<i>Chairman: S.E. Calvert</i>	
Trace metal geochemistry of Eastern Canadian estuarine and coastal sediments (0900)	<i>D.H. Loring and R.T.T. Rantala, Atlantic Oceanographic Laboratory, Bedford Institute of Oceanography, Dartmouth, N.S.</i>
Compositional changes of the particulate matter during estuarine mixing, St Lawrence Estuary (0920)	<i>B. d'Anglejan and M. Lucotte, Institute of Oceanography, McGill University, Montréal, (Qué.)</i>
Biologically available iron in estuaries: The effect of particle geochemistry (0940)	<i>A.G. Lewis, Department of Oceanography, University of British Columbia, Vancouver, B.C.</i>
The relationship between geochemical profiles and sedimentological variability in the Southern Nares Abyssal Plain during the Quaternary (1000)	<i>D.E. Buckley, R.E. Cranston and G. Vilks, Atlantic Geoscience Centre, Bedford Institute of Oceanography, Dartmouth, N.S.</i>
Coffee (1020 - 1050)	
The use of Pb-210 geochronology and sub-bottom profiling to study sedimentation in the Kitimat Fjord system (1050)	<i>R.W. Macdonald and D.M. Macdonald, Institute of Ocean Sciences; B.D. Bornhold, Pacific Geoscience Centre, Sidney, B.C.</i>
Kinetics and capacity of metal and radionuclide binding by bacteria in sediments (1110)	<i>Paul E. Kepkay, Marine Ecology Laboratory, Bedford Institute of Oceanography, Dartmouth, N.S.</i>
North Atlantic benthic paleocirculation (1130)	<i>E.A. Boyle, Department of Earth and Planetary Sciences, Massachusetts Institute of Technology, Cambridge, Massachusetts</i>
Early diagenesis in hemipelagic sediments at 21°N on the East Pacific Rise (1150)	<i>Tom F. Pederson, Department of Oceanography, University of British Columbia, Vancouver, B.C.</i>

DSDP Leg 85: Equatorial Pacific-wide seismic reflectors as indicators of major Middle and Late Miocene paleo-oceanographic events (1210)

Larry A. Mayer, Department of Oceanography, Dalhousie University, Halifax, N.S.
John A. Barron, Branch of Paleontology and Stratigraphy, U.S. Geological Survey, Menlo Park, California

Session 6E: Theory, Modelling, General Geophysics and Navigation

Friday 0900 - 1230, A&A 234

Chairman: M.J. Keen

Heat and mass transfer associated with exceptionally thick sedimentary piles (0900)

V.A. Saul, Department of Geological Science, McGill University, Montréal, (Qué.)

The "Prism Effect" of layered media (0920)

D.J. Hearn, Department of Geology and Geophysics, University of Calgary, Alta, and E.S. Krebes

A structural representation of the magnetotelluric impedance tensor (0940)

E.C. Yee, Department of Physics, University of Saskatchewan, Saskatoon, and K.V. Paulson

Length of day and atmospheric pressure dependence of absolute gravity (1000)

M.A. Jeudy, Earth Physics Branch, DEMR, Ottawa, Ont.

Coffee (1020 - 1050)

Inversion of cosmogenic nuclide data from meteorites (1050)

Steven J. Pearce, University of British Columbia, Vancouver, B.C. and R. Don Russell

Geomagnetic reversals - Flicker noise or chaos? (1110)

D. Crossley, McGill University, Montréal (Qué.) and O. Jensen

Coastal geophysics: Gravity measurements in Mahone Bay, N.S. with a shipborne sea-gravimeter (1130)

B.D. Loncarevic, Atlantic Geoscience Centre, Bedford Institute of Oceanography, Dartmouth, N.S. and J.M. Woodside

First Canadian experiences with the Macro-meter GPS positioning system (1150)

H.D. Valliant, Earth Physics Branch, DEMR, Ottawa, Ont., D.E. Wells and D. McArthur

The Ottawa Macrometer Experiment: An independent analysis (1210)

G. Beutler, University of Berne, Switzerland, R.B. Langley, H.D. Valliant, P. Vanicek and D.E. Wells

Lunch (1230 - 1330)

Friday afternoon, 1 June 1984

Session 7AB: Deep-Sea Oceanography II

Friday 1330 - 1610, LS 2805

Chairman: R.M. Hendry

Gas exchange during deep water renewal (1330)

R. Allyn Clarke, Atlantic Oceanographic Laboratory, Bedford Institute of Oceanography, Dartmouth, N.S.

Overflow through Denmark Strait (1350)	<i>C.K. Ross, Atlantic Oceanographic Laboratory, Bedford Institute of Oceanography, Dartmouth, N.S.</i>
Current-meter records from the North Atlantic Current (1410)	<i>J.R.N. Lazier, Atlantic Oceanographic Laboratory, Bedford Institute of Oceanography, Dartmouth, N.S.</i>
Mixing and the <i>T, S</i> characteristics of the water in Hudson Strait (1430)	<i>K.F. Drinkwater, Marine Ecology Laboratory, Bedford Institute of Oceanography, Dartmouth, N.S.</i>
Coffee (1450 - 1510)	
Oceanic thermal structure in the Canadian Western Arctic (1510)	<i>Humfrey Melling, R.A. Lake and D.R. Topham, Institute of Ocean Sciences; D.B. Fissel, Arctic Sciences Ltd; Sidney, B.C.</i>
Is potential vorticity conserved in the Gulf Stream? (1530)	<i>Dave Hebert, Department of Oceanography, Dalhousie University, Halifax, N.S.</i>
Mapping the local structure of the Gulf Stream near 60°W (1550)	<i>R.M. Hendry, Atlantic Oceanographic Laboratory, Bedford Institute of Oceanography, Dartmouth, N.S.</i>

Session 7C: The Nuclear Winter: Scientific Assessment in the Canadian Context
Chairman: P.H. LeBlond

Friday 1330 - 1530, LS 2815

Panel discussion sponsored by the CMOS Scientific Committee (1330)

Participants to be announced.

Session 7D: Geophysical Heat Flow
Chairman: K.E. Loudon

Friday 1330 - 1550, A&A 201

Heat flow studies in the Sohm Abyssal Plain, Western North Atlantic Ocean (1330)

M. Burgess, Earth Physics Branch, DEMR, Ottawa, Ont.

Heat flow through Old Ocean floor - Results from the Sohm Abyssal Plain, Northwest Atlantic (1350)

D.O. Wallace, Dalhousie University, Halifax, N.S., K.E. Loudon and R. Courtney

Heat flow variations with depth in Alberta (1410)

J.A. Majorowicz, Department of Physics, University of Alberta, Edmonton, Alta, F.W. Jones, H.L. Lam and A.M. Jessop

Heat flow in Alberta and its significance for the occurrence of hydrocarbons (1430)

J.A. Majorowicz, Department of Physics, University of Alberta, Edmonton, Alta, M. Rahman and F.W. Jones

Coffee (1450 - 1510)

Studies of the paleogeothermal field and its relation to the present heat flow pattern in southern Alberta (1510)

M. Rahman, Department of Physics, University of Alberta, Edmonton, Alta, J.A. Majorowicz and F.W. Jones

Geothermal and geophysical investigation of the distribution of permafrost and gas hydrates in the Mackenzie Delta and Beaufort Sea (1530)	<i>A.S. Judge, Earth Physics Branch, DEMR, Ottawa, Ont., A.E. Taylor, I.P. Norquay, and W.E. Bawden</i>
Session 7E: Magnetism <i>Chairman: P.A. Camfield</i>	Friday 1330 - 1630, LS 2805
Direct geophysical evidence for displacement along Nares Strait from low-level aeromagnetic data (1330)	<i>Peter Hood, Geological Survey of Canada, Ottawa, Ont., Margaret Bower, C.D. Hardwick and D.J. Teskey</i>
New aeromagnetic data from the High Arctic and Norwegian-Greenland Sea (1350)	<i>L.C. Kovacs, Naval Research Laboratory, Washington, D.C., and G.E. Vink</i>
Advances in the magnetic anomaly mapping program at the Geological Survey of Canada (1410)	<i>D.J. Teskey, Geological Survey of Canada, Ottawa, Ont., S.D. Dods and P.J. Hood</i>
Uplift studies and the nature of remanent magnetization in the contact zone of some Precambrian dykes (1430)	<i>E.J. Schwarz, Geological Survey of Canada, Ottawa, Ont., K.L. Buchan, A. Cazavant and G. Salvas</i>
Coffee (1450 - 1510)	
The paleomagnetic record of the Appalachians (1510)	<i>E. Tanczyk, Earth Physics Branch, DEMR, Ottawa, Ont., J.L. Roy and P. Lapointe</i>
New paleomagnetic data from Carboniferous redbeds and volcanics from central New Brunswick (1530)	<i>Maurice K.-Seguin, Université Laval, Québec (Qué.), A. Singh and L. Fyffe</i>
Paleomagnetic results from the Port-Daniel diabase sills and Middle Ordovician meta-sediments of the Mictaw Group, Gaspé (1550)	<i>Maurice K.-Seguin, Université Laval, Québec (Qué.), E. Gahe and G. De Broucker</i>
Paleomagnetism of the Ottawa Islands of the circum-Ungava belt (1610)	<i>K.L. Buchan, Geological Survey of Canada, Ottawa, Ont., and W.R.A. Baragar</i>

Abstracts

Session 1: The Marine Environment

Tuesday 0900 – 1220

The Halifax Explosion – December 6, 1917

D. W. Simpson and Alan Ruffman

Shortly before 9 a.m. on December 6, 1917, two ships collided in the Narrows between Halifax Harbour and Bedford Basin. The Belgian Relief ship *Imo* was outward bound for New York. The French ship, *Mont Blanc*, loaded with 2600 tons of high explosives, was arriving from New York to join a convoy in Halifax before crossing the Atlantic. At 9:04 a.m. the *Mont Blanc* exploded. Most of the north end of Halifax was completely destroyed; almost 2,000 were killed, 9,000 injured, and 25,000 left without adequate shelter. A severe snowstorm the next day compounded the disaster.

The 2.6-kiloton Halifax explosion was the largest man-made explosion prior to the detonation of the first atomic bombs in 1945 and remained the largest conventional explosion until the demolition of a 4,253-ton German munitions dump at Heligoland in 1947.

A horizontal pendulum Mainka seismograph at Dalhousie University recorded the explosion. The N-S component shows a clear, high-frequency arrival at 09:04 (local time) which offset the stylus and rendered this component inoperable. The E-W component shows three almost identical sets of low-frequency (6-s) oscillations lasting for 1 min at 09:04, 09:10 and 10:05. Because of their low-frequency nature, and the absence of any documented reports of major secondary explosions, these arrivals may be due to instrument malfunction.

The explosion was heard, and in some cases felt, over large parts of Nova Scotia and New Brunswick. Energy-magnitude relationships and data from underground nuclear explosions show a well-coupled 2.6-kiloton explosion to correspond to an earthquake magnitude of $m_h = 4.5 - 5.0$. Because of the location of the Halifax explosion on the water surface, the effective seismic magnitude may have been closer to $m_h = 2.5 - 3.0$

The East vs West Coasts of North America: Differences in the response of coastal waters to wind driving

K. H. Brink

In principle, the response of shelf waters to wind driving can be described using the same theoretical formalism off both coasts of North America. In practice, however, the differences are often so substantial as to obscure the common aspects. The dynamical formalism that unifies the two regions will first be discussed, with an emphasis on long coastal-trapped wave theory. It will then be shown that the broad East Coast Shelf tends, in contrast to most of the West Coast, to allow the barotropic limit to hold to a good approximation, and that the wind-driven response is confined primarily to the shelf itself. Along the West Coast, the predominant direction of storm motion tends to encourage free wave resonance, hence a relatively more energetic response. The dynamics of the East Coast Shelf are considerably complicated by the existence of gulfs, and banks, and by regions of very strong bottom friction induced by energetic tidal currents. This is not to say that the West Coast is geometrically simple, however. Finally, the relative significance of coastal upwelling is discussed, even though this process is not well described by linear wave theory.

The regional differences between the two coasts have led to rather striking differences between approaches to studying the shelf, but the underlying physics is indeed similar.

Critical problems in Quaternary Paleo-Oceanography

E.A. Boyle

Micropaleontological and isotopic studies of deep-sea piston cores have dramatically improved our understanding of the surface ocean's history in relation to continental ice-volume fluctuations and orbital variations. Refinements of these techniques will continue, but the next decade of research will concentrate on detailed studies of particularly good high sedimentation cores. The 3-D studies of deep-water hydrography and chemistry will also see major expansion. The orbital theory of climate change will serve as a focal point for these studies: How much of climate variance is due to orbital variations? Through what mechanisms are climate and orbital variations linked? What other factors influence long-term climate history, and to what extent is climate determinate?

Deep ocean hydrography is just now being unravelled and current data hints at a complex pattern of horizontal and vertical variability. Holocene ventilation rates may be determined using radiocarbon dating of milligram-size planktonic and benthic foraminifera. The problem of sea-level change will begin to yield to studies of pore-water salinity, $\delta^{18}\text{O}$ studies and submersible/drilling studies of stable oceanic islands. Studies of ice cores will provide information on the variations in the partial pressure and isotopic composition of atmospheric carbon dioxide. The development of reliable paleo-productivity indicators will continue to be of interest. Geochronologists will dream of improved dating methods with ± 5000 years accuracy to test the orbital tuning time-scale, and of dating techniques for cores lacking calcareous microfossils and for continental deposits. The calcium carbonate dissolution problem may begin to present a coherent global pattern. Studies of very high sedimentation rate cores will focus on variability at 500 - 5000 year periods. Progress in most of these areas will depend on the discovery and collection of long wide-diameter cores in areas of rapid sedimentation.

The AES Vector Computer: Opportunities for the future

I.D. Rutherford

In the autumn of 1983, AES acquired a Cray-1S vector computer to replace its CYBER 176, which had been in place for the previous ten years. The Cray-1S will itself be replaced by a Cray-XMP in 1986. This series of planned upgrades will make possible substantial improvements in operational weather forecasting and in the prediction of weather-driven phenomena such as sea state and sea ice. It will allow important advances in climate modelling and will allow more definitive long-range (seasonal) predictions. It will allow the running of a sophisticated model for the transport, transformation and deposition of air pollutants. Ocean circulation models, which are necessary for a complete description and understanding of the climate system, will also be a possibility. In addition, up to 10% of the CPU time will be made available to university researchers, through NSERC, for work on projects in these and other fields that require such a facility.

The transition to turbulence in finite-amplitude Kelvin-Helmholtz billows

W. R. Peltier

Kelvin-Helmholtz billows are the product of an essentially inviscid shear instability that onsets in stably stratified parallel flow when the gradient Richardson number falls below the critical value of $1/4$. These waves are ubiquitous structures in both the atmosphere and oceans where they are responsible for the generation of intense local turbulence. Although this association has been recognized for some time, the question of the mechanism through which the finite amplitude laminar wave enters the disordered state has been the cause of a great deal of controversy, with candidate mechanisms varying from centrifugal to convective in nature. This question has been addressed by testing the stability of two-dimensional non-linear and time-dependent Kelvin-Helmholtz waves against three-dimensional fluctuations of arbitrary spatial symmetry. The two-dimensional non-linear wave states were produced in a sequence of high resolution finite-difference simulations, while the stability analyses were performed using a Galerkin formalism to solve the extended Floquet problem. These analyses show that for sufficiently high initial Reynolds number the non-linear waves become unstable to an intense convective instability that is confined to thin superadiabatic sublayers that are produced by the roll-up of the isentropes in the recirculating regions of the wave. In the limit of large Reynolds number the bandwidth of this instability tends to infinity and there is an orientational degeneracy of the wavenumber vector of the fastest growing mode. Both of these properties are characteristic of a turbulence transition.

Barotropic instability in a slowly varying easterly jet

M. S. Peng, R. T. Williams and C.-P. Chang

The influence of downstream mean flow variation on the stability of an easterly barotropic jet is investigated with a multiple scale technique. Both a simple broken profile and a Bickley jet profile are studied, and the results from both types of flow show the same features.

For zonally symmetric downstream variations in the profile, the higher order corrections to the spatial growth rate and the local wavenumber are proportional to the downstream derivative of the symmetric variation, which is antisymmetric. Therefore, the spatial growth rate curve and its maximum are shifted downstream. A physical discussion of the results will be presented. The results correspond very well with a previous numerical study by Tupaz et al. (1978).

Barotropic stability of finite-amplitude, topographically-forced flows

John Fyfe and Jacques Derome

Steady-state solutions to the inviscid barotropic vorticity equation including finite amplitude topography have been obtained for cases where the potential vorticity is a linear function of the streamfunction. In this paper the stability of these equilibrium flows is investigated numerically. The relationship between the gradient of the basic state potential vorticity and perturbation growth rates and structure will be emphasized.

A barotropic study of waves and turbulence in a stationary zonal jet

Theodore G. Shepherd

A study is made of the behaviour of barotropic beta-plane turbulence in the presence of a large-scale, stationary zonal jet, in order to determine the extent to which the characteristics of standard homogeneous two-dimensional turbulence theory are affected by large-scale inhomogeneities in the flow field. The model is designed to mimic in the crudest possible manner the picture of the atmosphere suggested by Boer and Shepherd's (*J. Atmos. Sci.*, 1983) spectral observational analysis: namely, that of a quasi-homogeneous and isotropic regime of intermediate-scale or synoptic-scale transient turbulent eddies, interacting non-linearly with a large-scale, zonally-anisotropic (i.e. $L_x \gg L_y$), quasi-stationary flow.

The problem is investigated numerically by performing both spin-down and forced-dissipative equilibrium simulations with an eddy-resolving turbulence model, and the results are interpreted according to various theoretical approaches. The two principal conclusions of beta-plane turbulence theory – an arrest of the reverse energy cascade at the "Rhines radius" $k_\beta = \sqrt{\beta/2U}$, and a subsequent development of zonal anisotropy – are found to be inapplicable to this inhomogeneous flow. Instead, transient energy is transferred past k_β up to the scale of the inhomogeneity, and the interaction with the stationary jet introduces a tendency towards meridional rather than zonal anisotropy.

For this special case of a zonal stationary flow, and assuming a scale separation between the mean flow and the eddies, the transient kinetic energy is no longer a conserved quantity but the transient enstrophy remains so. It is shown that the stationary-transient interactions involve local transfers of enstrophy but nonlocal transfers of energy, and that this demands a careful interpretation of observed non-linear kinetic energy fluxes in the atmosphere.

Barotropic instability of the Gaspé Current

Yves Gratton

Based on calculations from Niiler and Mysak's (1971) model of barotropic instability for a coastal jet, Tang (1980) suggested that the wave-like motion of the Gaspé Current may be triggered by the increased instability of the current when it is away from the coast. This hypothesis is re-examined. The Gaspé Current is modelled as a continuous coastal jet flowing over a steep parabolic bottom slope. The relative importance of topographic and shear waves is investigated.

Non-linear meridional scale interaction in baroclinic instability

Charles A. Lin

Baroclinic instability of a zonal flow with latitudinal structure is examined using a non-linear quasi-geostrophic two-level β -plane model. An initially small perturbation with the structure of the linearly most unstable mode is allowed to grow to finite amplitude through non-linear interaction. Because of latitudinal asymmetries of the basic zonal flow, a spectrum of meridional modes is generated in the perturbation. The meridional modes resolved consist of the gravest mode between meridional boundaries and its subsequent nine harmonics. The perturbation zonal scale is close to the radius of deformation.

The time evolution of zonal wind and perturbation meridional structures, and their Fourier meridional mode spectra are examined. The time period selected is a 5-day period representing a typical sample of the statistically steady state.

A linear analysis shows the radius of deformation is an important meridional scale in the perturbation. This is found to be true also in the non-linear regime. Moreover, this scale also appears in the zonal flow meridional structure owing to non-linear interaction. During the baroclinic growth stage when eddy kinetic energy is increasing, baroclinic conversion of zonal available potential energy to eddy available potential energy is largely accomplished by the interaction of the largest meridional scales between the perturbation and the zonal flow. During the barotropic decay phase when eddy kinetic energy is decreasing and zonal kinetic energy increasing, interactions involving both the largest scales and the radius of deformation between the zonal flow and perturbation are important. Examination of the time series of energy conversions shows they vacillate about a mean value close to zero; thus there is no energy accumulation.

Momentum transport in thermohaline staircases

Barry R. Ruddick

Given the fine-scale temperature and salinity in an actively convecting thermohaline staircase, can the average eddy viscosity be estimated? A simple model for momentum transport in such a system shows that the average dissipation and viscosity are controlled by the regions of high dissipation and small eddy viscosity – the interfaces. The model results are combined with a mechanistic argument for momentum transport across the interfaces by convection-driven internal waves. The average eddy viscosity for the staircase is about $40 J_b / N^2$, where J_b is the buoyancy flux and N is the buoyancy frequency. By definition, the eddy diffusivity of the staircase is $-J_b / N^2$ and therefore the turbulent Prandtl number is constant and equal to -40 . The model predictions are consistent with the dissipation measurements in the Bahamas by Larson and Gregg (1983) and imply eddy viscosities of about $10^{-3} \text{ m}^2 \text{ s}^{-1}$.

Parameterizing double-diffusion

Dan Kelley

Accumulating evidence illustrates the importance of double-diffusive mixing on both medium scales (e.g. frontal intrusions and upwelling at ice edges) and large scales (e.g. the T - S properties of mid-gyre thermocline water masses and processes involved in the oceanic vertical salt balances). In this paper, it is noted that the literature is replete with particular examples of the occurrence and the importance of double-diffusion. What is needed now is a way of predicting the extent of this small-scale phenomenon based upon the characteristics of the ocean measured at the larger scales, which are well constrained by conventional data and are typical of conceivable theoretical and numerical models. Since the fluxes of S , T and ρ due to oceanic double-diffusion can be found by scaling the measurements made in laboratory experiments, one can make the required connection by parameterizing the relevant small-scale characteristics in terms of the properties of the larger scale structure. Simple reasoning is outlined, which suggests a form of such a parameterization. A comparison is made with oceanic data. These results are then integrated to give a formulation of the effective vertical diffusivity due to double-diffusion.

Practical problems of computing tidal residuals

J. Nasr and P.A. Bolduc

Different methods for computing tidal residuals are used on selected records with occurrences of storm surges. The results are compared and the differences discussed to ease the selection of a proper method for the problem at hand.

Preprocessing of water-level data for tidal analysis

Bryan F. White

The advent of reliable microprocessor-based data acquisition and telemetry systems permits the extension of water-level sampling methods to provide anti-aliasing filtering of the data beyond the stilling well response, and real-time extrema detection. A simple filtering scheme that derives the hourly averaged, zero phase shifted mean water level for logging has been implemented in an 8085-based water level gauge (TATS, Tidal Acquisition and Telemetry System). Comparisons of the filtered and conventional decimated (instantaneous) data sets and their respective analyses with the predicted filter transfer function are provided for gauges at Lauzon and Bamfield. The comparison of observed extreme levels with predicted highs and lows is shown for a number of gauging stations to be an aid in evaluating the accuracy of existing prediction practices.

Geodetic applications of tide gauge observations

G. Carrera and P. Vanicek

The three major functions of Geodesy are positioning, the study of the earth's gravity field, and the study of the earth's temporal variations. Tide gauge observations are useful in all of these three endeavours.

It is at tide gauge stations that the reference surface for height positioning is realized. An accurate knowledge of MSL and SST at as many locations as possible helps in making heights more accurate.

It is also at tide gauge stations that control of the geoid is established in the study of the earth's gravity field.

Temporal variations of MSL are at present the only account of continuous information on the vertical movements at single points.

Analysis of tide data collected during the Arctic winter of 1848

P.A. Bolduc and F. Barber

Her Majesty's ships *Enterprize* and *Investigator* were compelled to pass the winter of 1848-49 in Port Leopold, N.W.T. As a precautionary measure to prevent damage to their ships caused by the ice, 47 days of hourly sea-level data were obtained by reading a tide pole. Here we present an application of contemporary methods of tidal analysis to these historical data.

The modulation of tides

Lung-fa Ku

In addition to the modulation predicted by the equilibrium tides, the semidiurnal tides at Saint John and Yarmouth in the Bay of Fundy, and Halifax on the Atlantic Coast, undergo other modulations. They are found by passing both the observed and the predicted hourly tidal heights through a complex band-pass filter centred at M_2 frequency. The range of the modulation is about $\pm 3\%$ in amplitude and $\mp 5\%$ degrees in phase at all three locations. The most predominant feature in the changes of the modulation is the fortnightly variation and events that can be related to the meteorological disturbances. The seasonal changes in the modulation are also noticeable.

Sea level of Atlantic Canada

Keith R. Thompson

Along the Labrador (Nain) and Nova Scotian (Halifax) coastlines, monthly mean sea level is most responsive to the longshore component of local wind stress. The empirically determined gains suggest that the wind-forced currents are confined to within about 20 km of the coast. By contrast, sea levels in the Gulf of Maine respond more strongly to cross-shelf winds, presumably because of enhanced set-up in this semi-enclosed area.

The importance of density to the shelf circulation is clearly evident in the southward phase progression and amplitude attenuation of the seasonal oscillation of sea level. The difference in the seasonal amplitude between deep water (dynamic height) and the coastal gauges is consonant with a seasonally fluctuating baroclinic current at the shelf break as suggested by Csanady (1978). Finally the importance of vertical crustal movement and eustatic changes to the observed sea-level variations is discussed.

Sea-level response to atmospheric pressure and wind at Katakolon, Greece and Nain, Labrador

Chris Garrett, Fouad Majaess and Bechara Toulany

We have carried out a frequency-dependent multiple regression of sub-tidal sea level on atmospheric pressure and wind or wind stress derived from the geostrophic wind.

At Katakolon in the Eastern Mediterranean we find an isostatic response to pressure at low and high frequencies, but a less-than-isostatic and lagging response for periods centred on about 4 days. The results are consistent with a theory in which the response of the Mediterranean to travelling pressure fluctuations is affected by limitations on the flow through the Straits of Gibraltar and Sicily.

At Nain, Labrador, the response to atmospheric pressure is also slightly non-isostatic, owing to either the location of the gauge or the nature of the response of the waters on the Continental Shelf. The response to wind or wind stress is consistent at low frequencies with Thompson's (1984) results from monthly mean data, and corresponds to the set-up induced by longshore currents within only about 20 km of the coast. The frequency dependence of the results is compared with theory. No significant differences are found between the response for seasons with or without sea ice, so that meteorological influences can be removed quite simply from the sea-level data in any study of residuals due to other causes.

Impacts of the Caniapiscou cutoff on the Koksoak River Estuary

Danielle Messier

A dam, located 600 km south of Ungava Bay, was built on the Caniapiscou River, to allow the filling of the Caniapiscou Reservoir in order to increase the power production of the La Grande complex. Since 25 October 1981, the water flowing into Ungava Bay has been diverted towards James Bay through La Grande rivière. The head of the Koksoak River is located where the Caniapiscou meets the Larch River and the cutoff has reduced the Koksoak watershed by 30%, consequently, some hydrographic features of the Koksoak Estuary were modified.

During the July to October summer period natural daily flows varied from 2344 to 5133 m³ s⁻¹. In 1982, they were reduced from 3134 to 1067 m³ s⁻¹ and in 1983, from 2830 to 1152 m³ s⁻¹. Summer water flows were reduced by an average of 32%. Tidal levels were measured at three stations: km 1.6, km 29.0 and km 52.9. Flow reductions seem to have increased the tidal amplitude slightly, mostly by lowering lower water levels. The tidal phase was not significantly modified by the reduction of water flows.

At low tide, the limit of salt intrusion is located between km 30 and km 36, but salinity is higher during spring tides than neap tides. At high tide, salt-water intrusion will go farther since water flows are low, particularly during tides. In general, salinity has increased mostly in the middle part in the estuary.

At Kuujuaq (km 52.9), the lowering of the lower water levels is estimated to be 0.25 m for each 1000 m³ s⁻¹ of water flow reduction. Upstream, near the head, the lowering of the water level is in the order of 0.75 m since the Caniapiscou River cutoff.

The main consequences of the Caniapiscou River cutoff experienced by the users of the Koksoak River were increased difficulties to travel on the Koksoak River and possible effects on water resources harvesting.

An approach to benefit/cost analysis of storm surge forecasting

Eldon J. Oja

On 25 October 1983 a violent Atlantic storm struck Cape Breton, Nova Scotia, bringing with it enormous seas and a storm surge that raised the tides more than 2.5 ft above predicted levels. In the aftermath, \$2.7 million in damage dramatically illustrated the significance of the surge. The infamous "Ground Hog Day Storm" of 2 February 1976 brought devastation to Nova Scotia and New Brunswick as \$10 million in damage was estimated for each province. In the 1976 storm, the fisheries component bill of \$5.5 million in Nova Scotia alone puts a price tag on the 5-ft storm surge. Very few statistics or documented records are available on surges in Canada. How can one differentiate between surge related damage and all the other factors of a violent storm? How can one put a dollar value on the benefits of a specific and perhaps infrequent service? The Cape Breton storm provided the opportunity to develop a scenario approach to measure the costs and the benefits of storm surge forecasting. Scientists are developing surge prediction models and forecast techniques while others are recording the economic impact the storm surge had. The Benefit-Cost Analysis brings their purposes together since one measures the benefits to society in dollars and cents.

The doubtful value of snow survey data for run-off forecasting*R. F. Hopkinson*

Each year, water agencies across Canada devote substantial resources to snow surveys. An examination of the water equivalents for adjacent snow course and Nipher-shielded snow gauge sites revealed a high degree of variability for the snow course data when compared with accumulated precipitation. Although the catch efficiency of a particular snow course can be accounted for in statistical run-off models given a sufficiently long record, it could pose a major obstacle for the use of snow course data in physically based models. The moving of a snow course to a more representative location can radically alter the snow course - snow gauge relationship and thus destroy the usefulness of snow course data for use in statistical models. A number of examples from Saskatchewan and Manitoba are presented to illustrate these points.

The development of a new method for generating wind streamline charts from scattered station data*Robert R. Dickinson and Art Leganchuk*

A unique automated method for generating wind streamline charts from scattered station data for use in objective meteorological analysis has been developed to the level of a full-scale prototype. Work is continuing towards an operational system. The method is based on the intermediate generation of an isogon field (lines of constant wind bearing), rather than the generation of a regular rectangular grid of wind bearings.

Some features and advantages of the new system over existing systems are discussed. The theoretical basis of the methods used to construct streamlines from an isogon field are outlined. Some complexities associated with the generation of isogon fields from sparse data are reviewed, especially with respect to singularities.

Some typical charts are presented, illustrating some of the advantages of the system in the context of an operational forecasting aid. In particular, the accurate representation of vortices, cols and asymptotes is discussed with respect to the potential for monitoring their translation, intensification and/or decay with respect to time.

Finally, a summary of potential applications of the new method to other related sciences is given.

Tests of three objective analysis schemes*E.J. Goldberg*

Three objective analysis schemes have been implemented and tested on an HP minicomputer at AES Headquarters. These include the Cressman Analysis (currently in use at Weather Centres), a Barnes analysis, and an orthogonal polynomial analysis.

The techniques were tested extensively. Tables are provided comparing computer usage, and a series of figures illustrate the behaviour of the analyses.

As a result of this work, it was found that the Cressman scheme is the most efficient and flexible general purpose analysis technique of the three tested.

Computer-assisted, site-specific enhancement of digital PIXEL data

Philip R.J. Chadwick

Satellite sensing of the earth-atmosphere system reveals abundant, cost-effective and accurate real-time information. A revised enhancement scheme has been devised to maximize the amount of usable satellite data.

A computer-assisted enhancement scheme for the raw satellite data may be used to assign the optimum enhancement level to each picture element (PIXEL). The scheme uses an external normalization field defined over the area of interest to determine the enhancement to be applied to each of the corresponding PIXELS.

Operational implementation of this technique includes applications to both visible and infrared imagery.

With visible imagery, the contrast and amount of usable data can be optimized by using the surface solar flux as a normalization field. If the surface solar flux is defined as a function of radial displacement from the sun subpoint, one enhancement field can follow the sun across the area of interest, both diurnally and seasonally. The benefits of this scheme include artificially uniform illumination levels over the satellite sector, the optimization of contrast and detail, as well as the maximization of relative cloud thickness information.

With infrared imagery, many applications are also possible when surface temperature fields or other thermal fields are used as the normalization field.

Determining boundaries between areas of rain, snow and freezing rain in Ontario using TOVS data

T.C. Yip, B. Greaves and M. Leduc

The TIROS-N Operational Vertical Sounder (TOVS) is flown on the current TIROS-N and NOAA series of polar-orbiting satellites. It measures radiances in a number of channels in the visible, thermal infrared and microwave regions. From these data, the current AES data processing system can retrieve temperature profiles from the surface to 115 mb and moisture profiles from the surface to 300 mb. Thence, the thicknesses of different layers can be calculated. The horizontal resolution is 30 km at the subsatellite point for the infrared sounder and 110 km for the microwave sounder.

From 21 November to 16 December 1983, an experiment was conducted jointly by the Aerospace Meteorology Division, Meteorological Services Research Branch, at Downsview (ARMA), and the Ontario Weather Centre (OWC). TOVS data were analysed by the ARMA staff and transmitted to OWC on a daily Monday-Friday basis. A total of 5 charts were sent each day: 850- and 500-mb temperatures; and 1000 - 850, 850 - 700 and 1000 - 500 mb thicknesses. The OWC forecasters compared the TOVS data with radiosonde data, with respect to their overall patterns, and also in positioning and forecasting the location of rain /freezing rain/snow lines and rain/snow lines. The Koolwine (1975, M.Sc. Thesis, Univ. of Toronto) technique based on partial thicknesses was used.

From this experiment, we concluded that using the AES-TOVS data, we can delineate the rain /freezing rain/ snow lines as well as, and in certain cases better than, we can by using the radiosonde data alone.

Weather element prediction at CMC

N. Brunet and N. Yacowar

A new automated temperature forecast system has been operational since November 1982. Forecasts of daily minimum and maximum temperatures are produced to day 5. Verifications of these forecasts show positive skill for the minimum temperature to day 5. An error feedback correction has been developed that will reduce the mean absolute errors and will improve the skill for all forecast periods.

CMC has developed an MOS system to forecast the probability of precipitation for six consecutive 12-h periods. Experimental forecasts have been made for over one year. Verifications for the one-year period indicate that the MOS forecasts are superior to those produced by the operational perfect prog (POPA) system.

Automated worded forecasts for days 3 to 5

D. Soucy and N. Yacowar

It is the intention of the Atmospheric Environment Service to produce automated worded forecasts for days three to five. Weather elements for these days are now being produced, and prototype bilingual worded forecasts are being prepared for 94 Canadian stations.

The temperature forecasts are produced by a perfect prog regression system. Sky cover and probability of precipitation forecasts are prepared by analogue techniques. The terminology generated is based on the forecast weather element matrix.

Experiments in the development of marine weather forecasting techniques off the East Coast

J.I. Walker and L.J. Wilson

The development of wind forecast equations for marine areas using statistical techniques generally requires a compromise between sample size and the size of the area for which the equation is to be developed. Statistical techniques are, at least over land stations, quite site-specific. Small marine areas may not contain enough observations in the time period that overlaps the analysis or prognosis data bases to allow valid application of statistical techniques. Enlarging the acceptable observation data area may violate the site-specific constraints.

Another type of approach to the problem is to use the data from the nearest land station or from another marine area where data are more abundant. The validity of this must be established empirically.

As part of a larger study, a series of experiments were conducted to address this problem. Wind forecast equations (speed, U and V components) were developed using the Perfect Prog approach for 30 AES forecast regions off the East Coast, and for the regular observing station on Sable Island. The data from these 30 regions were then aggregated to form 12 regions, and another set of equations was developed. The observation data were extracted from the archives of ship observations from 1974 to 1979. Analysis data were extracted from the 381-km grid FNOC data base.

Data from 1979 were reserved as an independent test set, the remainder being used for equation development. Verifications were performed by comparing forecasts generated for 1979 from CMC prognosis data with the independent data set. A number of cases are presented and the differences between the performances of equations based on the large areas, small areas and Sable Island are discussed.

The results of these experiments provide objective measures of the benefits of increasing sample size versus the site-specific approach, and assess the validity of applying techniques developed in one area to another, including the particular case where a land station is used.

Software design for the development of marine weather forecast techniques

J.I. Walker, R.A. Gauthier and S. Martin-McGinty

A software system has been designed for developing and testing statistical weather forecast techniques. It has been implemented on the AES AS/6 computer system in Downsview, Ontario, and used on behalf of the Meteorological Services Research Branch in the development of techniques for forecasting wind, ceiling and visibility off the East Coast of Canada.

Some key features of the system are:

- The capability to use the MOS or Perfect Prog approach.
- Multiple screening regression and discriminant analysis are currently available; other analyses may be added relatively easily.
- Manipulations to produce raw, interpolated and derived predictors are specified in plain language expressions in a data file. The predictor names as given in this file are used in all subsequent analyses to label the output information.
- Up to twenty predictands may be included in a given run, and these may be manipulated where it is advantageous to use derived predictands, for example, using threshold functions.

The applications to date have been quite successful, and have shown the usefulness of the programs for both basic research and applied operations. The factors considered in the design of the system are discussed and a critical performance evaluation is made, which will provide guidance to other workers with a need to process and analyse large data bases.

Development and testing of MOS wind forecasts in Canada

W.R. Burrows

A MOS wind forecasting system designed for operational use has been developed for 159 stations across Canada. Separate equations for S , U and V forecasts were derived for 12-, 24-, 36-, 48- and 60-h projection times for each of 00 and 12Z issue times in 3 seasonal stratifications. The reduction of variance for these wind forecast equations approaches that of similar operational equations developed for the United States by the National Weather Service. An analysis of the predictors selected for the forecast equations is given. Although 105 predictors were originally offered for selection, one could comfortably use 40 or less. Forecasts of wind speed and direction were verified for 22 stations for a 7-month period independent of the development period. Forecast errors are found to be reasonably low for operational purposes at most stations, even at 60 h. "Inflation" of the wind speed is found to be a useful method for sharpening the forecasts, as has been found in the United States. Experiments using forecast equations developed for one projection time on model data valid for other projection times to generate forecasts at those times (termed Improper MOS, or IMOS, here) show that one can use this approach without an undue increase in forecast error. This would be an alternative to the need to develop a separate set of back-up equations at many stations to cover cases when a current observation is missing in order to generate 12-h forecasts, and 24-h forecasts at a few stations. The technique also points to a useful method for generating forecasts for longer projection times from equations developed for shorter projection times (48- and 60-h direction errors actually decreased somewhat when equations developed for 12-, 24- and 36-h projection times were used to generate forecasts) - this may significantly reduce development computer time requirements, possibly for even longer projection times than 60 h. Using the IMOS approach, 6- and 18-h wind forecasts will be generated operationally from 12-h MOS equations, and 30-h forecasts from 24-h equations.

Winnipeg Radar Data Base Management System

G. Machnee

A system has been designed to automatically retrieve radar data from several Enterprise radars and store the information in a 72-image data base. The system has the capability to display the information on colour monitors or to print the information on a 6-colour hard copier. The presentation will describe the system organization and show sample outputs and pictures of the equipment.

A biometeorological model of an encephalitis vector

R.L. Raddatz

Two prerequisites for a Western Equine Encephalitis (WEE) epidemic are the presence of the disease-causing agent, the WEE virus, and the vectors of the disease plentiful enough to effectively transmit the pathogen from infected animals to susceptible humans. In Southern Manitoba, the primary vector of WEE is considered to be the (female) *Culex tarsalis* mosquito.

Multiple linear regression techniques and seven years of data were used to build a biometeorological model of Winnipeg's mean daily *Cx. tarsalis* capture-counts. Hydrologic accounting of precipitation, evapotranspiration and run-off provided estimates of the wetness of the presumptive conditions, while the warmth of the season was gauged in terms of a threshold antecedent temperature regime.

Winnipeg's capture-counts are not always indicative of the natural population. The impact of mosquito abatement measures was included in the model via a control effectiveness parameter. An activity-level adjustment, based on mean daily temperatures, was also made to the counts.

This model can, by monitoring the weather, provide forecasts of *Cx. tarsalis* populations for Winnipeg with a lead time of three weeks, thereby contributing to an early warning of an impending WEE outbreak.

Session 2D: Marine Chemistry

Tuesday 1400 - 1710

Surface coagulation in sea water

Bruce D. Johnson

The process of the aggregation of dissolved, colloidal and larger particulate substances at air-water interfaces is described. This surface coagulation is treated from a theoretical standpoint and is seen to explain the observations of those who have produced particles by bubbling sea water, e.g. Batoosingh et al. (1969).

The rate of surface coagulation is examined in relation to coagulation by Brownian motion and shear. The potential significance of surface coagulation is explained in terms of the specificity for surfactants, the near-surface locus of activity, and the facility with which the process occurs relative to other modes of coagulation.

Isotopic profile of a 32-m ice core from the Ward Hunt Ice Shelf

Martin O. Jeffries and H. Roy Krouse

A 32-m ice core from the Ward Hunt Ice Shelf exhibits an interesting isotopic and salinity profile. The mean $\delta^{18}\text{O}$ value of the upper 10 m is -30.7‰ , consistent with local precipitation values. The depth interval 10 to 19 m has $\delta^{18}\text{O}$ values near SMOW, diagnostic of ice formed from sea water. At 19 m the $\delta^{18}\text{O}$ values abruptly become negative again (-26‰) but at 20 m return equally abruptly to SMOW, and remain there for the lowermost 12 m.

In principle, there are three mechanisms that could establish such an isotopic profile. The portion above 19-m depth could represent a later oceanic flooding event and subsequent freezing upon the original sea-ice basement. Thereafter, there was a surface addition of local precipitation. This seems quite unlikely since the original sea ice would have to remain submerged and undergo minimal melting while the upper sea ice accumulated. In the second mechanism, one ice-sheet might simply have rafted upon another. The third mechanism recognizes the ice from 10 to 19 m to constitute the original basement ice. The 19 to 20 m stratum represents the freezing of a shallow freshwater flow beneath the ice shelf, which was probably established during a warm period. Sea ice has subsequently formed below this fresh ice stratum. The mean salinity for the 10 to 19 m interval is about 3‰. This value is also found in the sea ice just below 20 m, but the salinity steadily increased with depth to 16‰. Such a salinity is remarkably high for ice and possibly resulted from long-term infiltration of underlying sea water. A long-term contact of the under-surface of the lower sea ice is consistent with the time required for the uppermost 10-m accumulation of precipitation. In contrast, the original sea-ice basement would have been in contact with ocean water and the shallow freshwater flow for a relatively short time. If this relative chronology is correct then the second mechanism is favoured.

Tritium measurements currently in progress might provide a better understanding of the chronology and mechanisms of ice-forming events at this location on Ward Hunt Ice Shelf.

Chemical changes in a light crude oil on a sandy beach

Peter M. Strain

Chemical changes in a crude condensate from the Scotian Shelf have been followed in small quantities of oiled sand exposed to natural environmental conditions in the intertidal zone of a low-energy sandy beach. The oil composition has been monitored for changes that are due both to the fractionation of components by variations in their physical-chemical properties and to (bio)chemical reactions.

Early results show that even very light oils at the relatively low oil/sand concentrations used in these experiments can be surprisingly persistent. In addition, the composition of the oil changes both in different ways and at different rates than oil on supratidal sand exposed to ambient air temperatures.

Recent laboratory studies have suggested that some of the light aromatic constituents in crudes may be partially oxidized photochemically and that these oxidation products may explain the observed higher toxicity sometimes noted for weathered versus unweathered oils. No accumulation of such compounds was noticed despite the detailed GCMS analyses performed in this study. However, tests show that some simply oxidized naphthalene derivatives have lifetimes of the order of hours or days in intertidal sands, compared with months or years for the parent oils. Presumably the greater solubility of the oxidized materials is responsible for their rapid removal.

Reactive mercury in the central North Atlantic Ocean

J.A. Dalziel and P.A. Yeats

The levels of reactive mercury in pelagic waters near the Mid-Atlantic Ridge south of the Azores and in the Sargasso Sea north of Bermuda were measured by cold vapour atomic absorption spectrophotometry. The reactive mercury content at both locations was shown to be uniform with depth and equal to 2.5 ± 0.5 picomoles per litre. The profiles show no indication of a simple mercury nutrient relationship. The deep water from the FAMOUS area was also sampled and shows no elevated mercury levels.

Heavy metal levels of commercially valuable seaweeds near point sources of pollution

G.J. Sharp, H.S. Samant and O.C. Vaidya

Tissues of *Laminaria longicuris*, *Laminaria digitata*, *Ascophyllum nodosum*, *Fucus edentatus* and *Chondrus crispus* were analysed for all major heavy metals. Concentration factors reached 14,300 for Cd, 84,000 for Pb, and 394,000 for Zn near a point source of heavy metal pollution. In contrast, tissue concentration factors of these metals in commercially active harvest areas were a factor of 10 below the "worse case" site. Longevity within or between species did not have a significant effect on total metal accumulations. As a whole, the marine plant resources of the Scotia-Fundy region are unaffected by the few point sources of heavy metal pollution.

Simultaneous determination of nitrate, nitrite and ammonia in water by HPLC

R.M. Gershey and E.C.V. Butler

A chromatographic system comprising an anion exchange column with both U.V. and gas-sensing ammonia electrode detectors has been developed. Nitrate, nitrite and ammonia can be determined simultaneously using small sample volumes (500 μ L). Total analysis time is less than ten minutes. The method has been used to study the effects of ultraviolet radiation on these nitrogen species in artificial sea water at concentrations in the range of 10^{-4} - 10^{-5} mol. The use of a preconcentrator column allows the determination of natural levels (10^{-3} - 10^{-6} mol) of nitrate and nitrite in fresh waters. A similar concentration scheme for sea water is under development.

Development of an *in situ* water sampler

David Green

Over the last ten years, water sampling techniques have failed to keep pace with analytical methods and requirements. Conventional water sampling relies on messenger-activated Niskin or Nansen-type bottles. This approach is not suitable for obtaining the large volume water samples necessary for many organic and inorganic pollutant analyses, nor can time-integrated samples be taken. The sampling bottles themselves pose contamination problems; and the water samples, once obtained, must frequently be extracted in the field providing further opportunities for contamination.

Biological sentinel organisms provide a method of water quality monitoring that circumvents a number of these problems but introduces others, particularly biological variability.

This paper describes a sampling instrument that uses extraction columns to extract organics and metals from water *in situ*. This sampler provides a reproducible and reliable method of obtaining large, time-integrated samples. It is simple and straightforward, functional in both moored and hydrowire configurations, and equally useful for organic and inorganic sampling.

The extraction efficiencies of the various columns that have been developed for the sampler are summarized, and results of field experiments with the sampler are described.

Disposal of PCB-contaminated dredged sediments from Petit-de-Grat, Nova Scotia

S. MacKnight

In Canada, ocean disposal of dredged materials is regulated by the Ocean Dumping Control Act, the purpose of which is to provide a mechanism to review and control the disposal of contaminated materials into the marine environment. Included within the list of regulated substances are organochlorine compounds, (e.g. polychlorinated biphenyls; PCBs). In the Atlantic region, a regulatory screening limit of 100 ng g⁻¹ is used. This can be compared to typical harbour concentrations of 10 - 20 ng g⁻¹.

In 1977, Public Works Canada proposed the dredging of a cove area adjacent to a fish meal processing operation in Petit-de-Grat, Nova Scotia. Sediment concentrations of PCBs in excess of 100 ng g^{-1} were reported. Subsequent surveys between 1977 and 1981 further defined and delineated the problem area, with concentrations as high as $20,000 \text{ ng g}^{-1}$ being reported. It was found that the dredged material actually consisted of two layers: the upper layer (8% of the total volume), being composed of decomposed fish wastes and oils, was the source of contaminants; the underlying layer (92% of the total volume) was a "clean" glacial till material.

The solution to the problem was to suction-dredge the fish wastes into a containment facility; the underlying till could be ocean dumped. To promote settling and dewatering of the fish "muck", a high-cationic polymer was added. This addition was found to reduce settling times by approximately a factor of three and to give an effluent water with acceptable PCB and suspended solids concentrations.

Session 2E: Lithospheric Stress I

Tuesday 1400 - 1740

Intra- vs inter-plate tectonics in Soviet Central Asia

D. W. Simpson

The southern part of Central Asia (including the Soviet Republics of Tadjikistan, Uzbekistan and Kirgizia) lies in a broad zone of deformation related to the India-Eurasian collision. Between the Tien Shan Mountains, which form the southern edge of Asia, and the Himalayan frontal thrusts lie a number of distinct terrains that are either blocks that have been sutured to Asia during the closing of the Paleotethys (e.g. Pamir) or basins that have not yet completely closed (e.g. Tadjik Depression). Seismicity in the region includes true intraplate seismicity on reactivated structures within the Tien Shan (e.g. Talas-Fergana and Gissar-Kokshal fault zones); shallow activity within the foreland-fold-and-thrust belt of the Tadjik Depression; and the intermediate depth seismicity of the Pamir-Hindu Kush zone.

The post-Jurassic sediments of the Tadjik Depression appear to lie on thinned continental crust, the eastern part of which is being subducted beneath the Pamir. At the northern edge of the Depression, sediments are being thrust northward, over the hinge zone of the ancient continental margin, to lie on top of the Paleozoic rocks of the southern Tien Shan. The load of the thrust sheets, added to the regional NW compression, reactivates high-angle faults inherited from the extensional stage of passive margin development, producing the large magnitude earthquake activity of the Gissar-Kokshal zone.

Induced seismicity is occurring at two large hydro-electric projects in Central Asia. At the 315-m high Nurek dam in the Tadjik Depression, a ten-fold increase in seismicity was observed during rapid filling in 1972 and 1976, including two earthquakes of magnitude 4.5. A clear correlation is seen between the level of seismicity and time of rapid changes in the rate of filling. Toktogul Reservoir in Kirgizia is still filling and the induced seismicity has been confined to low magnitude activity directly beneath the dam. No increase in seismicity has yet been observed on the Talas-Fergana fault, which crosses the reservoir 15 km upstream from the dam.

Long axis orientation in elongated boreholes and its correlation with rock stress data

John W. Cox

Several detailed studies of borehole elongation, as measured with 4-arm dual caliper systems, have been made for specific geographical areas of North America. The authors of these studies have shown that a correlation exists between the orientation of elongation and the orientation of known principal horizontal stress.

Borehole elongation alone may not be a reliable indicator of unequal horizontal stress, however, and some guidelines are presented to assist the user of such data in distinguishing potential stress-related elongations from those of other causes.

A compilation of data from other authors in addition to newly acquired data is compared with existing rock stress measurements in several areas of the United States. The resultant correlation shows excellent agreement in orientation, and supports major continental-scale trends as well as regional differences.

Because a large amount of rock stress data exists in North America and other parts of the world, this paper attempts to expand the correlation of horizontal stress and borehole elongation to tectonic provinces not previously documented in this respect, and to other continents where, with limited data, trends appear to exist.

Initial results of the study strongly suggest that borehole elongation information may give significant support to the understanding of plate tectonics, seismicity, and rock failure characteristics. The oil and gas industry particularly has shown increasing interest in rock mechanics and its application to reservoir performance during hydraulic fracturing and production operations. Information presented in this paper may provide assistance in these fields.

Stress orientations from breakouts and their application in the Western Canadian Basin and Rocky Mountain Foothills

J.S. Bell, D.I. Gough, C.K. Fordjor and E.A. Babcock

Borehole breakouts measured from dipmeter logs run in more than 100 wells provide a detailed picture of present-day principal stress orientations in the Western Canadian Basin and adjacent Rocky Mountain Foothills. These data corroborate stress orientations implied by subsurface induced fractures and surficial stress release phenomena. They are also compatible with relative stress magnitudes measured in mines and wells.

The pattern that emerges is one in which the stresses are unequal in magnitude, and the regional stress regime responds to basin architecture. In northern and southern areas, NW-SE trending breakout axes show that the larger horizontal principal stress, S_H , is oriented NE-SW. In the central area, between 55 and 57°N, S_H trends NNE-SSW. This deflection coincides areally with the Peace River Arch, which is believed to cause the observed change in orientation of the principal stress axes.

Breakouts have been identified between depths of 200 to 5000 metres in wells in Western Canada. They provide principal stress axes, which can be used to predict hydraulic fracture orientations, and therefore aid hydrocarbon exploration and production programs. Other applications include designing multiple fracture programs for inclined wells, interpreting stress release fractures in cores and planning well configurations for heavy-oil production.

Stress orientations in the North American plate

D.I. Gough, J.S. Bell and C.K. Fordjor

Fourteen stress provinces have been identified by Zoback and Zoback in the conterminous United States, by means of overcoring stress measurements, hydraulic fracture data, earthquake mechanisms and geological data on recent displacements across active faults. Each stress province is characterized by nearly constant directions and the relative magnitudes of the horizontal principal stresses. The largest province in the United States, the Mid-Continent Stress Province, extends from the east front of the Rocky Mountains of Colorado to New England and the Atlantic Provinces of Canada. In this province the greater horizontal principal stress, S_H , is oriented northeast-southwest. We have used breakouts in oil wells to show that this S_H orientation extends through the Western Canadian sedimentary basin to the Arctic coast at the Mackenzie Delta. Cox has recently found evidence of similar stress orientations from borehole breakouts, in the Atlantic Archipelago, and it appears very probable that the northeast-southwest orientation of S_H extends through the whole of the North American craton. In the Yukon and far western Northwest Territories breakouts indicate a NNW-SSE direction for S_H in an Alaskan stress province, which we associate with traction of the subducted Pacific plate lithosphere against the North American plate. Stress orientations found by Nakamura, Jacob and Davies, from earthquake mechanisms and volcanic satellite cones in Alaska, show NNW-SSE directions for S_H in harmony with the breakout data. Part of the boundary between the North American craton and the Alaskan stress provinces is located by our breakout data, and lies well within the North American plate and craton.

Stress orientations in North America and mantle dynamics

D.I. Gough

There is now a considerable data set on stress orientations in North America. The craton east of the Rocky Mountains, including the Shield, appears to be dominated by a NE-SW greater horizontal principal stress S_H . This is believed to indicate a basal traction to the northeast on the cratonic part of the plate. Such a traction could be produced either by the plate sliding southwestward over a passive asthenosphere, or by convective flow in the mantle driving the plate northeastward. Stress orientations in the Basin and Range Province, and the abundant evidence of an east-west extension there, support the "active drive" hypothesis and are difficult to explain on the "passive sliding" view. Some general implications for plate tectonics will be developed.

Ground stress gradients in the Canadian Shield

G. Herget

On the basis of ground stress determinations by overcoring in underground mines located in the Canadian Shield, various trends of the increase of horizontal and vertical stresses with depth have been identified. The results have been obtained over a depth range from the surface to 2200 m below the surface. The data show considerable scatter but the trends shown below are significant:

Increase of vertical stress component (S_v) with depth (m):

$$S_v = 0.0260 \text{ to } 0.0324 \text{ MPa m}^{-1}$$

$$S_v \text{ (extreme)} = 0.0603 \text{ MPa m}^{-1}$$

Increase of average horizontal stress component (S_{Ha}) with depth (m):

$$0-900 \text{ m} \quad S_{Ha} = 9.86 \text{ MPa} + 0.0371 \text{ MPa m}^{-1}$$

$$900-2200 \text{ m} \quad S_{Ha} = 33.41 \text{ MPa} + 0.0111 \text{ MPa m}^{-1}$$

$$\text{Extreme Values} \quad S_{Hae} = 12.36 \text{ MPa} + 0.0586 \text{ MPa m}^{-1}$$

Change of ratio of the horizontal stress to the measured vertical stress (σ_H/σ_v):

$$\sigma_{Ha}/\sigma_v = \frac{251.68}{\text{Depth (m)}} + 1.14$$

$$\sigma_{Hmax}/\sigma_v = \frac{253.87}{\text{Depth (m)}} + 1.45$$

$$\sigma_{Hmin}/\sigma_v = \frac{279.72}{\text{Depth (m)}} + 0.88$$

Rock stresses at the north shore of Lake Ontario

K. Y. Lo, B. Lukajic and C. F. Lee

In connection with the design and construction of the Darlington Nuclear Generating Station, measurements of the initial state of the stresses in rocks were required for the purpose of: (i) designing the rock-concrete interface of the powerhouse and other structures; (ii) evaluating the potential "rock squeeze" problem in the construction of the intake and discharge tunnels; and (iii) evaluating the regional stress distribution for the assessment of tectonic safety. The program of stress measurements included both the over-coring method using the USBM deformation gauge and the hydrofracturing method in the limestones of the Black River-Trenton Group.

It was found that the results of the two different methods agreed well with one another. The state of horizontal stresses is markedly anisotropic, with the major principal stress P increasing from 10 MPa near the surface to 14 MPa at 70-m depth. The horizontal minor principal stress Q showed a similar trend. The orientation of the major principal stress P is remarkably constant, being $N70^\circ E$.

Along the north shore of Lake Ontario, stress measurements for engineering projects have been performed at four other sites extending from west of Toronto to Port Hope. The results of these off-site measurements were compared with those obtained at Darlington. No evidence of any stress anomaly was found. However, while the magnitudes are comparable, the direction of the major principal stress did not show a consistent trend on a regional basis.

Geological processes such as pop-ups and the heave of quarry floors in this general area were also studied. The results were generally consistent with expectations based on the results of stress measurements and the mechanical properties of the rocks.

During the rock excavation for the foundations of the surface facilities, observations of minor folds were made and monitoring of rock movements was carried out. Analyses of the results obtained showed that these were stress-induced phenomena and both the magnitude and direction of the bedding plane displacements are consistent with the stress regime. The effect of blasting on these geological features and observations is also discussed.

From the results of stress measurements at the site, together with off-site results of stress measurements, analysis of rock movements, and geological phenomena, it is concluded that there is no discernible evidence to suggest that the construction of the engineering structures at the site can remotely affect this area.

Stress relief bed slip in the Canadian Rocky Mountains

J.S. Bell

Recent NE-directed updip bedding plane displacements of several centimetres were recorded by borehole offsets in road cuts in the southern Canadian Rocky Mountains of Alberta. In the Exshaw area, 47 boreholes were offset 2–6 cm on 13 bedding planes exposed in six road cuts excavated between 1968 and 1979. In the Kananaskis area, 15 boreholes were offset 1–4 cm on four bedding planes in two road cuts excavated in 1975. Borehole offsets were generally consistent for each displacement surface. The measurements were made in SW-dipping Paleozoic carbonate sequences contained in four thrust slices.

The borehole offsets do not appear to be recording recent thrusting as interpreted from similar phenomena in the Appalachians, because: (1) apparent movement rates are unrealistically high; (2) no active thrusting is known to offset any wells in the adjacent overthrust Rocky Mountain Foothills; and (3) the area is not seismically active. Instead, their geometry is compatible with surficial stress release within an anisotropic stress regime, where $S_H > S_h > S_v$ and S_H is oriented NE-SW.

Finite-element models of lithospheric flexure during thrusting

Paul Lloyd

The tilting and flexure of fault-bounded blocks of the lithosphere can account for the Laramide basins and uplifts that characterize the Rocky Mountain foreland in Wyoming and Colorado. Where the lithosphere is tilted or flexed downward a basin will form; where it is tilted or flexed upward a mountain range will form. Such tilting and flexure may result from horizontally directed forces applied to a lithosphere with pre-existing faults. A quantitative model of this mechanism is useful for: a) determining whether horizontal forces can in fact produce the required amount of tilting, b) finding the amount of material that must have been eroded to produce the present topography, and c) relating the stratigraphy of a basin to the horizontal driving forces, thus helping us to understand the histories of basins in the region.

A two-dimensional numerical model has been developed that allows horizontal forces to be applied to a length of lithosphere having a single, pre-existing fault. It is assumed that the lithosphere behaves elastically, and finite-element solutions of the elasticity equations are employed. The fault is simulated by a thin zone whose elastic modulus is about two orders of magnitude lower than that of the lithosphere. The model includes the effects of sediment loading in the basins, and erosion of the uplifts. Results from the model are compared with observations from the Green River Basin and Wind River Mountains in Wyoming. Future work will include the use of a plastic material in the fault zone instead of a weak elastic one, and the introduction of a second fault.

Lithospheric stress and seismic ground motions

H.W. Asmis

Lithospheric, or in situ, stress is found to control the three most important parameters of seismicity that determine the character of seismic motions reaching buildings or other facilities on the surface of the earth. These parameters are: location of the source, energy release, and attenuation. This paper will highlight recent work on reconciling observed data with mechanical models and the known properties of rock to show how the distribution of in situ stress controls all three parameters. Location, including hypocentral depth, is determined by the interaction of tectonic driving forces and in situ stresses, taking into account geologic structure. A mathematical model has been developed that shows that most larger seismic fault ruptures should initiate at the ductile-brittle interface. The second parameter, energy release, is also shown through models to be dependent on in situ stress. Total seismic energy release, as measured by distant seismometers, differs from the energy release that is significant to civil structures in the near field; the most important determinant of energy release in the frequency band of structural interest is simply the size of fault rupture. The third parameter, attenuation, is most significant for structures located on rock. The state of in situ stress may control the stress amplitude of seismic waves, which then determines the seismic effect of stiff structures located on rock or facilities, such as tunnels, actually within rock. Computer models that incorporated non-linear rock properties derived from rock mechanics demonstrated that seismic waves most probably propagate with low stress. This then defines the relationships between frequency, displacement, acceleration and velocity. Non-linearity in the rock with regard to seismic stress amplitude can be considered as the primary control on seismic waves in the near field.

Session 3A: Geophysical Fluid Dynamics II Wednesday 0900 - 1220

Topographic generation of the Sitka Eddy

Gordon E. Swaters and Lawrence A. Mysak

A mathematical model is formulated that describes the interaction between a baroclinic current and order Rossby number topography along a coastline. The lead term solution, in an asymptotic expansion in the Rossby number, is obtained for the pressure, density, velocity and mass transport fields. The lead term solution is found using a normal mode analysis and a Green's function technique. The solution is applied to the possible topographic generation of the Sitka Eddy in the northeast Pacific Ocean. The numerical calculations of the model and the observed location, dimensions, velocities and transports of the Sitka Eddy are in good agreement.

On tidally-generated internal hydraulic jumps and solitary waves

H. Sandstrom and J.A. Elliott

Observations on the Scotian Shelf indicate that the baroclinic tides that are generated near the shelf edge dissipate their energy while propagating on the shelf by a process of non-linear steepening to form internal undular hydraulic jumps or to break up into solitary waves. Both forms have been observed to occur and will be discussed in the context of other physical parameters, such as strength of tidal current, stratification and sea bottom topography.

Forced finite-amplitude local baroclinic waves of constant form

William Perrie

What is the finite-amplitude inviscid dynamics of baroclinic waves in the 2-layer, β -plane model when bottom forcing is present and the layers are of unequal thickness? The governing equations are multiple-scaled in both the 1-dimensional and 2-dimensional cases. Resultant envelope relations are mapped via Gibbon et al. (1979, *Proc. R.S. Lond.* **A367**:219) to the so-called self-induced transparency equations. Assuming analytic functions obeying the Cauchy relations the extension of Gibbon et al.'s mapping to the 2-dimensional case is obvious. These latter equations are solvable via inverse scattering transform and have soliton solutions. It is seen that, in this situation when layers have unequal thicknesses and there is bottom forcing, Pedlosky's (1982, *J. Atmos. Sci.* **39**:555) work pointing at the presence of critical layer dynamics does not apply.

Coastal flows driven by a local density flux

Motoyoshi Ikeda

A two-layer model with a rigid lid and a flat bottom on an f -plane is employed to study a flow field driven by a density flux through the sea surface or the coast. The negative (positive) density flux is modelled by entrainment of the lower (upper) layer by the upper (lower) layer. The sub-inertial flow pattern constrained by the coast has two components: one is a baroclinic eddy nearby matching the entrainment region, and the other is a forced, internal Kelvin wave along the appropriate half of the coast.

A solution-scheme for the convective-diffusion equation

P.J. Sullivan and H. Yip

This paper presents a versatile solution-scheme for the convective-diffusion equation. A small-time, asymptotic, solution for an instantaneous point source of scalar contaminant is expressed as a three-dimensional, Hermite polynomial expansion and manipulated, using superposition, to generate the contaminant concentration field that results at larger times and for an arbitrary, continuous or instantaneous, source contaminant distribution. This equation is commonly used to model contaminant dispersion in complex environmental flows, so that the considerable degree of generality, flexibility and efficiency of this solution-scheme highly commends it to this application. The off-diagonal terms in the diffusivity tensor and the non-zero gradient of this term and the mean-velocity field are shown to make a significant contribution to the evolution of the contaminant concentration field resulting from the instantaneous release of contaminant from a point source.

Ringdown of inertial waves in a spheroidal shell of rotating fluid

S. Stergiopoulos and K.D. Aldridge

The role of inertial waves in the dynamics of the Earth's fluid outer core has been investigated through laboratory experiments. In these experiments inertial waves of azimuthal wavenumber one, Ekman number $O(10^{-5})$, Rossby number $O(10^{-3})$ were excited in a rotating spheroidal shell of fluid by precession of an inner body. Proximity to resonance was achieved by adjusting the ratio of the frequency of precession of the inner body to the rotational speed of the container to be near the eigenfrequency of the inertial wave mode being studied. Once the system was near resonance the perturbation was stopped and decay records were obtained. An iterative linearized

least squares inversion method was applied to the digitized disturbance pressure data. Amplitude, eigenfrequency and decay rate were simultaneously recovered for the principal and neighbouring modes excited.

The recovery of the complex eigenfrequencies from digital pressure records has given experimental verification of the existence of non-axisymmetric inertial waves in this shell geometry. For those waves of azimuthal wavenumber one, a significant non-linear interaction among modes is inferred from the simultaneous recovery of neighbouring modes. Other non-linear effects include a mean azimuthal flow that appears to be stable for the low spatial order modes studied. These results contrast with the highly unstable mean flow found experimentally in similar experiments carried out in cylindrical geometry.

Transient multiple vertical wavenumber convective instability in a rotating fluid

C. Quon

In the past, the classical Bénard instability problem has been investigated in a thin layer of fluid in either a stationary or rotating frame of reference (Chandrasekhar, 1961). When the fluid layer is thin, the dominant unstable mode has vertical wave number unity. The aspect ratio of the unstable cells is $O(1)$. When the aspect ratio of the fluid container itself is $O(1)$, then the convective instability permits multiple vertical wavenumbers. In a rotating fluid, this instability is closely related to the Stewartson boundary layer near the vertical walls. The potential application of this problem to large-scale oceanic and atmospheric circulation will be discussed.

A computer movie of the transient states of 5 different sets of parameters will be shown.

CHANDRASEKHAR, S. 1961. *Hydrodynamics and Hydromagnetics Instability*. Oxford Press, 654 pp.

Session 3B: Scientific Services to the Offshore Industry

Wednesday 0900 – 1230

Calculation of extreme design parameters for offshore drilling units

Langley R. Muir

Regulations for the design of offshore drilling units contain a phrase to the effect that the unit must be able to survive the "statistical 100-year storm", but they do not give any further guidance as to what this phrase actually means. In practice, it has been taken to mean that the design parameters for the unit must be the 100-year return values for the winds, waves, currents and water levels and that each parameter is calculated independently. Economics dictate that the design parameters and the joint-probability distributions should be known with some precision, while safety requirements dictate that the confidence limits should also be known.

Fisher and Tippet (1928) showed that the distribution of the maxima of independent samples drawn from an identically-distributed population will tend asymptotically to one of three limiting types, which are independent of the distribution of the original population. These three distributions, as well as a number of others, have been used routinely to calculate extreme design parameters. Lawless (1970s) showed how to calculate confidence limits for the Fisher-Tippet distributions, although this is seldom done.

This paper is a critical review of the various methods available for the computation of extreme design parameters. It considers the various statistical distributions, methods of fitting data, the assumptions made, computation of confidence intervals, and, above all, the statistical interpreta-

tion of the results. Although the review is primarily aimed at the computation of extreme winds and wave heights, some attention is paid to the peculiar problems of extreme currents and water levels. Specific recommendations will be given that are applicable to the Canadian offshore.

Marine climate information systems for offshore engineering

A. Saulesleja, V. Swail, T. Agnew, L. Mortsch and T. Mathews

Marine climate information systems have been developed by the AES Canadian Climate Centre to produce climatic summaries of meteorological and oceanographic data in tabular and graphic form. They were designed primarily for offshore engineering applications, but are useful for environmental assessment, contingency planning and research as well.

The interactive software systems produce a wide range of statistical analyses on a variety of environmental parameters originating from observed and derived data fields.

MAST (marine statistics), LAST (Land Statistics) and GASP (Grid Area Statistics) produce a series of univariate and bivariate analyses and graphs of marine observations, climatological observations from land stations and objectively analysed fields from the U.S. Naval Environmental Data Network data set, respectively. A brief overview is provided. Recent improvements include the calculation of monthly mean fluxes of momentum, latent and sensible heat over the oceans, and a provision for obtaining analyses preconditioned by the occurrence of a specified environmental condition.

A contour analysis software package (CONAN) has been developed to map environmental data from observed and analysed fields. CONAN contours the means, medians, modes, standard deviations, percentile values and other statistics for any user-specified area and draws these and a background map on a polar stereographic projection. The user can compare fields by contouring differences, ratios and per cent differences between two fields. Directions are displayed as arrow plots.

A duration statistics package (DUST) automates the production of duration statistics and extreme value analyses. There is considerable flexibility to handle data gaps and threshold values. Output is in the form of tables and graphs, and DUST is interfaced with CONAN to map return periods of extremes and durations of climatic elements.

The climatological analysis systems described are designed to be user friendly but powerful and flexible enough to suit the needs of offshore engineering design and contingency planning. The systems are available through AES regional offices and through the Canadian Climate Centre. The public and private sectors may also access the systems directly via telephone lines by obtaining an account with the AES computing facility in Downsview.

The function and capabilities of these systems and the application of their outputs for marine climatology is described.

Searching for long-distance wave group correlations at Hibernia

P.H. LeBlond, D. Cumming and G. Staples

Simultaneous measurements of sea-level variations, obtained from a pair of Waverider buoys at the Hibernia site on the Grand Banks, have been compared in a search for correlations between groups of waves that might be interpreted as possible envelope solitons. Group coincidences were calculated for a range of lags and for different wind directions. Not unexpectedly, given the 17-km separation between sensors, no statistically significant coincidences were found.

Sable Island wind comparison

William Richards and Erik Banke

To determine the relationship between the boundary-layer (10-m) winds at the Atmospheric Environment Service (AES) observing station on Sable Island and winds over the open sea, wind measurements at the island site were compared with those simultaneously measured on the beach during Bedford Institute of Oceanography (BIO) experiments, and with those collected by ships at sea.

Seventy-eight pairs of simultaneous AES BIO winds and 17 sets of AES, BIO and ship winds were used in the comparison.

The analysis demonstrates that winds measured at the AES station are 10 – 15% lower than BIO winds on the beach. It was further found that the BIO winds were on average 20% lower than the ship winds. More work should be performed to "calibrate" the long-term AES wind data from Sable Island before they can be used with high confidence for design purposes.

Oil spill tracking buoy research and applications

Douglas White

A Lagrangian buoy to accurately track oil spills has been developed at the Bedford Institute of Oceanography during the past three years. Although signal transmitting buoys may approximate the actual surface water motion, their motion is a combination of wind and wave drag forces. Evaluating the performance of a buoy is complicated by the fact that surface water velocities are not easily measured owing to the change in velocity structure with depth and turbulent and dispersive effects. The above problems have been empirically approached by developing an experimental reference buoy whose surface-following performance characteristics are now well known. These characteristics were investigated by documenting how changes in the buoy's shape and mass distribution affected its performance.

The buoy has been field tested against other commercially available buoys and against a real oil spill. Although this buoy was developed for the application of oil spill monitoring, it has potential for use in ocean surface current research.

Initial Stabilization of man-made islands in Grande-Entrée Lagoon, Îles-de-la-Madeleine

Georges Drapeau and Mario Gagnon

A 7.8-km long navigation channel was dredged to enable 20,000-ton salt carriers to reach Mines Seleine wharf on the northern side of Grande-Entrée Lagoon at Îles-de-la-Madeleine in the Gulf of St Lawrence. The sand dredged to excavate the 125-m wide and 7.5-m deep navigation channel was dumped at preselected locations mostly to form two artificial islands. One island (Ilot B), 2 km south of Mines Seleine wharf resulted from the dumping of 1,500,000 m³ of fine sand over a flat portion of the lagoon at an initial water depth of 3.5 m. The island formed by the dredged material is 1000 m long and 200 m wide, and its low profile reaches 3 m above the lagoon water level. The second island (Ilot C) is located some 500 m north of Grande-Entrée Harbour and parallels the dredged navigation channel. At that location the original water depth was only 1 m and 1,400,000 m³ of dredged fine sand formed a 1200-m long by 300-m wide island that reaches in places 4 m above the lagoon water level.

Repeated surveys of these two islands in 1982 and 1983 show that they are stabilizing rapidly. Initially the islands had steep beach slopes that could reach 1:5. Two years after the completion of the dredging operations the beach slopes are of the order of 1:10 to 1:20 and the nearshore profiles average 1:60. Wind, wave and bottom current measurements indicate that the rate of bottom sediment transport is tempered by the hydrodynamic conditions prevailing in the lagoon and that the final configuration of the beach and near-shore profiles will eventually compare with those of natural islands in other parts of the lagoon.

However, as we are dealing with artificial islands, the near-shore beach profile equilibrium concepts used in natural environments are not sufficient to model the evolution of these artificial islands. Potential energy was built up because of the piling up of the dredged sand. As a result, the centre of gravity of the islands is lowering as stabilization processes take place and an analogy can be drawn with the concept of entropy. This implies that additional sources of sediment from the upper portion of the beach have to be taken into account for the modelling of the evolution of these artificial islands. One approach is to consider these artificial islands as if they were subjected to a quasi-instantaneous transgression of sea level.

A simple summary wave-hindcast model

David P. Krauel

A simple summary wave-hindcast model based on the Sverdrup-Munk-Bretschneider equations is presented and the results are compared with those of a more detailed hindcast model and with observed wave data. The frequency distributions of significant wave height and period by direction are calculated directly from frequency distributions of wind speed and direction. Summary hindcast wave climates compare favourably with the more detailed hindcast model results and with observed waves in coastal waters with fetches of up to 500 km. Improvements in the summary model results can be effected by including a persistence factor for the wind data. The persistence factor removes the assumption that the waves are fetch limited and extends the reliable application of the summary hindcast model to locations with longer fetches. It is shown that the simple and quick summary hindcast model yields an average wave climate that is sufficiently accurate for most studies involving coastal geomorphology or coastal engineering.

Real-time operation of Spectral Ocean Wave Models (SOWM)

Simon G. P. Skey and Bassem M. Eid

At the present time there are, to the best of the author's knowledge, only two Spectral Ocean Wave Models being run in a real-time mode, namely the SOWM of the Fleet Numerical Oceanography Centre (FNOC) and the ODGP (Ocean Data Gathering Program) model being run by Oceanweather Inc. (Cardone and Ross, 1979)

The value of these models to Canadian offshore users depends on the individual user requirements and the locations of the forecast grid points. The models use widely different grid projections and different versions of the growth and decay subroutines. Comparisons of the two models, verified against buoy and rig data, point out the relative strengths and weaknesses of the two models.

Use of the models in an operational sense is dependent on the timing of the output from the models as well as the speed with which one can turn a spectral forecast into an operational forecast. The paper looks at the models available to Canadian users and assesses both their usefulness and their proposed future developments.

On the development of an operational spectral wave model for the Canadian East Coast offshore

M.L. Khandekar

The Atmospheric Environment Service (AES) has identified a requirement of a spectral wave model for operational ocean wind-wave prediction in Canada. This paper describes some of the developmental studies in spectral ocean wave modelling that are currently in progress in the AES Meteorological Services Research Branch.

Following a brief review of the development of operational wave prediction techniques, the basis of spectral wave modelling is discussed and some of the products obtainable from a spectral wave model are presented. Two spectral wave models are identified for possible implementation in the AES forecasting system. These two models are closely examined to assess their applicability to the East Coast of Canada where major marine activities are in progress. Possible modifications of these models for application to shallow water areas are also discussed.

Finally, some aspects of wind data requirements for the spectral wave model are considered.

Session 3C: Agricultural and Forest Meteorology

Wednesday 0900 - 1020

The effects of terrain and moisture on lightning activity over southern British Columbia

Larry Funk

The Pacific Weather Centre places heavy emphasis on GOES-WEST satellite imagery and lightning strike data for its fire weather forecast program. The lightning strike location network was expanded to cover British Columbia during the summer of 1983 and the data are now being assessed on their own merit. The presentation deals with lightning strikes over southern British Columbia and links them to satellite image features.

The basic approach was to plot the lightning strike data on geographical maps using small time intervals. The maps were then recorded on videotape. Playback at an appropriate speed results in an animated sequence, which illustrates the time dependence of the lightning patterns.

In the past, conventional theory suggested a random occurrence of heavy convection. Wide-spread thunderstorm and lightning activity was usually forecast across the southern Interior when strong surface heating, high dew points, and orographic lift were deemed significant. Random thunderstorms were forecast along windward coastal areas when cool unstable air moved onshore from the Pacific.

By studying animated lightning strike and satellite imagery, it now appears that the convective activity is more ordered than previously believed. Though lift and heating remain key parameters for convection, valley orientation and low-level moisture tongues appear to be the critical factors for the incidence and location of lightning events.

This presentation demonstrates that valleys and coastal inlets of southern British Columbia act as funnels for moisture and wind thus creating steep gradients along the valley walls and enhancing thunderstorm and lightning activity. Animated sequences are used to illustrate the relationship of valleys and moisture to: lightning occurrence, well-defined lightning corridors, convergence zones, intensification areas and cloud tops.

Airflow measurements above a forest canopy during spray trials in New Brunswick

R.E. Mickle

In a well-established aircraft spray program in New Brunswick, approximately 1.5 million hectares of forest are sprayed each year against the spruce budworm. The off-target drift and subsequent environmental impact of the chemicals used is a continuing concern. Meteorological conditions, particularly wind and temperature above the canopy, have a strong influence on eventual spray fate. Just above and within the forest canopy, the characteristics of the canopy, particularly height and density are important modifiers.

As part of an ongoing impact assessment, an attempt is being made to produce a realistic Monte Carlo computer model of spray dispersion and its subsequent fate. In order to provide the best possible parameterizations for the model, complementary field studies were undertaken in 1982 and 1983 near Upper Blackville, N.B. to study the in- and above-canopy ambient airflow and turbulence during spray trial simulations. In addition, a special study of the evolution of the spray aircraft wing-tip vortices, a major influence on the spray dispersion, was conducted.

A climatology of historical drought on the Canadian Prairies

Roger B. Street

A systematic study of the complexities of drought in terms of timing, extent, duration and severity is essential for developing strategies and designs against future drought impacts. This study addresses the problem of characterising drought on the Canadian Prairies. It provides an objectively based means of assessing the relative characteristics of individual historic drought events during the period from 1926 to 1980.

The basis of the analysis is soil moisture values estimated on a rectangular grid system using a climatic water budget. The climatic water budget uses grid values of the maximum and minimum temperatures, precipitation, solar radiation and physiographic descriptors to produce water status reports each 10 days on a calendar-year basis.

A statistical analysis of the grid water status reports has revealed some regional homogeneity in the soil moisture estimates. Eight distinct soil moisture status regions have been defined across the Canadian Prairies. The characteristics of soil moisture in each of these regions are analysed to determine the drought climatology of the individual regions. Included in the analysis are regional statistics that assess the temporal and spatial values of drought and the susceptibility of the regions to drought.

An on-line drought index for forest fire management purposes

Monique Loiselle

An automated on-line, near real-time drought index was developed for forest fire management purposes for 22 AES core observing stations in Ontario. A Shear and Steila index, reflecting the departure of the soil moisture status from the long-term mean was used. The actual moisture status was calculated from soil moisture values obtained from a modified Thornthwaite water budget. A few historical cases are developed to demonstrate the application of this index.

A comparison between climate parameters in an open site and a farmed forest site

Philip J. Sajecki and Roger B. Street

Few observations of climate data are available within a farmed forest system. In addition, a lack of documentation of such essential boundary conditions as synoptic climatological conditions, forest canopy structure and physiological state of the stand makes the generalization of existing research results difficult and their extrapolation hazardous. Well-documented field experiments are needed to assess the farmed forest microclimate.

Measurements of climatological factors were made during the 1982 growing season within a hybrid poplar plantation in eastern Ontario. The climate parameters measured included solar radiation, soil temperature, air temperature and relative humidity, precipitation and wind speed and direction. The influence of the hybrid poplar stand on the climate is quantified by comparing the observations with coincident measurements taken at an adjacent open site. The measurements are kept in the proper perspective by referencing them to specific synoptic weather types.

On the basis of the daily totals of solar radiation received at the open site, the existing climate data bases for the Codrington site were separated into three distinct classes: clear, partly cloudy or cloudy. The individual climate parameters were also separated into these classes and statistical comparisons were carried out on the farmed forest and open-site data. In addition, the synoptic weather conditions associated with the observation days are described to provide a background for interpreting the analysis.

Session 3CC: Air Pollution Meteorology **Wednesday 1050 – 1230**

A preliminary assessment of wood smoke emission levels from residential sources in Canadian urban centres

Ambury Stuart and William Lowe

A simple model of wood smoke emissions and dispersion was developed to identify those Canadian urban centres where pollution from this source was most intense. Following a review of provincial studies of wood use for residential heating, an emissions model was constructed that took into account the size of each of 428 urban centres, its inventory of housing types, local heating requirements and the popularity of wood as a fuel in the centre. Then a dispersion model was developed that estimated nocturnal mixing heights, average surface winds and the effect of precipitation on smoke particles likely to be harmful to human health. Finally, a ranking procedure was applied to these emission and dispersion estimates to identify those urban centres where high emission rates and/or low dispersive capacities indicate the necessity of further studies.

Many urban centres in the Western Cordillera climate zone were highly ranked in most seasons. Many centres in Atlantic Canada were also considered noteworthy. Other centres were located in the Laurentian mountain area, northern Québec and northern Ontario.

This study was the first of its kind to cover most urban centres in Canada. Its simplified approach precludes its application to the estimation of actual wood smoke pollution levels. Instead, it is intended that the results would serve as guidance in the selection of urban centres for more thorough field studies or simulation models.

Meteorology, Long Range Transport of Air Pollutants and health: An integrated study

F. Fanaki and M. Raizenne

Industrial pollutants, pollen and particulates disperse and change their chemical composition as they travel in the atmosphere. The mechanism of dispersion is a function of many meteorological parameters (e.g. atmospheric turbulence and thermal stability) as well as topography and the distance travelled. With the existence of tall industrial stacks, pollution is no longer limited to local areas but can be transported over hundreds of kilometres. Hence, isolated areas are subjected to air pollutants from distant sources, commonly referred to as LRTAP (Long Range Transport of Air Pollutants). The acute health effects associated with the degradation of air quality from these remote sources are not well defined in the literature.

This paper describes a field study that was carried out in June 1983 at Lake Couchiching, Ontario, Canada. Of 120 residential campers, 52 children (age 8-15) volunteered to participate in the study. Twenty-three of the subjects were asthmatic. Measurements of lung function were made twice daily and children answered a brief health/symptom diary. The camp was equipped with meteorological sensors to monitor wind speed, wind direction, temperature, atmospheric pressure and relative humidity. A bivane was used to measure wind fluctuations. Various pollutant measuring units were used to determine the air quality of the area during the study period. Measurements included SO₂, O₃ and size fractionated particulates. Comparison of the observed concentrations of particulates within a canopy and outside it suggested that the trees act as filters for certain size particles and play a role in the deposition process.

Back-trajectory modelling was used to determine the history of the air masses interacting with the research area. The trajectory analysis has shown that the camp area was subjected to air masses that had travelled over pollution sources in the United States and Canada. The associated increase in LRTAP pollutants coupled to meteorological measurements produced modest changes in the health indices. The extent of the interactions and the limitations of this study will be stated.

Further investigation of local wet sulphur deposition patterns around Halifax and Dartmouth, Nova Scotia

R. W. Shaw

An earlier study by the author (*Atmos. Environ.* **16**: 337-348) indicated that approximately 50% of the deposition of sulphur by precipitation in 1979 at a station 25 km from Halifax/Dartmouth may have originated from sources in that city, and the other 50% from more distant sources in central Canada and the eastern United States. Since that time, precipitation event sampling has been continued and expanded to include two additional stations. This larger data set was analysed. Comparisons are made among the measured wet deposition values of the hydrogen and sulphate ions at the three local stations and with those measured at a more distant, regionally representative station at Kejimikujik National Park to estimate the contribution of sources in Halifax/Dartmouth. In addition, the observations are compared with the predictions of a meso-scale climatological deposition model to gain an insight into the magnitude of the washout coefficient during precipitation.

The detectability of trends in wet deposition data

R.E. Munn and D.M. Whelpdale

A workshop on the Detection of Trends in Wet Deposition Data was held 17-18 November 1983 at the Institute for Environmental Studies, University of Toronto. The 20 participants included atmospheric modellers, atmospheric chemists and statisticians. The emphasis was on methods rather than on results, and special attention was given to the question of estimating the length of time that would be required to detect a future change in regional emissions of sulphur.

The following scenario was selected for the North American reduction in sulphur emissions to be expected once a Canada-U.S. accord on acidic deposition has been signed: 1, 10, 20 and 28% decreases after 2, 5, 7½ and 11 years, respectively. Assuming linear chemistry, this would lead to equivalent per cent reductions in wet sulphate deposition. However, year-to-year variability in the relevant climatic factors is so great that the change would be difficult to detect. Four ways of reducing the noise in the time series are as follows:

1. Combining point measurements to obtain spatial averages, e.g. by Kriging or Thiessen polygons
2. Data stratification, e.g. sector analyses
3. Normalization for meteorological influences, e.g. using sulphate concentrations in precipitation rather than wet deposition amounts
4. Use of model-derived time series rather than observed ones

In any case, the data sets to be used for detecting a trend consist of "before" and "after" time series. These are to be compared in a purely statistical way. The techniques available for this part of the analysis include Box-Jenkins intervention and ridit methods.

The paper concludes with a brief discussion of methods (signal-to-noise ratios and Kriging) for improving the existing wet deposition networks, and with the Workshop recommendations.

Automated minitube air sampling system

Don Barnett, Terry Locke and Orville Olm

The Canadian Centre for Advanced Instrumentation has developed an automated air sampling system for the Department of National Defence. The system consists of a number of field-based microprocessor-controlled samplers, a radio transmitter to trigger the start of sampling and a specially modified gas chromatograph to perform the analysis.

Air samples are taken by pumping the air to be sampled through a minitube packed with a polymer adsorber. Each field sampler is fitted with a carousel housing fifty minitubes. A program module in each sampler controls the minitube selection, sampling time and flow rate. Program modules can be easily changed in the field.

It is anticipated that this system, or some modification of it, would be useful for pollutant monitoring, and the verification of downwind transport modelling.

This paper will give a brief introduction to the Canadian Centre for Advanced Instrumentation and describe the development and operation of the Automated Minitube Air Sampling System.

A model of the Ice-Age cycle*W.R. Peltier*

Times series analyses of the $\delta^{18}\text{O}$ signal in deep-sea sedimentary cores have very clearly established that ice volume fluctuations throughout the late Pleistocene have been dominated by an almost periodic oscillation with a characteristic time-scale of 10^5 years. Although statistically significant variance is also found at the expected Milankovitch periods corresponding to the precession of the equinoxes and to the variation of orbital obliquity, the dominance of the 10^5 -year signal has been difficult to understand because the strength of the astronomical forcing at this period is negligibly small. The analysis presented here shows that this period arises naturally in a new model that includes the non-linearity due to ice-sheet flow and a more accurate description of the process of glacial isostatic adjustment than has been employed previously.

Orbital periods in climatic records of the Ice-Age North Atlantic*W.F. Ruddiman*

Ice-Age sediments of the Atlantic Ocean from 40 to 65°N contain a clear and systematic record of three periodicities linked to variations in the earth's orbit around the sun (eccentricity at 100,000 years; tilt at 41,000 years; and precession at 23,000 years). These signals are recorded by temperature-sensitive marine microplankton, which form shells in surface waters, die, fall to the sea floor and leave in the layered sediments a record of past ocean history. From census counts of these shells, combined with regression analyses of their modern temperature preferences, it is possible to derive records of the changes in estimated sea-surface temperature (SST) during past geologic history.

Over record lengths covering the last several hundred thousand years, the ocean at all latitudes from 40 to 65°N shows a strong 100,000-year SST rhythm. At latitudes north of 50°N, this signal is in phase with measures of Northern Hemisphere ice volume recorded by independent geochemical parameters. There is also a strong 41,000-year SST signal north of 50°N that is in phase with ice volume. These relationships suggest that the North Atlantic at very high latitudes responds quickly and passively to changes in ice volume. The full sequence appears to be: Summer insolation controls ice buildup on land, the ice then controls air temperatures by means of albedo-temperature feedback, and the air temperatures then control the heat content of the surface ocean. This basic regime at high latitudes has existed since about 850,000 years ago, before which ice-volume buildup and SST coolings at the 100,000-year cycle were smaller.

South of 50°N, the 41,000-year period weakens considerably and the 23,000-year rhythm becomes dominant. The SST signal at this period lags behind that of ice volume by 6000 years ($\frac{1}{4}$ wavelength). As a result, the mid-latitude North Atlantic tends to be warmest during the growth of ice-sheets on adjacent continents and coldest during their decay. The origin of this signal is not yet fully clear, but the implication of the SST lag is that the mid-latitude North Atlantic could provide major amounts of moisture for ice growth and cut off that moisture during ice decay, thus amplifying insolation changes at that cycle.

Deglacial melt water plumes in the North Atlantic: Isotopic evidence*Richard H. Fillon and Douglas F. Williams*

Estimates of the $\delta^{18}\text{O}$ of North Atlantic surface waters ($\delta^{18}\text{O}_{\text{SW}}$) during the last deglaciation corrected for global effects can be made from down-core $\delta^{18}\text{O}$ analyses of tests of the planktonic foraminifera *Neogloboquadrina pachyderma* (left-coiling) and faunal estimates of sea surface

temperature. The ca. 13,000 B.P. peak deglacial level has been identified in 25 North Atlantic area cores with suitable $\delta^{18}\text{O}$ records, thus providing adequate areal coverage to reconstruct deglacial sea surface paleo-oceanographic gradients in $\delta^{18}\text{O}_{\text{sw}}$. The most striking feature of this reconstruction is a significant, more than 2-fold increase in area of ^{18}O -depleted surface waters ($\delta^{18}\text{O}_{\text{sw}} < -0.7\text{‰}$ vs PDB). Today, waters depleted in ^{18}O to that extent are confined to the Canadian and East Greenland Currents, which transport ^{18}O -depleted run-off from Arctic and sub-Arctic Canada, Greenland and the Arctic Ocean. This leads us to believe that planktonic foraminiferal tests in the North Atlantic Ocean record an accelerated discharge of ^{18}O -depleted fresh water into marginal seas during disintegration of the late Pleistocene ice-sheets.

Planktonic foraminiferal, palynological and oxygen isotopic stratigraphy of CESAR 83-102 and 83-103: A 1-Ma record of Arctic Ocean climate

A.E. Aksu and P.J. Mudie

Two gravity cores from the southeastern Alpha Ridge area of the Arctic Ocean include a continuous sedimentary record of the last 1 Ma (lithofacies I to M as defined by Clark et al., 1980). Paleomagnetic data show that both cores penetrate a complete record of the Brunhes normal polarity chron (ca. 0.73 Ma) and into the upper Matuyama negative chron. Planktonic foraminifera are the dominant component of the biogenic skeletal debris in the $> 63 \mu\text{m}$ fraction with pteropods, benthic foraminifera, ostracodes and pelecypods not exceeding 2%. *Neogloboquadrina pachyderma* (left and right coiled) and *N. cryophila* and the major planktonic foraminifera; *N. polusi*, *Globigerina quinqueloba*, *G. egelida* and *G. bulloides* are secondary in abundance. Oxygen isotopic composition of *N. pachyderma* together with the foraminiferal and palynological data suggest that:

1. Large-scale decreases in planktonic foraminiferal abundances may be the result of (i) dilution of the surface waters by increased run-off, as suggested by the ^{18}O data and palynological data; if the surface salinity dropped below the tolerance level of planktonic foraminifera, this would result in low total foraminiferal counts in sediments regardless of the primary productivity in the water column and regardless of climate; (ii) increased calcium carbonate dissolution on the sea floor that would also give lower total foraminiferal counts regardless of climate and productivity, as seen near the base of core 83-103; and (iii) thicker sea ice that may decrease primary productivity and also result in lower foraminiferal counts.
2. Although the absence or very rare occurrence of foraminifera in the Arctic Ocean sediments does not necessarily indicate low productivity, high abundances of foraminifera strongly suggest relatively high productivity in the water column.
3. The absence of gravity flow deposits in the cores suggest that most of the $> 63 \mu\text{m}$ fraction is ice-rafted. The near-uniform occurrence of ice-rafted coarse clastics throughout the gravity cores indicates that Northern Hemisphere glaciation was underway prior to 1 Ma B.P.
4. There is no evidence in the faunal or floral record of the cores to suggest pack-ice free conditions during the past 1 Ma.

Patterns of sedimentation in the Arctic Ocean: Key to a high latitude Late Cenozoic chronology?

David L. Clark

Most sedimentation in the Arctic Ocean during the Late Cenozoic has been a result of ice transport. Pack-ice and icebergs carry their unique cargo of sediment to all parts of the Arctic Ocean

and only in the deeper basins (e.g. Canadian Basin) have other sedimentation processes been significant. A Late Cenozoic stratigraphy for sediment of the Chukchi-Alpha Ridges includes 13 lithologic units that can be correlated with magnetic reversal dating and with sediment deposited in the Makarov Basin and on the Lomonosov Ridge as well. The turbidite dominated sediment of the Canadian Basin has its own stratigraphy.

Textural analysis of the Chukchi-Alpha sediment cores provides a spiky record of abundant coarse grained sediment ($> 62\mu\text{m}$) alternating with intervals of finer grained debris. The consistency of this record throughout the area of correlation of the various stratigraphic units suggests climatologic controls and chronologic significance.

Climatologically, an abundance of coarse grained sediment generally correlates with global ice minima (low $\delta^{18}\text{O}$) and low coarse grained sediment concentration is in phase with global ice maxima (high $\delta^{18}\text{O}$). This confirms the intuitive conclusion that a product of deglaciation is an abundance of coarse grained sediment. Pack-ice transport probably accounts for most of the finer grained sediment deposited between times of active deglaciation. In the central Arctic Ocean deglaciation generally is incomplete and T-3-size icebergs continue to transport coarser sediment following the most active stages of deglaciation.

Preliminary study of the plots of coarse sediment at 1-cm intervals shows that the texture record has a superficial similarity with the $\delta^{18}\text{O}$ record. Additional $\delta^{18}\text{O}$ and texture comparisons are necessary to quantify this correlation. A deglaciation record correlated with $\delta^{18}\text{O}$ variations would be a unique high latitude chronology. It is also possible that the textural record of deglaciation could be used as a measure of Northern Hemisphere ice volume, or, at least, the degree of completeness of deglaciation.

Foraminifera from the Lomonosov Ridge and adjacent basins, Central Arctic Ocean

G. Vilks and Ali Aksu

Shipek surface grabs from 11 stations along a traverse across the Lomonosov Ridge yielded 55 benthic foraminiferal species, 14 of which are agglutinated types. The major species suggest different environments in the Makarov Basin (water depth 3900 m), Lomonosov Ridge (1500-1900 m) and Fram Basin (4200 m). Makarov Basin is characterized by *Eponides tener*, and the Lomonosov Ridge by *Cassidulina laevigata*, *Planulina wuellerstorfi* and *Trochammina rotaliformis*; the Fram Basin is dominated by agglutinated species, such as *Hyperammina fragilis*, *Reophax nodulosus*, *Psammosphaera fusca* and *Trochammina nitida*. The calcareous forms *Stetsonia horwathi* and *Elphidium subarcticum* are abundant in both basins.

Foraminifera are most abundant between 2-5 cm in closely spaced Shipek Grab subsamples. Below 5 cm of sediment, foraminiferal numbers and diversity are sharply reduced.

Two Benthos gravity cores from Makarov and Fram Basins show distinct turbidite textural characteristics and contain very few foraminifera below the surface, 0-2 cm. The agglutinated genus *Hyperammina* that is common in the Fram Basin core was found only in the 78-80 cm interval of the Makarov Basin core.

The dominance of arenaceous species in the Fram Basin may reflect the deeper and colder bottom waters to the east of Lomonosov Ridge. The arenaceous assemblages of the Fram Basin are comparable to those in other areas of cold water, turbidite sedimentation and/or reduced salinities. Similar assemblages are found, for example, on the inner Labrador Shelf where Labrador Current water temperatures are as low as -1.5°C , in fjords, such as Lake Melville, and in waters below the Carbonate Compensation Depth of the Sohm and Nares Abyssal Plains.

The ^{18}O values of the benthic foraminifera *Planulina wuellerstorfi* will be compared with those of the planktonic form *Neogloboquadrina pachyderma* in sediment and plankton tows to determine the influence of run-off and meltwater in the upper 200 m of water, and to provide data that will aid in establishing the boundary between isotopic stages 1 and 2 in the bioturbated near-surface interval of the two gravity cores.

Palaeoclimate reconstruction from deep ground temperatures, Canadian Arctic Archipelago

Alan Taylor and Alan Judge

In this paper, we examine temperature profiles to 850 m at 20 sites in the Canadian Arctic Archipelago, concentrating on what the geothermal analysis can contribute to three types of climatically related episodes.

- 1) Several sites within the coastal margins of some of these islands have emerged only recently from the sea owing to isostatic uplift. In the Arctic, the effect of emergence on the present subsurface thermal regime is substantial because of the large temperature contrast experienced as the submerged site became sub-aerial. The geothermal analysis is used to test possible dates: In the Canadian Arctic Archipelago, our analysis suggests that the recent period of marine submergence probably began no earlier than 10,000 years B.P. and that dates of emergence are in general agreement with uplift curves published for the region. The geothermal analysis demonstrates how the increase in permafrost thickness noted away from coastal margins may be attributed to the submergence history of the region.
- 2) The geothermal analysis was used to attribute approximate temperatures to the major climatic episodes in the past few thousand years. Little Ice Age temperatures were probably 5 K lower than today, but the earlier Climatic Optimum and Hypsithermal suggest that temperatures in the past few thousand years were higher by a degree or so than today.
- 3) The nature and extent of late Wisconsin glacial ice cover over the Canadian Arctic has generated some conflicting views in the past decade. The depth extent of the profiles is insufficient for a detailed study but the geothermal analysis favours surface temperatures similar to those of today during that period. This is consistent with some geologic evidence that suggests a lack of a continuous ice cover over the central Arctic Archipelago.

Late glacial to recent stratigraphy and sedimentary processes: Newfoundland Continental Slope and Rise

C.T. Schafer, F.C. Tan, D.F. Williams and J.N. Smith

Micropaleontology, pollen, sediment and $\delta^{18}\text{O}$ studies point to considerable variation in sedimentary processes and water mass characteristics on the northeast Newfoundland Slope and Rise during late Wisconsinan and Holocene time. Allochthonous shelf and upper slope foraminiferal species suggestive of turbidity current activity occur relatively frequently in rise sediments during a presumed early to middle Wisconsinan interval, dated by extrapolation from a probable 9300-year old ash horizon. A single late Wisconsinan turbidity current deposit involved a much larger volume of sediment than that noted for the earlier events and it appears to have originated primarily on the middle slope. In conjunction with a widespread late glacial interval of fecal pellet deposition, this larger event suggests an increased flux of suspended particulate matter (SPM) to the continental margin prior to and following the late Wisconsinan glacial maximum. The higher SPM flux appears to have stimulated the productivity of zooplankton during a late glacial interval of rapid ice ablation.

Within the late Holocene interval of the rise sediments, there is some micropaleontological and sedimentological evidence for an intensification of the Western Boundary Undercurrent (WBU) that appears to have started about 1000–2000 years B.P. Over the same period of time, the surface water circulation seaward of the northeast Newfoundland Shelf appears to have changed from a mode that was dominated occasionally by a northern component of relatively warm North Atlantic Drift water to one that is dominated today exclusively by Labrador Current water.

The influence of sea level rise on the Bay of Fundy–Gulf of Maine tidal ranges from 7500 B.P.

David B. Scott and David A. Greenberg

Previous studies of sea level and tidal amplification in the Bay of Fundy suggested a linear increase of tidal amplitude as relative sea level rose. New data presented here are used in a numerical tidal model in an effort to reproduce paleo-tidal regimes over the last 7000 years. Five new sea-level curves covering the last 4000 years and some previously published data extending the record back to 7000 years B.P. are used as the data base. These data, when used together with the tidal model, indicate that tidal amplitudes increased much more rapidly between 7000 and 4000 years ago than in the period 4000 years to present. It is also shown that changes in depth within the Bay of Fundy produce little effect on the tidal amplitudes, while such variations in water depth on Georges Bank account for almost all the change. This calculation of tidal-amplitude changes allows a calibration to be made for the Bay of Fundy of sea-level curves that were obtained using higher high water indicators.

Session 3E: Lithospheric Stress II

Wednesday 0900 – 1240

The Miramichi earthquake sequence of 1982–1984 and its relation to regional crustal stresses in New Brunswick

John Adams and R.J. Wetmiller

Analyses of the four principal 1982 Miramichi earthquakes (m_b 5.7, 5.1, 5.4 and 5.0) and subsequent smaller aftershocks indicate thrust faulting with rupture up-dip on conjugate west- and east-dipping planes. Composite P -nodal solutions from the smaller aftershocks suggest that both planes steepen from 7 km up toward the surface. All aftershocks appear to have occurred within a homogeneous granite pluton. An aftershock survey in July 1983 showed most activity has remained in the V-shaped volume defined in 1982; however a new zone of activity 5 km to the northwest was also located, and the region of aftershocks may have spread out with time.

The m_b 5.7 main shock produced an average dislocation of 25–35 cm. The field studies in 1983 were designed to find surface and near-surface evidence for the west-dipping plane(s). Till cover was scraped off 100 m \times 30 m of bedrock around a small N-striking thrust found in 1982: it proved to represent the earthquake-triggered release of near-surface stresses rather than primary faulting. A pop-up that occurred two weeks after the till was removed provided further evidence of E-W compression. These features confirm the near-horizontal E-W compression shown by “ P ” axes from the Miramichi composite solutions (average azimuth 265° with a mean plunge of only 9°), from an independent earthquake at Trousers Lake in June 1982 (300°/02°), and agree with stress measurements in a 1000-m deep mine 75 km to the northeast (55 MPa ESE, 37 MPa NNE). Direct stress measurements and a further clean-off are intended for 1984.

It is not yet known from aftershock distribution if the ruptures occurred on single curved planes or on shallow-dipping principal faults that splay upward into more steeply dipping faults. If they occurred on a curved fault plane, there are important geometrical implications for stress changes that might explain some of the unusual features of the earthquake sequence.

Stress-drops of aftershocks of the Miramichi earthquake recorded in July 1983

E. Cranswick

Recent work has demonstrated that the site response of a seismograph station has an effect on the high-frequency content of the recorded seismogram that is comparable to the effect of the instrument response of the seismograph itself. In an attempt to obtain seismic wave-forms that had the greatest fidelity to their original source shape, aftershocks of the 9 January 1982 Miramichi Earthquake (magnitude 5.7 m_b) were recorded at seven exposed glaciated crystalline basement sites in the aftershock zone during a field program conducted jointly by the EPB, Ottawa and the USGS, Menlo Park in July 1983. The GEOS digital seismographs used in this study recorded three components of ground velocity at 400 sps per component at relatively high gain (greater than 42 dB) that had been anti-alias filtered at 100 Hz. A very pronounced high-frequency resonance that was commonly observed in the aftershock records, and which is known not to be caused by instrument malfunction, complicates the spectral shapes of this data set.

Preliminary analysis of the 29 events that were recorded at three or more stations, and which have an estimated magnitude range of 0.0 to 2.0 mbLG yields moments up to 10^{19} dyne-cm and stress-drops that are generally a fraction of a bar. The spectra of the tangential component of S -phases have corner frequencies as high as 50 Hz, but most of the corner frequencies range between 12.5 and 25 Hz. The displacement wave-forms are usually simple though some are two-sided pulses rather than the single-sided pulse expected from simple slip on a fault, and peak amplitudes are on the order of 0.01 to 1.0 mm.

These stress-drops are much lower than those calculated for the main shock and larger aftershocks of the Miramichi earthquake sequence, and taken at face value, this difference would indicate that stress-drop decreases with moment in this region over this magnitude range.

Recent and historic seismicity of southeastern Maine

John E. Foley, John E. Ebel and Alan L. Kafka

The occurrence of 5 felt earthquakes (all $M_c > 3.0$) since August 1983 in eastern Maine near the New Brunswick border has prompted a re-examination of the earthquake activity of that region. A search of the historic seismicity showed frequent earthquakes throughout the 111-year historic record as well as sporadic episodes of stronger seismicity. The largest of the events from this region to date occurred on March 21, 1904. During this event intensity VIII was experienced near the Calais, Maine epicentre and intensity VII at Saint John, N.B., 85 km away. A period of increased seismicity took place in the 1920s when 6 events of intensity III or greater occurred.

The two predominant tectonic features in the area are the Passamaquoddy Bay, which is subsiding at a maximum rate of about 9 mm year⁻¹, and the Oak Bay Fault, which trends NW and is nearly perpendicular to the subsidence axis. The recent 5 events occurred at 4 separate epicentres, all of which were west of Passamaquoddy Bay and south of the Oak Bay Fault. The August 12 ($M_n = 3.6$) event was located 50 km west of the bay while the December 8 ($M_n = 3.2$) event was located 35 km more to the east. The January 14 earthquakes ($M_n = 3.4$ and 3.6) had origin times less than a minute apart and were located 5 km east of the December event. The latest and largest

event was on January 19 ($M_n = 3.8$) and had an epicentre 20 km SW of the January 14 events. Although poorly constrained, a fault plane solution for this last event indicates a thrust mechanism striking WNW. The ground acceleration of this earthquake did not trigger two accelerometers set at 0.01 g, each of which was located less than 10 km from the epicentre.

The recent seismicity near the Passamaquoddy Bay was not unexpected because there is a statistical preference for larger New England events to occur in regions of such coastal irregularities as Passamaquoddy, Penobscot and Casco Bays, Maine; and Cape Ann, Massachusetts. The cause of this pattern is not presently understood. The relation of the seismicity with the local tectonic features is also unclear.

Grenville structure and the Central Adirondack seismic zone including the October 7, 1983 main shock-aftershock sequence

L. Seeber, N. Barstow, E. Cranswick, J.G. Armbruster, G. Suarez, K. Coles and C. Aviles

Seismic zones can be recognized in the Adirondacks from ~ 10 years of epicentral data produced by a regional network. Two arcuate E-NE epicentral belts are correlated with structural trends of Grenville age. One is near the southeast limit of the Adirondack Lowlands and another farther south is adjacent to the root zone of the Wakely Mountain nappe. Individual earthquakes in these belts are found, however, to rupture NNW striking faults with reverse slip consistent with ENE subhorizontal P -axes. These faults cannot be related to any known Grenville structural trend. Thus, the control of the seismicity by the Grenville structure is not by simple reactivation of weaknesses directly associated with this structure, but must be indirect, possibly through the control that structure has on the spatial (depth) distribution, of particular rock types.

The aftershock sequence of the October 7, 1983 Goodnow earthquake in the central Adirondacks is well constrained by data from a temporary network and conforms with the pattern of earthquake faulting found in the Adirondacks. The time-space distribution of 96 aftershocks delineate a circular zone dipping $\sim 60^\circ$ with a diameter of ~ 1.5 km, extending from a depth of ~ 7 to ~ 8.5 km. If this small aftershock zone is an upper-limit of the size of the main rupture, a relatively high stress-drop is obtained for the main rupture. Both the fault-plane solution from the main shock and the composite solution for most of the aftershocks indicate reverse faulting on a N $10 - 20^\circ$ W plane dipping $60 - 70^\circ$ west. On the tenth day of the aftershock sequence an apparently conjugate fault became active and the activity migrated up and west from the main aftershock plane. This shallow-dipping "conjugate" fault is subparallel to and displaced by only a few kilometres from a 20-km downdip extrapolation of the Blue Mountain Lake fault active during swarms in 1971-1973. The Goodnow and Blue Mountain Lake faults, if extrapolated beyond the currently active segments, delimit a wedge-shaped block that is being uplifted by the fault movement. The high topography that characterizes this block may be related to this motion. The 40-km long NNW Catlin Lake lineament is subparallel to the inferred Goodnow rupture zone and close to the surface intersection of the planar extrapolation of this fault. The rapidly growing constraints on active faulting from seismicity and on Grenville structure from surface mapping are expected to improve our understanding of the complex interaction between Precambrian structure and the current state of stress in generating seismicity in the Adirondacks.

A large intraplate stress-strain event from seismicity changes associated with the 1886 South Carolina earthquake

L. Seeber and J.G. Armbruster

Seismicity before and after 1886 in the southeastern United States was re-examined by a search of newspapers published from 1830 to 1890. This search consists of two phases: a systematic search where all issues of selected newspapers are scanned; and a specific search where all pertinent newspapers are searched for maximizing information on each earthquake discovered. By this approach we optimize uniformity and completeness of coverage at manageable levels of effort. About 40,000 newspaper issues from South Carolina, North Carolina, Georgia, and Tennessee were scanned for the period 1830 to 1890.

Results indicate that previously available earthquake data were not only poorly constrained and incomplete, but also systematically biased. We find that the 1886 main shock is followed by a 3-year burst of seismicity consisting of ~ 500 recognized events, with a $(\text{time})^{-1}$ decay, typical of an aftershock sequence. Unlike previous compilations that locate all the aftershocks at the same epicentre near Charleston, S.C., we locate this sequence over a wide area across the Coastal Plain and part of the Piedmont, similar to the currently observed South Carolina-Georgia seismic zone. For 50 years prior to 1886, seismicity is very low in the 1886-90 aftershock zone while the several tens of events observed are located in the surrounding area. The space-time pattern of seismicity associated with the 1886 earthquake resembles in character and dimensions patterns typically associated with major plate boundary earthquakes. It indicates an abrupt widespread change in stress suggestive of a similarly widespread strain event. This event may or may not be seismic and coincide with the 1886 main shock. From these and other data we suggest back-slip on the Appalachian master detachment and splay thrusts as a possible cause of the 1886 event, in particular, and of Appalachian intraplate neotectonics, in general.

Historical seismicity, 1983 OBS Experiment and seismic hazard along the southeastern Canadian margin

John Adams, J. Reid and P.W. Basham

The eastern offshore has been the locus of continuing seismic activity – although with the exception of the Ms 7.2 "Grand Banks" earthquake in 1929 these earthquakes have been largely unnoticed. Magnitude 5 earthquakes occurred in 1951, 1954 (2), and 1975, but were barely felt on land. Reports from Sable Island (1927) and southern Newfoundland (1864) may refer to similar offshore events. Monitoring of the offshore is now complete to $ML > 3.5$; in 1983 four earthquakes were located.

A thorough analysis of available instrumental records relocated most earthquakes in a restricted zone 100 km E-W by 30 km N-S near the mouth of the Laurentian Channel. Dewey and Gordon's 1983 relocation of the 1929 earthquake places it at the east end of the zone; the 1950s M5 earthquakes lie to the east of centre, and the 1975 earthquake lies at the western end. Recent small earthquakes tend to lie towards the ends rather than the centre. This suggests that they may be belated aftershocks releasing stresses concentrated at the ends of an E-W fault ruptured in 1929.

A joint EPB/AGC ocean bottom seismicity experiment in June and July 1983 recorded a very low level of microseismic activity, which in view of the four earthquakes in 1983 may suggest episodic activity. The one confirmed earthquake occurred at the east end of the zone.

While contemporary seismicity suggests that high-hazard regions offshore are restricted, an alternative speculative source model that assumes that large earthquakes are equally likely at any location along the margin produces 4-fold differences in probabilistic seismic ground motion. Such differences are of considerable significance to offshore developments and point out the need for a better understanding of all seismicity off Eastern Canada.

Post-glacial rebound and the focal mechanisms of Eastern Canadian earthquakes

Garry Quinlan

A detailed numerical model of post-glacial rebound for Eastern Canada has been constructed and is able to account for observed uplift patterns as recorded in the relative sea-level record. These uplift patterns show regional trends, and so the same model can be used to interpolate between data sites and to estimate the uplift history at any arbitrary site within the study area.

By treating the lithosphere as a thin elastic plate, spatial variations in the uplift pattern can be translated into estimates of lithospheric stress. The stress so calculated is treated as a perturbation to an ambient stress field having its origin in other processes. Post-glacial rebound is shown to be capable of triggering earthquakes in pre-stressed regions but rarely capable of dictating the focal mechanisms of these earthquakes.

Tilt observations from three inland stations in Western Canada

P. Rouleau, J.S. Rogers, F.W. Jones, K. Hutchence and L.W. Vigrass

Tilt measurements provide information on the physical properties of earth materials that are complementary to that obtained from seismological and other geophysical methods. Pairs of relatively inexpensive short baselength mercury level tiltmeters installed on standard Energy, Mines and Resources seismic piers at Regina, SASK, Leduc, ALTA and Penticton, B.C. have recorded signals of various lengths and qualities. Analysis in the time domain shows that meteorological noise more significantly perturbs the secular stability of the tilt signal for piers coupled to unconsolidated porous media than for those coupled to consolidated material. This perturbation is not necessarily unpredictable. Analysis in the frequency domain shows that noise power varies approximately as the inverse of the squared frequency and that signal-to-noise ratios of 30 dB can be obtained in the semidiurnal band with this type of instrument and installation. Tilt observations at the principal semidiurnal frequency M_2 agree, within experimental uncertainties, with the predictions of linear elastic theory.

Tidal tilt observations around the Bay of Fundy and Gulf of Maine: Implications for crustal structure and ocean tides

P. Rouleau

Measurement of the loading effects produced by ocean tides can yield information about the elastic constants of the crust and upper mantle provided that the distribution of the loading function is well known. Deflection of the gravity vector has been observed with a pair of ANAC tiltmeters installed in a shallow vault at Shelburne, N.S. Results from this station complement a network of tilt sites northeast and southwest of the Bay of Fundy and Gulf of Maine area. Tidal analysis shows that for the principal semidiurnal constituent M_2 the west component of the observed deflection at Shelburne differs by 12% from theory. The discrepancy increases towards the west

and suggests the influence of lateral heterogeneities beneath the Gulf of Maine. Possible causes for the observed trend are examined in terms of both local and regional features. Also, differences between the loading function used in the theory and that given by the Schwiderski M_2 tide model are examined in light of the tilt observations.

Analysis of tidal tilt and gravity measurements at the Fredericton earth tides station

Spiros Pagiatakis and Peter Vanicek

Eight months of uninterrupted tilt data have been recorded from two Verbaandert-Melchior quartz horizontal pendulums and five months of uninterrupted gravity data have been obtained from a LaCoste-Romberg G gravimeter. The instruments are operating at the UNB Earth Tides Station located in the vicinity of Fredericton, about 90 km north from the shore of the Bay of Fundy and 170 km west from the shore of the Gulf of St Lawrence. The records show a strong influence of ocean tide loading. In addition, since the station is a near-surface installation, both the tilt and gravity data are significantly affected by atmospheric pressure and thermal variation.

Simultaneous records of atmospheric pressure, bedrock, instrumental chamber and surface temperatures are analysed and the response of tilt and gravity data to these atmospheric variations is studied. The performance of the UNB Earth Tides Station is evaluated from the record analyses on the S_1 , S_3 , S_4 and M_4 frequencies.

Tidal tilt in the Charlevoix seismic zone

J.A. Peters

Temporal anomalies in the earth tidal amplitudes and phases measured by tiltmeters is expected, in a similar way to v_p/v_s seismic velocity anomalies, to indicate parallel time changes in the regional elastic parameter distribution.

An array of three borehole tiltmeters has been established in the Charlevoix seismic region of Québec. Two of the tiltmeters (in boreholes 1 and 2, 80 m apart) are operating at 47-m depth and the third, more recent, installation is operating at a depth of 110 m. Tidal analysis results from two years of simultaneous measurements in boreholes 1 and 2 are presented for the main diurnal (O_1) and semi-diurnal (M_2) constituents. Based on 2-monthly overlapping harmonic analyses, the absolute size of the amplitude variations is shown to be in the range of 3–5 nrad for most constituents. This represents a range of 5–6% for M_2 and 30–40% for O_1 . The pattern of variations is very similar between boreholes, indicating that the effects are probably regional. An identical analysis of the tide gauge data from the nearby St Lawrence River shows a good correlation with the tilt results. Since approximately 70% of the tilt signal is caused by loading from the marine tide in the river, most of the measured variations are due to the loading. It is expected that correction of the tilt results for the effect of the non-stationary marine tide input will reduce the M_2 baseline variability to the 2% level. This is consistent with the M_2 baseline established elsewhere in an aseismic zone. Thus the potential exists to detect short- and long-term anomalies in the earth response at tidal frequencies, particularly M_2 , where the anomaly exceeds 2–4%.

Eliminating the interpolation associated with the semi-Lagrangian scheme*Harold Ritchie*

In the original semi-Lagrangian method, in order to predict a field value at grid point (X_i, Y_j) it is necessary to calculate the trajectory over one time step for the fluid element that arrives at (X_i, Y_j) . One then moves along this trajectory in order to extract the field value at an upstream location, which generally lies between the grid points, and hence requires the use of interpolation formulae.

This trajectory can be represented as a vector. In the new scheme, the trajectory vector is considered to be the sum of two other vectors – a first vector joining (X_i, Y_j) to the grid point (X_u, Y_u) nearest the upstream location, and a second vector joining (X_u, Y_u) to the upstream location. The advection along the first vector is done via a Lagrangian technique that displaces the field from one grid point to another and, therefore, does not require interpolation. The advection along the second vector is accounted for by an Eulerian approach with the advecting winds modified in such a way that the Courant number is always less than one, thus retaining the attractive stability properties of the original semi-Lagrangian method.

There are several reasons why it is desirable to eliminate the interpolation in the semi-Lagrangian method. Interpolation leads to smoothing and is also the most costly operation associated with the original technique. Furthermore, its elimination produces a scheme that is more readily adaptable to a spectral model.

Here the non-interpolating scheme is applied to a model of the shallow water equations and its performance is assessed by comparing the results with those produced by one model that uses the original semi-Lagrangian technique and another model that uses a conventional fourth-order approach.

The representation of the boundary layer in atmospheric circulation models: A choice?*Yves Delage*

Modellers of atmospheric circulation numerical models used for weather forecasting or climate studies must incorporate an adequate treatment of the exchange of momentum, heat and moisture at the earth's surface. With the current available formulations of these processes, they are compelled to put several levels in the first kilometre above the surface in their models. While this may be a desirable practice, since it allows the modelling of boundary-layer processes such as the low-level jet or low-level clouds, it has not yet been demonstrated that the higher resolution near the surface is in itself beneficial to the present-day circulation models or, at least, is cost effective. In order to give modellers a choice of the vertical resolution they would like to use or test in their models, schemes for surface fluxes and near-surface temperatures were developed with the interesting property of being applicable to models with virtually any vertical resolution. Verification tests of these schemes are shown using the Wangara data. Such schemes that allow a full representation of the diurnal cycle have been successfully used in the Canadian operational forecast model for more than five years. In this model the lowest wind level is around 500 m and the lowest temperature level around 250 m above the surface.

Impact of turbulent energy modelling in an NWP model

Robert Benoit and Jean Coté

The coupling of the atmospheric boundary-layer model of Mailhot and Benoit (1982) with a three-dimensional primitive equations numerical weather prediction model has been completed. Details on the coupling strategy were presented at last year's Congress. The distinctive feature of this scheme is the introduction of time-dependent rate equations for turbulent energy and length scale; the vertical resolution used is high, by NWP standards, with 10 levels below 700 mb. The emphasis is put here on three-dimensional results obtained with the full atmospheric model.

Boundary-layer fields will be shown together with their impact on short-range forecasts prepared with the RPN finite-element model.

A spectral analysis of error in the CMC forecast system

G.J. Boer

The operational error characteristics of the CMC forecast system for a winter month and summer month is studied. An analysis is carried out in terms of the scales of atmospheric motion via a spectral decomposition of the error. The separation of the error into that due to initial errors in the data and that due to model imperfections is also obtained.

The growth of error with time is studied in terms of the mechanisms of error production and redistribution among the scales. The predictability of the flow resides in the region of low wavenumbers. The behaviour of the error and its components differs markedly with season at these scales.

Session 4AA: Climate Change and Variation Thursday 1050 – 1230

Some questions associated with assessing carbon dioxide buildup in the oceans

E.P. Jones

The buildup of CO₂ in the atmosphere has been very well documented. One of the most important questions regarding predictions of future atmospheric CO₂ concentrations is how much fossil fuel CO₂ has entered the oceans from the atmosphere and how much can be expected to enter in the future. Because of the large carbon reservoir in the oceans, changes in oceanic carbon associated with the atmospheric buildup are hard to detect. Several recent papers that attempt to assess these changes rely on a specific model to account for carbon contributed from the decay of organic matter. Since this contribution is generally much larger than that from fossil fuel CO₂, the assessment of the CO₂ buildup will depend strongly on the model for organic decay. Data from Baffin Bay that show some difficulties with this model are presented, and a modified version of the model that may help overcome them is described.

Computer experiments on the climate sensitivity to a doubling of CO₂ with an atmospheric general circulation model coupled to a simple mixed-layer ocean model

Warren M. Washington

A simple slab ocean of 50-m depth that allows for seasonal ocean heat storage but no ocean heat transport is coupled to a global spectral general circulation model. Globally averaged, annual mean surface warming due to a doubling of CO₂ is 4.2°C. This is greater than that computed in a

previous study with the same atmospheric model coupled to an energy balance or "swamp" ocean with annual mean solar forcing. This result differs from previous studies performed by other groups and can be partly accounted for by the fact that different ocean parameterizations produce significantly different climate responses. Zonal mean air temperature differences indicate stratospheric cooling and tropospheric warming as seen in other CO₂ modelling studies. The greatest increases of surface air temperature in the 2 × CO₂ case compared to the control occur near the sea-ice margins. Retreat of sea ice in the 2 × CO₂ case results in ice-free areas of ocean maintaining the heat flux to the overlying air. Warmer temperatures then occur in areas that are much colder in the control case because of the insulating effect of the sea ice, especially in winter. Increases of zonal mean precipitation are evident at all latitudes owing to increases of available moisture evaporated from the warmer oceans. Seasonal means of soil moisture show decreases in tropical and subtropical continental areas and increases at high latitudes, but at mid-latitudes the change depends on the season. An analysis of the statistical significance of the geographical distribution of seasonal means of surface air temperature and soil moisture differences is given for the 2 × CO₂ case compared with the control. Comparisons with other modelling studies using similar models will also be shown.

The effect of ozone photochemistry on atmospheric and surface temperature changes due to increased CO₂ and volcanic aerosols in the atmosphere

R.K.R. Vupputuri

Increased atmospheric CO₂ and volcanic aerosols can affect indirectly the ozone by altering the atmospheric temperature structure and the photochemical coupling. The radiative effects that result from the local ozone perturbations would in turn modify the initial temperature changes due to the increased CO₂ and volcanic aerosols. In this paper a coupled 1-D radiative-convective and photochemical diffusion model is used to study the influence of ozone photochemistry on changes in the vertical temperature structure and surface climate resulting from the doubling of atmospheric CO₂ and from the El Chichón volcanic eruption. It is found that when the CO₂ is doubled the total ozone column increased by about 5% (with maximum enhancement of 20% in the ozone mixing ratio between 40 and 45 km), and the resulting growth in the solar heating by the enhanced ozone contributed to the smaller temperature decrease in the stratosphere (1–3 K recovery in the upper stratosphere). The effect of ozone-temperature coupling on the surface temperature change is negligibly small in comparison to the direct heating due to double CO₂, although it contributed to slight additional heating.

It will also be shown that the interaction of the ozone photochemistry with the stratospheric aerosol cloud resulting from the El Chichón eruption would lead to a 2% depletion in the total ozone column, which in turn has the effect of enhancing the cooling at the surface while causing additional warming below the cloud centre in the lower stratosphere.

Positive and negative El Niños – Modelling the atmospheric response

G.J. Boer

The El Niño of 1982/83 has been identified with an array of meteorological phenomena some of which are very remote from the El Niño region. The modelling of events such as this using the CCC GCM is reviewed. The results of 5 separate experimental integrations is analysed in an attempt to infer the statistical reliability of extratropical responses to the El Niño.

The case of a "negative El Niño" or colder than normal sea surface temperatures in the equatorial Pacific provides a contrast to the more usual case. Both the local response and possible extratropical effects are examined in these simulations.

**Session 4B: Coastal Oceanography I -
Circulation Driven by Winds and Tides**

Thursday 0900 - 1230

Dynamical balances of the mean barotropic circulation of the Gulf of Maine

D.A. Greenberg, J.W. Loder, P.C. Smith and D.G. Wright

Numerical models have been used to investigate the mean currents in the Gulf of Maine. The significant residual circulation can be attributed to (a) the divergence in tidal momentum flux resulting from interactions of the tide and topography, (b) sea-surface gradients along the cross-shelf boundaries and (c) steady wind forcing. The dynamical balances indicate regions where the residual currents are locally driven and regions where they are balanced by pressure gradients resulting from large-scale continuity constraints.

Gulf of Maine response to wind stress

Daniel G. Wright, David A. Greenberg, John W. Loder and Peter C. Smith

The response of the Gulf of Maine to surface stress is studied using a 2-D numerical model. The examination of the influence of conditions at cross-shelf boundaries reveals that results are more sensitive to conditions specified across the Scotian Shelf than to those across the New England Shelf. Further, consideration of an infinite shelf model with straight parallel isobaths indicates that set-up across the Scotian Shelf could dominate the response of the Gulf to wind stress. However, observed sea-level gains at Halifax (Sandstrom, 1980, *J. Geophys. Res.* **85**:461) are much less than those predicted by the infinite shelf model and this is explained in terms of Csanady's work on wind forcing over a finite extent of the shelf (Csanady, 1978, *J. Phys. Oceanogr.* **8**:47). Using Csanady's results and the observed gains at Halifax, an appropriate boundary condition is determined.

Model results for currents and set-up in the Gulf associated with steady, spatially uniform wind stress are presented. Results are discussed in terms of previous theoretical investigations and compared with observed sea-level response at several coastal stations in the Gulf.

Wind-driven circulation on the Northwest Shelf of Australia

Ian Webster

This paper presents a theoretical study of the wind-driven circulation on the Northwest Shelf of Australia. Because the shelf is wide and its tidal currents are strong, bottom frictional effects are of major significance. A numerical model is developed to simulate the depth-averaged wind-driven circulation along the length of the shelf. Using the model, the roles of bottom friction and of the temporal and spatial forms of the wind stress driving the circulation are investigated. The results of the model can readily be interpreted in terms of the generation of frictional continental shelf waves. The apparently anomalous result that an increase in bottom friction may cause an

increase in the model response can be understood using this interpretation. The friction parameter determines the magnitude of the shelf response through its influence on the form and decay rates of the shelf waves generated by the wind stress. These in turn determine the model's sensitivity to the specifications of boundary conditions and wind forcing. Thus, the choice of friction parameter has major implications for the application of circulation models to wide shelves such as the Northwest Shelf.

Wind-driven circulation models of Lake Melville

T.E. Keliher and A.S. Bhogal

Lake Melville, Labrador, is the largest sub-Arctic fjord in North America. It is a very important waterway to the inland Labrador communities of Goose Bay and Northwest River and is located in an area where industrial, timber and mineral developments are taking place. A number of numerical models of wind-driven circulation have been adapted to study the circulation features of Lake Melville. Two of these models are a steady-state homogeneous model and a time-dependent homogeneous one, both driven by a constant wind. The results indicate that the complex bottom topography of the lake forces a complicated circulation pattern that is relatively unaffected by the value of the bottom stress coefficient. For a constant wind of 7 m s^{-1} , the vertically averaged horizontal velocity is about 1 cm s^{-1} suggesting a surface velocity of $5\text{--}10 \text{ cm s}^{-1}$. These values and the general circulation features are consistent with observations.

Tidally-induced residual upwelling and downwelling on the sides of Georges Bank

Kim-Tai Tee

It has been found that the rectification of the strong tidal current on Georges Bank partially drives the residual clockwise circulation around the bank. Steady upwelling/downwelling on the bank can be induced by the divergence/convergence of these tidally rectified currents in horizontal planes. By using a weakly non-linear depth-dependent tidal model, we have computed the residual vertical motion on the sides of Georges Bank. On the northern section of the Bank, downwelling occurs near its shallow and deep ends, and upwelling at intermediate locations. On the southern section, downwelling also occurs near the deep end, but upwelling extends over almost all of its shallow portion. The sensitivity of these vertical motions to different vertical eddy viscosity coefficients and stratifications in the water column will be discussed.

Tidal rectification off southwest Nova Scotia

Peter C. Smith

Long-term measurements off southwest Nova Scotia reveal the following features of the mean circulation:

- a) a westward longshore current ($4\text{--}20 \text{ cm s}^{-1}$) near the coast,
- b) an anticyclonic gyre around Browns Bank ($5\text{--}15 \text{ cm s}^{-1}$).

The investigation of coherent modulations (monthly and fortnightly) in the semidiurnal tidal streams and low-frequency currents reveals that tidal rectification supports both the coastal and gyral circulations. However, the magnitudes of the rectified currents, reaching 40 cm s^{-1} in the gyre and 50 cm s^{-1} near-shore, generally exceed the observed velocities. To resolve this discrepancy, the vertical and horizontal structure of the tidal residual circulation is compared to the results of a 3-D non-linear numerical model. In addition, some possible baroclinic effects associated with temporal variations in tidal mixing are discussed.

Current-meter measurements near Sable Island: Their features and dynamics in conjunction with local boundary conditions

Bassem M. Eid and Simon G.P. Skey

Recently, the increasing activities associated with the exploratory drilling programs offshore Nova Scotia have led to the acquisition of a large amount of oceanographic and meteorological data, especially near Sable Island. In situ current-meter measurements were carried out during 1983-1984 at several locations on Sable Island Bank. At each site, at least two current meters (e.g. one near the surface and one near the bottom) were moored. In relatively deeper waters (e.g. greater than 20 m), an additional current meter was installed near mid-depth. Current speed as well as temperature and salinity were continuously recorded for extended mooring periods ranging from one to three months. These measurements were complemented by complete records of the meteorological (e.g. wind speed and direction, and air temperature) and sea-state conditions at or near the mooring sites.

The spatial and temporal variability resulting from wind and tidal forces as well as local boundary conditions was evident in all measurements made on Sable Island Bank. The extreme variability in oceanographic measurements was studied in relation to the driving forces. The dynamics of the mean circulation around Sable Island were examined and their relation to the large-scale circulation on the Scotian Shelf were reviewed.

Evaluation of the direct influence of the freshwater run-off on the coastal zone of the northern part of the Gulf of St Lawrence

Denis Lefavre

Two surveys, one in July 1980 and one in May 1981, were carried out to collect temperature and salinity data over a dense array of stations along the northern coast of the Gulf of St Lawrence. Presentation of the data set includes temperature and salinity data in horizontal cuts at a constant depth, along with vertical sections from the coast. A water mass analysis using *T-S* diagrams will be given along with an evaluation of the horizontal and vertical density contrasts. These contrast evaluations are introduced with seasonal wind data and the water levels along the coast as external parameters in a linear diagnostic model of circulation. This model proposed by Csanady (1976, *J. Geophys. Res.*) allows the evaluation of the variation of the circulation with depth. It also gives the relative influence of every external parameter on the circulation.

The Beaufort Current on the Continental Slope

Paul Greisman

In 1981, current-meter moorings were deployed in the Canadian and U.S. sectors of the Beaufort Sea in a joint experiment conducted by IOS and the U.S. Coast Guard. Three moorings on the Continental Slope east of Prudhoe Bay at 146°W yielded five current data sets. These data show currents of up to 0.5 m s⁻¹ to the east and reversals of up to 0.25 m s⁻¹. Both the continental slope data and the data from instruments deployed on the Mackenzie Shelf show mean eastward flows at depths up to 250 m.

The measured vertical current shears are in agreement with the geostrophic shears computed from CTD measurements; however, a relatively large eastward barotropic component of flow is

superimposed. Westward flows appear to be confined to the upper 30 m of the water column. An hypothesis explaining the mean eastward flows in the presence of westward ice drift is that the longshore flow is driven by the longshore gradient of the longshore wind stress – the dynamics of a coastal undercurrent. Coherences between the wind stress gradients computed from the atmospheric pressure field and the currents are examined.

Session 4C: Boundary-Layer ProcessesThursday 0900 – 1230

Boundary-layer flow over a low hill – The Askervein Experiments*Peter Taylor, Hans Teunissen, Bob Mickle and Jim Salmon*

Askervein is a low hill (~125 m) on the west coast of South Uist in the Outer Hebrides (Scotland). As a part of the International Energy Agency Programme of R&D on Wind Energy Conversion Systems (WECS) a detailed study has been made of airflow and turbulence at this site, which was selected as being typical of a good potential wind turbine location. Canada is the "operating agent" for the project and is coordinating the study. Other participants are groups from Denmark, Germany, New Zealand and the United Kingdom.

Two intensive field experiments form the core of the project, but numerical and wind-tunnel modelling activities also play a major part since the object of the exercise is to determine how well these approaches can predict the detailed local variations of mean flow and turbulence caused by the topography.

The first field experiment, ASKERVEIN '82, was conducted during September/October 1982. This provided excellent and detailed data on the spatial variations in mean flow above the hill, as well as some preliminary turbulence data. ASKERVEIN '83 was conducted during September and October 1983 and concentrated on the turbulence measurements. Two 50-m towers provided upstream and hilltop data while additional 30-, 17- and 10-m towers provided details of spatial variations on the upstream and lee faces of the hill. Approximately fifty towers were deployed.

Data from both experiments will be presented and discussed in the light of current theories.

MS3DJH/3R – The incorporation of variable surface roughness in a simple model of boundary-layer flow over low hills, with application to a barchan sand dune*John L. Walmsley, Peter A. Taylor, Alan D. Howard and Tim Keith*

MS3DJH/3R is an offspring of the 3-D model of neutrally stratified boundary-layer flow over low hills described by Taylor (1983) at the 17th CMOS Annual Congress. The incorporation of variable surface roughness allows the model to be more widely applicable. MS3DJH/3R is compared with results for idealized situations (step changes and sinusoidal variations) from a 2-D finite-difference model. If proper care is taken in the choice of scaling the roughness lengths, quite good agreement is achieved.

An application to a barchan sand dune is discussed. In this case the effective roughness length is a function of wind speed, and an iterative procedure is used to obtain the results.

A control-volume-based, finite-difference technique applied to the planetary boundary layer over homogeneous surfaces

D. Rooney and G.D. Stubbley

A knowledge of the vertical structure of the mean wind and turbulent intensities in the planetary boundary layer is critical in air pollution studies. Model equations can predict the boundary-layer structure in terms of prescribed synoptic and surface conditions. These equations based on the standard kinetic energy-dissipation Reynolds stress model are sufficiently complex that a numerical solution technique must be used to obtain a solution.

The control-volume-based, finite-difference technique is an ideal one for solving the boundary-layer equations. The advantages of the technique are that the approximations are determined by the physics of the problem and that local and global conservation can be maintained.

It will be shown that the use of the conservative control volume technique gives improved accuracy for a given number of grid points when compared to the use of non-conservative techniques.

Predictions of the steady-state profiles of the mean wind and turbulence intensities for baroclinic and barotropic atmospheres of neutral stability will be presented. Extensions to allow for non-neutral stabilities and transient effects will be discussed.

Vertical structure in the nearshore zone

John W. Haines

Theoretical models of bedload and suspended load transport of sediment require various parameters describing the fluid flow. Bedload models depend on near-bed measurements that are difficult or impossible to obtain. Suspended load models often require an accurate vertical resolution of the flow. The difficulty in measuring such variables has led to parameterisations of the flow field based on largely untested models of the vertical velocity structure. The applicability of these flow models in the near-shore zone was the subject of a field experiment in Pointe-Sapin, New Brunswick. Data were collected from a vertical array of (Electro-Magnetic) flowmeters. Results are compared with theoretical models and the data sets collected by Sallenger in the United States and Bowen in Nova Scotia.

Saturation-point analysis of STREX boundary-layer/cloud-layer data

Gordon A. McBean

During the Storm Transfer and Response Experiment (STREX), extensive vertical profiles of thermodynamic parameters were made through the boundary layer and cloud layer. Betts (1982, 1983, *J. Atmos. Sci.*) has shown that the mixing processes can be more clearly examined using the air parcel saturation point. The application of this technique to the STREX data will be described. Because of the complexity of the mid-latitude storm environment, as opposed to the Trade Wind stratocumulus situation that Betts studied, it is not possible to clarify all points. However, it is possible to assess the mixing in the boundary layer and cloud layer and to examine the exchanges with the atmosphere aloft.

The profile structure of wind over sea ice

K. Shirasawa

Wind profiles above a first-year sea-ice sheet were collected over a terrain ranging from bare smooth ice to hummocky ice and were used to compute surface drag coefficients. In near-neutral stability, the drag depended on surface topography. Most of the values of the drag coefficient for bare ice were smaller than its limiting value for a hydrodynamically smooth flow. This theoretical value was calculated using the roughness Reynolds number, defined as $U_* Z_0 / \nu$, where U_* is the friction velocity, Z_0 is the roughness length, and ν is the kinematic viscosity of air. The drag coefficient for snow-covered flat ice varied with the surface snow conditions and was higher than that calculated for bare ice.

Wind profiles above a hummocked surface exhibited the logarithmic shape typical of rough sea ice. At the sail height of nearby ridges the wind speed gradient (slope of the profile) decreased gradually. Values of the friction velocity calculated from wind profiles over a roughened surface compared favourably with those obtained by the eddy correlation method using a sonic anemometer.

Studies on the variability in space and time of boundary-layer fluxes

P.H. Schuepp, P. Alvo, R.L. Désjardins and J.I. MacPherson

The variability of the fluxes of sensible heat and CO_2 recorded from aircraft- and ground-based observation platforms will be examined. An attempt will be made to link it to tentatively identified meteorological and terrain-related factors such as atmospheric stability, changes in wind direction and radiation conditions, and to specify turbulence scales predominantly identified with variability.

Such studies are needed for the interpretation of data obtained in the mapping of large-scale distributions of environmental sources and sinks of such quantities as heat, water vapour and CO_2 .

Eddy correlation measurements of CO_2 flux over the sea near Sable Island

Stuart D. Smith and E. Peter Jones

In a series of measurements of the CO_2 flux over the sea the mean flux was near zero even though the surface water had a substantially higher partial pressure of CO_2 than the air. Hourly variations in wind speed were well correlated with the flux, suggesting that a process such as wave-breaking may drive additional CO_2 into the water as the wind speed increases.

CO_2 exchange on a regional scale

R.L. Désjardins, P. Alvo, J.I. MacPherson and P.H. Schuepp

The flux densities of CO_2 and sensible heat were measured over a distance of 200 km at an altitude of 150 m using aircraft-mounted sensors. Repeated measurements were also obtained over a 40-km strip at altitudes of 75 and 150 m.

The CO_2 concentrations and exchange values will be related to the underlying ground conditions. The variability of the cospectra of the vertical wind with heat and CO_2 will also be examined.

The use of ocean colour data to map surface dynamic features

Jim Gower, Gary Borstad and Dawson Truax

Satellite infrared imagery is widely used in physical oceanography. Ocean colour imagery is now becoming available and should make an additional major contribution. Images from the Coastal Zone Colour Scanner on Nimbus-7 show western boundary currents, eddies and coastal patterns delineated by colour differences. These differences are due to variations in the phytoplankton concentration or suspended or dissolved material, and provide a tracer that is in some cases better than thermal differences, especially where the thermal contrast is small.

The FLI (Fluorescence Line Imager) project, funded by ICS and DFO, is developing an advanced sensor to provide higher spectral resolution and sensitivity for airborne and eventually satellite imagery.

Freshwater-driven eastern boundary current in the Pacific

Mikio Miyake, Gary Borstad and Jim Gower

Since the West Coast of North America closely follows a great circle, the discharged fresh water generates a density current that is circum-basin to the mid-Pacific. The diffusion of this water takes substantially different forms, depending on the stability of the upper ocean mixed layer at different seasons. This can be seen through colour images from space. The narrowness of the stream is such that satellite imagery and continuous underway sampling are required to delineate the structure.

Satellite remote sensing of the spatial and temporal variations of coastal phytoplankton patches

Soon T. Kim

An attempt is made to evaluate current satellite remote-sensing capabilities in studying the spatial and temporal variations of coastal marine phytoplankton patches. Three elements involved in the satellite measurements are discussed: 1) the sensor's spatial (ground) resolution in relation to the length scale of coastal plankton patches, 2) the spectral and radiometric resolutions of the sensor to estimate the chlorophyll concentrations in turbid coastal (Case II) waters, and 3) the frequency (repeat coverage) of the satellite observations in relation to the temporal scales of coastal phytoplankton.

The Thematic Mapper (TM) and Multispectral Scanner (MSS) aboard Landsat 4/5 are capable of resolving 85- and 170-m patches, respectively. The Nimbus-7 Coastal Zone Colour Scanner (CZCS) and the NOAA 7/8 Advanced Very High Resolution Radiometer (AVHRR) may be able to resolve at best 1.5- and 2.0-km patches, respectively.

The physics of separating chlorophyll spectra from the spectra of suspended inorganic sediments in Case II waters is unknown to date. However, a multispectral, stochastic approach defining the chlorophyll observations in a multi-dimensional spectral domain appears to be promising; a TM wavelength-based multispectral algorithm was able to produce chlorophyll estimates

within $\pm 9\%$ of shipboard measurements from the near sea-level spectra obtained in the Mississippi Sound, $\pm 35\%$ from 2.0-km altitude (M2S Multispectral Scanner) data in the New York Bight, and $\pm 50\%$ from 2.4-km altitude (M2S) data in the James River estuary. The results seem to indicate the possibility of an adequate prediction model for a wide range of turbid coastal waters.

Radiometrically, it has been reported by Gordon et al. (1983) that the CZCS water-leaving radiance (L_w) may be calculated within $\pm 21\%$ of ship measurements. Detailed quantitative assessment of the TM and MSS radiometric data quality is scarce for Case II waters, however, several empirical studies have indicated good results for estimating surface chlorophyll concentrations from MSS digital data. Initial TM data obtained in the Mississippi Sound seem to indicate an excellent data quality for delineating water colour structures in turbid coastal waters.

Landsat (TM / MSS) and Nimbus-7 (CZCS) have nominal 16- and 2 to 3 day repeat coverage, respectively, for mid-latitude oceans. NOAA 7/8 (AVHRR) have one-day repeat coverage. Thus the temporal variation of coastal phytoplankton distribution may be resolved at about a 30-day or less time-scale.

Potential capabilities of the Ocean Colour Imager (OCI), a NASA future ocean colour sensor planned for the later 1980s, are also discussed.

Sediment mapping by remote multispectral techniques

B.J. Topliss and C.L. Amos

Remote multispectral scanners respond to changes in water colour caused by variations in the quantity and composition of the material suspended or dissolved in the surface layers of a water mass. Three different sensor platforms have been used on separate occasions to monitor the sediment-dominated upper reaches of the Bay of Fundy. Images from nine channels of a Canada Centre for Remote Sensing (CCRS) multispectral aircraft scanner, 3 bands of the Landsat multispectral sensors and 5 channels of the Nimbus-7 Coastal Zone Colour Scanner (CZCS) have been used to examine simple algorithms for suspended material. The different sensors cover different spatial resolutions for mapping sediment patterns on scales from metres to kilometres. Calibration data were collected either by ship, launch or helicopter depending on the aerial coverage of the remote platform. In situ optical measurements were used to examine the physical interpretation of the algorithms, and the design limitations of the sensors. Factor analysis was used to examine the errors associated with the calibrations. Sediment algorithms were also affected by large quantities of biological material, river discharge and bathymetric effects. Consideration is given to the reasons behind the success of using colour imagery for mapping suspended sediments within the Bay of Fundy and to whether such mapping techniques would be applicable elsewhere.

Analysis of time-lapse radar imagery of the ocean's surface

M.J. Press and H.J. Duffus

Time-lapse pictures of radar imagery have been taken of the Strait of Juan de Fuca south of Victoria, B.C. every 5 min for about 18 months. Approximately 150,000 individual images have been recorded on film. Many interesting features can be identified. These include surface clutter, tidal wave-fronts and internal wave streams. For analysis, selected radar images can be digitized with a 256 pixel by 240 pixel resolution and a 16-level grey scale, using a Tecmar video digitization system.

During the past year selected images have been digitized. Software has been developed to transmit these images from the digitization system to a Honeywell DPS 6/52 mainframe for analysis. A preliminary study involving two-dimensional correlation has shown that there is enough information to identify regions reliably within a single image and to identify these regions in a sequence of images as they evolve with time.

In a typical image there are generally two different length scales. The small wavelength features correspond to the surface clutter that moves with the general tidal flow. Longer wavelength features are the result of deep ocean waves and internal wave streams. These have a significant velocity with respect to the tidal flow. To separate these features, two-dimensional FFTs will be performed, and the different wavelength regions correlated separately. If this proves successful the technique can be applied to a sequence of images to measure the velocities of the different features that are observed. The FFT process would also provide statistics on the nature of the surface clutter itself.

To help identify important features and to isolate unwanted events, such as boats, programs have been developed to display the transmitted images on a Tektronix 4113 graphics terminal. This allows interactive selection of regions to be correlated, expanded or visually enhanced using false colour for closer visual inspection.

The appearance and movement of surface features will ultimately be correlated with a tidal model of the Strait and with local weather and STD measurements.

Winds over ocean surfaces determined from satellite measurements of passive microwave brightness temperatures

I. Rubinstein

Multifrequency measurements of thermal-microwave natural-surface emissions are routinely being collected by the Nimbus-7 satellite Scanning Multichannel Microwave Radiometers (SMMR). These brightness temperature data allow the extraction of ocean surface characteristics and the estimation of variations in the intervening atmospheric water content.

An empirical model has been derived at Ph.D. Associates Inc. that utilizes horizontal and vertical polarized SMMR data (18 and 37 GHz) to derive wind speed near the ocean surface plus atmospheric liquid and water vapour content. A preliminary validation of this linear model with in situ surface observations suggests that the wind speed results are accurate within 15-20%.

These results, plus a comparison with the results of a five-variable theoretical model derived by F. Wentz, will be discussed in the light of the possible operational implementation of near real-time wind speed mapping production.

Atmospheric icing of some wind speed sensors

E.M. Gates and W.C. Thompson

Four commercially available wind speed sensors have been tested in an icing wind tunnel to determine the relative susceptibility of each to atmospheric icing and to determine the influence of ice accumulations upon the operation and accuracy of each. A comparison of the relative susceptibility to icing was carried out using an average collection efficiency. A clear advantage of the large sensors over the smaller ones was found. The operation of each sensor is affected by ice accretion in three specific ways: i) the interference of ice on the support structure with the hub of the rotating assembly, ii) the growth of ice from the support into the volume swept by the rotating

assembly and iii) a change in cup shape. The latter causes a reduction in sensor accuracy; the magnitude of the reduction is approximately proportional to the mass of the accreted ice.

An estimate of an "effective" operating time under expected icing conditions was made. The results of this calculation indicate that the useful operating life is only on the order of hours.

An application of automated Data Collection Platforms on ships

John Elliott and R. Vockeroth

While satellites provide considerable quantities of data from remote areas of the globe, they have not as yet eliminated the requirements for quantitative surface-level observations. To fill some deficiencies in the real-time meteorological data from ocean areas, equipment has been developed and deployed that is capable of automatically reporting weather parameters from buoys or ships. This paper reviews the recent and current use of such systems in the Northwest Atlantic, and elaborates on a new series of automated shipboard data platforms (SDPs), the first of which was installed on a ship in Halifax in December 1983. This type of SDP uses the ARGOS system on the NOAA polar-orbiting satellites to relay its reports and to provide locating parameters. The SDP can be operated as a simple automatic station, or an observer may key in additional parameters to provide a practically complete marine meteorological report.

Acoustic measurements of wind speed, precipitation and near-surface bubbles over a continental shelf

David D. Lemon and David M. Farmer

During the summer of 1982, and again during the winter of 1982-1983, underwater ambient noise measurements were made at two sites on the British Columbia Continental Shelf. The experiments were designed to compare the relationship between ambient noise and wind speed over a continental shelf with similar previous measurements made in the deep ocean. During the summer, ambient noise measurements made in three frequency bands centred at 4.3, 8.0 and 14.5 kHz and simultaneous surface wind observations were consistent with the previously-determined relationship

$$20 \log V = a(\text{NSL}) - b$$

where V is the surface wind speed at 3 m in m s^{-1} , NSL is the observed noise spectrum level in dB re $1 \mu\text{Pa}^2 \text{Hz}^{-1}$ and a and b are frequency-dependent constants. The resulting coefficients are similar to those found previously and allow a fit between ambient noise and wind speed to within $\pm 1.5 \text{ m s}^{-1}$ over the observed range of 0-12 m s^{-1} . Although the data are sparse, a clear acoustic signal associated with precipitation was observed and compared with rainfall measurements made at nearby coastal light stations. Using *Franz's (1959)* theoretically-determined calibration, the results show good agreement with the presence or absence of rain and agreement to within a factor of 2 in the measured quantity.

A second set of ambient noise measurements in bands centred at 4.3, 8.0, 14.5 and 25.0 kHz was obtained in the same area during the following winter, with surface wind speeds in excess of 20 m s^{-1} being encountered. At sufficiently high wind speeds ($> 15 \text{ m s}^{-1}$) noise levels at 14.5 and 25.0 kHz were found to level off and eventually decrease with increasing speed. A simple model has been developed that accounts for the effect through the scattering and absorption by a near-surface bubble layer. The changes in the ambient noise field as a function of frequency and wind speed allow the bubble populations and size distributions to be inferred, which were found to be consistent with previous photographic and bubble trap measurements. These near-surface bubble effects, which must be taken into account in planning wind and precipitation measurements using ambient noise, may also serve as a probe with which to study other effects at the air-sea interface.

Sea-ice and sea-surface wind mapping: Now operational from satellite measurements of passive microwave thermal emissions

Frank W. Thirkettle

Nimbus-7 Satellite measurements of thermal-microwave natural-surface emissions provide global observations every second day, from which near real-time map products are being produced. For the first time, sea-ice maps of contoured ice concentration and ice type and, on a more limited basis, ocean-wind maps of contoured wind speeds derived from these passive microwave data are being operationally produced and disseminated. These same user products are also generated from historic satellite data for uses such as a published ground-truth validation performed for March and October 1979.

This paper will illustrate examples of these maps, which are operationally produced and telecopied out to users within 4 hours of data reception at the Toronto offices of Ph.D. Associates Inc. The flexibility in user-definable mapping areas, projections and scales, and the availability of plotted or digital, telecopied / electronic or couriered information services will be highlighted. The routine incorporation of these services by the Canadian Atmospheric Environment Service's Ice Central for daily sea-ice forecasting will be noted.

The University of Toronto balloon radiometer

J. R. Drummond, D. Turner and A. Ashton

The University of Toronto balloon radiometer is a new balloon-borne instrument designed to make measurements of the concentrations of minor constituents of the stratosphere. It uses limb-scanning and pressure-modulation techniques to increase the useful signal-to-noise ratio of the emission signals from stratospheric species in concentrations of 1 ppb or less.

The instrument is designed to be flexible enough to measure many stratospheric constituents and to measure as many as three of these simultaneously, using the same air volume. It was equipped on its engineering flight to "measure" formaldehyde and carbon monoxide. This flight was also a trial of a double-sided limb scan technique for measuring the orientation of the optical beam relative to the atmospheric horizontal.

The instrument design will be discussed together with some test results from the engineering flight in August 1983. There will also be a discussion of the scientific aspects of the experiment and the possible improvements to the instrument in 1984-85.

Session 4E: Arctic Expeditions, CESAR, LOREX and FRAM: I

Thursday 0900 - 1230

Bathymetry and gravity of the Alpha Ridge

J. R. Weber and D. W. Halliday

In cooperation with the Canadian Hydrographic Service some 1300 individual depth soundings and gravity measurements were established over the Ellesmere Island Continental Shelf and Alpha Ridge to the 116° W meridian. In addition, some 120 line kilometres of echo sounder and

gravity recordings were established along the drift track of the CESAR station. A 100-m contour bathymetric map and a 10-mGal contour free-air gravity anomaly map were compiled which include data collected from Ice Island T-3 between 1969 and 1974. Unlike the Lomonosov Ridge the bottom topography is very complex and rugged. The minimum depth recorded over the Alpha Ridge is 1087 m. The ridge joins the Continental Shelf at a depth of between 1800 and 2000 m. Generally, the free-air anomalies mirror the ridge topography. Over this portion of the Continental Shelf the gravity map shows the same sort of positive elliptical free-air anomalies that have been discovered all along the Canadian and Alaskan Continental Shelf and that are indicative of the transition between continental and oceanic crust.

CESAR cores: Lithostratigraphic correlation and paleoenvironmental interpretation of Alpha Ridge Cretaceous and Late Cenozoic sediments

Peta J. Mudie and Ali E. Aksu

During CESAR, sixteen Benthos piston cores and twelve gravity cores recovered up to 6 m of sediment from the southeastern Alpha Ridge. The cores provide the first information on the lithology and age of sediments covering the northern Alpha Ridge crest and adjacent graben. Initial lithostratigraphic, biostratigraphic and magnetostratigraphic studies show a correlatable sequence of litho-facies that range in age from Late Cretaceous to Recent. The graben and basins on the flanks of the Northern Ridge are filled with about 250 m of unconsolidated sediment of which the top 6 m is a continuous section of Lower Pliocene (ca 5 Ma) to Recent mud. Most facies of this mud can be correlated with USGS cores from the Southern Ridge, western Alpha Ridge and Chukchi Rise. The surficial mud consists of alternating siliclastic and carbonate-rich sediments that represent glacio-marine deposits (debris from icebergs, sea ice and rivers flowing over ice) and hemipelagic material. Cretaceous biosiliceous sediment of Late Campanian to Maastrichtian age was sampled on the edge of a fault block on the north side of the Alpha Ridge graben. The siliceous sediment contains a complex sequence of laminated diatom ooze that was probably deposited in a shallow marine environment isolated from continental terrigenous sources. Ferromanganese micronodules and low organic content suggest that the sedimentary environment was strongly oxidizing. Thin mud stringers with a high aluminum content may indicate local volcanic activity but there is no evidence of diagenetic alteration of the biogenic Opal-A, which would indicate high temperatures or deep burial. The biosiliceous sediment is overlain by unfossiliferous sand and clay that may be a volcanic ash deposit. There appears to be a major lithostratigraphic unconformity between this sediment and a thin surface layer of Late Tertiary mud.

Geothermal measurements on the Alpha Ridge during CESAR

Alan Judge, Vic Allen and Alan Taylor

Ten heat flow stations were occupied on the Alpha Ridge during the CESAR project. A 3-m oceanographic probe recorded precise sediment temperatures at 7 thermistor positions along its length, and enabled the calculation of an *in situ* thermal conductivity through the analysis of a short heat pulse generated along the length of the probe. In addition, measurements of physical properties were made on core retrieved in the Marine Geology program. About 750 individual thermal conductivity measurements were made at 10-cm intervals on these cores. Approximate values of the DC electrical resistivity and the volumetric water content were obtained for 14 cores using the Time Domain Reflectometry method.

Thermal conductivities are higher in the upper metre of each core, decreasing somewhat deeper in the sediments, and are in qualitative agreement with core descriptions from the geology program. Ninety per cent of the conductivities lie between 1.2 and 1.8 W mK⁻¹; these values are half again or more higher than those typical of deep ocean sediments. Only core CR-06 in the lower few metres had conductivities of 0.8 W mK⁻¹, which are more typical deep ocean values.

Volumetric water contents are generally around 50%, somewhat less than that typical of deep ocean sediments. Both results are consistent with the hard, compacted sediments found on the Alpha Ridge.

Using these thermal conductivity determinations and the temperature gradient, estimates of the terrestrial heat flow have been calculated. These measured heat flows are low to moderate in value. At most stations, however, the heat flow varies measurably with depth in the 3-m sediment section; this variation may arise from several effects but is consistent with a change in bottom water temperature by several tenths of a degree during the preceding few months. If the measured heat flow is corrected for this transient effect, a more constant and generally lower heat flow is obtained.

The CESAR heat flow values are comparable to the values obtained more than a decade ago on the Alpha Ridge from Ice Island T-3. The low-to-moderate heat flow values determined during CESAR suggest several plausible origins for the Alpha Ridge. Such values would be typical of a fragment of continental crust or of an island arc remnant sufficiently old that any thermal signature has dissipated. Options such as a major volcanic origin or a spreading centre may be discarded because of the lack of evidence of enhanced heat flows during CESAR or the T-3 transects across the Ridge.

Seismic reflection profiles across the Lomonosov Ridge and on the Alpha Ridge, Arctic Ocean Basin

A. Overton

Seismic reflection profiles from LOREX (1979) and CESAR (1983) show distinctly different sedimentation patterns associated with, and structural patterns of, the Lomonosov and Alpha Ridges. The Lomonosov Ridge is shown to be an asymmetric, block faulted structure rising 2700 m above flat lying sediments at depths exceeding 4000 m in adjacent basins near the north geographic pole. The ridge surface has an irregular morphology having slopes exceeding 7° on the Amerasian slope and less than 7° on the Eurasian slope. Lithologic stratification on the tops of fault blocks is evident, but somewhat obscured by strong, scattered reflections from the rough ridge surface. Seismic events from within the ridge core suggest that the ridge is underthrust by the crust of the Eurasian Basin. Sediments on the Amerasian side of the ridge form a graben approximately 2 km thick with well-defined stratifications thickening toward the centre of the graben. A pronounced reflection from a synclinal structure about 1 km below the seafloor suggests a marked change in depositional environment. The sediments of the graben abut unconformably against the Lomonosov Ridge and another ridge buried by, and barely penetrating seafloor sediments on the southside of the graben. This buried ridge may be part of the Marvin Seamounts seen on bathymetric charts, and may represent the northern boundary of the Alpha Ridge. Sediments on the Eurasian side of, and abutting unconformably against, the Lomonosov Ridge show even more pronounced stratification with total thicknesses exceeding 2 km. An unconformity separates an upper flat lying sequence of about 1 km thickness from a lower, homoclinal sequence that thickens in excess of 1 km away from the ridge. In contrast the Alpha

Ridge seismic reflection profiles show no definite separation of distinct structures. The drift paths of the CESAR camps traversed small segments near the crestal region of the much larger areal extent of the Alpha Ridge. Seismic reflection profiles suggest a complex pattern of ridges and valleys. Stratified sediments in the valleys are generally less than 1 km thick. Stratification is not seen in the ridges. Basement features beneath the sediments are poorly defined on the seismic profiles.

Magnetotelluric measurements over the Alpha Ridge

E. R. Niblett, C. Michaud and R. D. Kurtz

A magnetotelluric (MT) recording station was established near the CESAR base camp early in April 1983. Three-component magnetic variations were measured with a standard fluxgate digital recording magnetometer mounted on the sea ice and programmed to sample the field at 1-min intervals. Horizontal telluric variations were derived from a north-south, east-west array of silver/silver chloride electrodes suspended in the sea water through holes in the ice. Data were acquired in the period range from 120 s to DC for all five components; in addition a band-passed telluric output was recorded separately for the range 120 - 30,000 s (8.3 h). The band-pass filters were included to reduce the possibility of contaminating the data with spurious potentials generated by ocean tides or ice drift velocities.

Good quality low-pass data were obtained for only 18 consecutive days because one of the telluric channels was adversely affected by low ambient temperatures during the early part of the experiment. However, the band-pass system yielded 30 days of high quality data. The geomagnetic transfer functions are very small and do not reveal any prominent contrasts in the electrical structure of the ocean crust. The apparent resistivity data are anisotropic at the longest periods, an effect that may be attributable to tidal influences. A preliminary interpretation indicates the presence of a highly conducting zone at a depth of about 90 km beneath the Alpha Ridge, which could be associated with partial melt in the asthenosphere.

Alpha and Lomonosov Ridge crustal structures

D. A. Forsyth and R. Jackson

Reversed crustal refraction profiles recorded along and across the Lomonosov Ridge (LOREX) in 1979 and the Alpha Ridge (CESAR) in 1983 indicate:

- a) The Lomonosov Ridge has a crustal thickness of about 28 km which thins to the north and south beneath the Fram and Makarov Basins. LOREX results show 5 km of 4.7 km s^{-1} upper crustal material overlying 15-20 km of 6.6 km s^{-1} material. The suggested upper mantle velocity is 8.3 km s^{-1} .
- b) Cross-over distances to upper mantle velocities of close to 200 km indicate the Alpha Ridge has a crustal thickness near 35 km and is clearly not typical oceanic crust. The velocity structure, however, does have some oceanic similarities - clarification requires analysis of the shallower structure.
- c) The crustal structure of the Alpha Ridge is significantly different from the structure of the Lomonosov Ridge near the Pole. Evolutionary schemes that suggested the two features should be similar are therefore in need of modification.
- d) The Alpha Ridge is much broader than perhaps has been realized. A corollary to this is that the Makarov Basin, if indeed there exists a basin with typical oceanic crust between the Alpha and Lomonosov Ridges, must be a rather narrow feature quite near the Lomonosov Ridge.

Petrography and geochemistry of the CESAR "Hard Rock": Possible implications for the origin of the Alpha Ridge

Nancy A. Van Wagoner and Paul T. Robinson

During the CESAR expedition 20 bedrock samples were dredged from the walls of a major graben on the Alpha Ridge. These rocks represent the only bedrock ever recovered from the Alpha Ridge and, therefore, provide the only direct evidence for the nature, composition, and possibly origin, of the Ridge. All bedrock samples recovered were presumably similar in character, and were sent to institutions across Canada for analysis. This report is based upon the analysis of one of those samples.

The sample is a fragmental volcanic rock and, although it is highly altered, many primary textures are preserved. It comprises 85 to 90% clasts that are 0.5 to 4.0 mm in size and angular to subround in shape, although some rounding may be due to alteration. Rare clasts display curvilinear and vesicle-controlled boundaries. The rock is heterolithic and the three clast types observed are 1) brown to orangish-yellow, apparently aphyric, clasts (~ 93%), 2) yellowish-brown clasts containing subhedral pyroxene crystals that are 1-2 mm in size and constitute up to 30% of the clast (~ 5%), and 3) dark-brown clasts containing 3-5% plagioclase microlites up to 0.2 mm in length (~ 2%). Most of the clasts are moderately to highly vesicular or scoriaceous, but the third clast type tends to be moderately to sparsely vesicular. Vesicles generally are either 0.5-1 mm in diameter and apparently spherical in shape, or 2-4 mm in size and irregular in shape. Most fragments contain both types of vesicles. Vesicles are rarely elongate perpendicular to grain boundaries. The presence of plagioclase microlites and the absence of abundant relict crystals suggests the clasts were flossy to very fine-grained. Geochemical analyses are in progress.

The high vesicularity and vitric or very fine-grained nature of the clasts suggests shallow water, perhaps phreatomagmatic, eruption. The fragments may have been transported after initial deposition but little reworking is suggested because 1) Although the rock is heterolithic, a single clast type predominates, 2) Many of the grains are angular in shape, and 3) Any amount of reworking would be expected to result in the destruction of the delicate, scoriaceous clasts.

Constraints on the tectonic origin of the Alpha Ridge

H.R. Jackson, D.A. Forsyth, P. Mudie and C. Amos

The results from the CESAR programs of geologic sampling, seismic reflection and seismic refraction are combined to interpret the tectonic history of the Alpha Ridge. The age of the Alpha Ridge is limited by fossils that indicate a minimum age of about 70 million years. An estimate of basement age is made using sediment thickness, rates and velocities. This estimate is found to be compatible with constraints on age suggested by the magnetic characteristic of the Alpha Ridge of about 100 million years. The basement of the ridge is inferred to be basaltic based on such data as: dredged samples, the high intensity magnetic anomalies of up to 1500 nt, and the velocities typical of basaltic crust measured on the refraction lines. The reflection profile shows the basement is rough and irregular. Faults are obvious in many areas, particularly in cross-strike profiles. A major valley, a graben-type structure, is clearly identified. The refraction data indicate there is homogeneity of crustal structure along strike, which is supported by the magnetotelluric data. The Alpha Ridge has a deep crustal root of nearly 38 km. The crustal structure is compared and

contrasted to the structure of the Lomonosov Ridge, the Canadian Arctic Islands and various oceanic plateaus such as Iceland. Based on crustal structure, probable age and geologic controls from the Arctic Islands, the tectonic evolution of the Alpha Ridge is described.

**Session 5A: Large-Scale Dynamic
Meteorology**

Thursday 1400 - 1540

Effects of stratospheric mean wind variations on the solar semidiurnal barometric oscillation

Kevin Hamilton

A simple perturbation procedure was developed to incorporate the effects of the mean winds and meridional temperature gradients in calculations of the atmospheric tidal fields. This method was applied in a numerical computation of the solar semidiurnal surface pressure oscillation ($S_2(p)$) employing various wind distributions appropriate for different phases of the stratospheric quasi-biennial oscillation (QBO). The results indicated that the effects of the stratospheric QBO on the excitation and propagation of the semidiurnal tide ought to produce a QBO in $S_2(p)$ of about 0.04 mb peak-to-peak amplitude. This prediction will be compared with some observations of the long-period variability of $S_2(p)$ at several Pacific Island stations during the period 1958 - 72.

Stratospheric "prehistory" revealed by observations of the solar semidiurnal barometric oscillation

Kevin Hamilton and Rolando R. Garcia

The solar semidiurnal tide is believed to be largely excited by the direct absorption of solar radiation in the stratosphere. Thus the observed solar semidiurnal surface pressure oscillation ($S_2(p)$) ought, in principle, to respond to changes in solar flux (particularly in the ultraviolet), ozone concentrations and stratospheric winds and temperatures (particularly in the tropics). Barometric measurements appropriate for the determination of $S_2(p)$ extend well back into the nineteenth century at some stations. This is potentially interesting since regular radiosonde observations of the tropical stratosphere began only in 1950 and reliable measurements of stratospheric ozone and the solar ultraviolet flux have an even shorter history.

In the present investigation monthly mean determinations of $S_2(p)$ at Batavia (6.2°S, 106.8°E) were computed from hourly barometric measurements taken between 1866 and 1944. There was a fairly clear indication of a roughly 26-month oscillation in the resulting $S_2(p)$ series, and it seems reasonable to infer that the stratospheric quasi-biennial oscillation must have been present in essentially its familiar form during the period 1866-1944. Also evident in the present observations are other indications of long-period variability in $S_2(p)$ that may be most reasonably interpreted in terms of large variations of the solar ultraviolet flux.

Mean wind evolution in the tropical lower stratosphere

Kevin Hamilton

A detailed study of the evolution of the zonally averaged zonal wind at the 30- and 50-mb levels during the period 1972–81 was conducted. Over 5000 monthly mean wind observations at 79 stations between 20°S and 20°N were employed. The wind behaviour was naturally dominated by the familiar quasi-biennial oscillation (QBO). A number of hitherto unnoticed features of the QBO were revealed by the data analysis. For example, there was a great difference in the meridional structure of the wind transitions from easterlies to westerlies and *vice versa*. In particular the initial westerly mean wind accelerations were concentrated in a very narrow region around the Equator, while the easterly accelerations were found to be broader in their latitudinal extent. In current theoretical models of the QBO the westerly wind accelerations are produced by the Reynolds stress divergence associated with a vertically propagating equatorial Kelvin wave. An explicit numerical integration of a Kelvin wave/mean flow interaction model was performed. For realistic parameter ranges it was found that the model's westerly mean wind accelerations were much broader than the observed accelerations. Possible resolutions of this discrepancy will be discussed.

Another interesting finding concerned the possibility of *in situ* barotropic instabilities in the tropical stratosphere. In each cycle of the QBO there was a considerable period near the extreme easterly phase during which Rayleigh's criterion for barotropic stability was strongly violated.

An interesting Southern Hemisphere wavenumber two

Steven Lambert

During late September and October of the FGGE year, a striking wavenumber two was observed in the Southern Hemisphere stratosphere. Wavenumber two will be shown to consist of two eastward propagating transients with periods of 14 and 28 days. The structure of the 28-day wave indicates that it is a global-scale free external Rossby wave. The 14-day wave appears to be a free internal Rossby mode with nearly the same horizontal structure as the 28-day wave.

The effect of gravity wave drag on simulations of the lower stratospheric general circulation

N.A. McFarlane

In an earlier CMOS Congress the author presented some preliminary results on the effect of including a simple parameterization of the wave drag due to breaking topographically generated gravity waves in the AES/CCC atmospheric general circulation model. Since that time the impact of this parameterized process on simulations of the atmospheric general circulation have been studied more extensively using longer simulation periods.

Among other things it has been found that the simulated behaviour of the lower stratospheric circulation is very sensitive to the way in which the momentum flux divergence due to the gravity wave breaking is represented. In particular, allowing a small amount of wave energy to leak up from the troposphere into the stratosphere alleviates some of the deficiencies that are common in most general circulation model simulations of the Northern Hemisphere winter-time circulation in the lower stratosphere.

Results will be presented to illustrate the effects of the gravity wave drag parameterization on simulations of the Northern Hemisphere winter-time circulation with the AES/CCC atmospheric general circulation model.

Session 5AA: Cloud PhysicsThursday 1610 - 1730

Numerical simulation of the chemistry of convective clouds*André Tremblay and Henry Leighton*

There is observational evidence that air motions associated with cloud and precipitation formation redistribute pollutants in the vertical, with the consequence that long range transport may be influenced. It is also well known that precipitation systems provide efficient mechanisms for the deposition of pollutants at the surface.

In order to provide a framework to improve the understanding of convective clouds in redistributing, chemically changing, and removing pollutants, a three-dimensional cloud model is being modified to include certain cloud chemical processes. Interaction of cloud and precipitation with sulphur dioxide, ammonia, nitric acid, hydrogen peroxide and sulphate aerosols are all included in the model. Preliminary results will be presented.

A simple estimator of collision efficiency for ice accretion models*K.J. Finstad and E.P. Lozowski*

The variation of the local collision efficiency of water droplets on the surfaces of cylinders and airfoils has been calculated using a detailed theoretical model. The results have then been fitted with a simple trigonometric function of the local surface slope, requiring only one independent parameter, which is the collision efficiency at the stagnation line. The fitted function is shown to be an excellent estimator for a variety of conditions applicable to both atmospheric and marine icing.

The estimator has been used in a simple "dry" ice accretion model, on the assumption that the local collision efficiency at a point on the most recently accreted surface is the same as for a point on the original surface having the same slope. Comparisons with results of the detailed model show excellent agreement at a substantial decrease in computing costs. Some comparisons with wind-tunnel experiments will also be presented.

Utilisation de spectres de gouttes de pluie pour évaluer les performances des radars à polarisation multiple*Gilles Boulet et Enrico Tortolasi*

On évalue les possibilités du radar à polarisation linéaire et du radar à polarisation circulaire pour estimer les distributions de gouttes de pluie. Des données de disdromètre mesurées dans le sud de l'Ontario par le Service de l'environnement atmosphérique du Canada durant l'été 1977 ont servi de base à nos calculs.

Ces données sont d'abord converties en spectres de gouttes pour ensuite être lissées dans le temps sur des intervalles de 5 et 20 min. On calcule, pour chaque spectre lissé, les observables du radar à polarisation linéaire et du radar à polarisation circulaire. Ces observables, ainsi obtenus,

sont interprétés en termes d'un modèle des spectres à 3 paramètres à partir duquel on évalue un contenu en eau liquide et un taux de précipitation. Les spectres calculés et les spectres lissés sont finalement comparés ainsi que leurs propriétés intégrales.

Les résultats obtenus indiquent que les deux techniques étudiées (polarisation linéaire et polarisation circulaire) sont équivalentes pour la mesure de la pluie. De plus, en comparant les performances du radar conventionnel à celles du radar à polarisation multiple, on réalise que le radar à polarisation permet d'améliorer appréciablement la mesure du contenu en eau liquide et du taux de précipitation.

On the retrieval of the wind field in storms from single Doppler radar measurements

J. Zawadzki and R. Hogue

The acquisition of a Doppler radar by the Atmospheric Environment Service makes the use of such equipment in research and operations of particular interest. In this work we examine the possibility of retrieving the three wind components from the measurements of reflectivity and one Doppler velocity. This is possible in principle by the use of the continuity equations for water substance (rain and cloud) with a suitable parameterization of the process leading to conversion from cloud to rain.

Session 5B: Coastal Oceanography II – Inlets and Fjords

Thursday 1400 – 1520

A numerical model of Burrard Inlet and Indian Arm, B.C.

Donald S. Dunbar

A finite-difference numerical model has been developed for the Burrard Inlet - Indian Arm fjord system located near Vancouver, B.C. Indian Arm is a typical West Coast, glacially carved fjord with a maximum depth of 220 m, a length of 18 km, and an average width of 1.3 km. The flow into Indian Arm is restricted by a shallow, 18-m sill at the mouth, which is connected to the Pacific ocean through Burrard Inlet and the straits of Georgia and Juan de Fuca. Tides in the area are semidiurnal with a range of 4.5 m and provide most of the energy for the intense mixing observed in the vicinity of the sill and the narrows.

Realistic bathymetry and tidal forcing at the mouth have been included in the model. Horizontal and vertical currents, tidal elevations, and salinity are calculated on a fixed staggered grid having vertical and horizontal resolutions of 10 m, and 1 or 2 km, respectively. Turbulent mixing and the diffusion of salt are simulated using a standard eddy coefficient approach, while surface and bottom stresses are modelled using a quadratic stress law. The model is time-dependent and retains the non-linear advection terms. Pressure is calculated using the hydrostatic approximation and density is assumed to be a linear function of salinity. Results from the model are compared to long-term tide gauge data and current meters. Baroclinic model runs have simulated the replacement of resident bottom water in Indian Arm by denser inflowing water.

Tidally-generated internal waves at the sill of a deep, tidally-energetic inlet

Michael W. Stacey

The interaction of the barotropic tide with the sill of Observatory Inlet, a fjord located on the coast of British Columbia, has been studied using tidal height, CTD, and current data. The tidal

height observations were used to calculate the power removed from the barotropic tide as a function of time. There are significant seasonal variations in the power removed from the tide because of seasonal changes in the stratification of the water column.

A simple theoretical model and the current observations show that most of the power is fed into a linear, progressive, semidiurnal, internal tide that propagates away from the sill. The first two internal modes, which account for almost all of the energy flux, respond quite differently to changes in the stratification. Although the energy flux of the first mode was insensitive to the summer increase in the surface stratification, that of the second mode increased by about a factor of four. On the other hand, only the energy flux of the first mode increased as a result of a deep water renewal event that occurred in the inlet.

Vigorous, non-linear, internal motions occur in the vicinity of the sill. These motions are more vigorous during spring tides than neap tides and so more energy is available for mixing during spring. Because of this, a significant baroclinic current occurs at the beat frequency of the M_2 and S_2 tides. This current is most vigorous near the surface of the inlet where its magnitude ($\approx 11 \text{ cm s}^{-1}$) is greater than that of the M_2 barotropic current.

Observations of an internal resonance in a fjord

J. R. Keeley

Current-meter, CTD and tide gauge data collected in a sill fjord in northern British Columbia are considered. Annual changes in stratification are such that the natural internal period of oscillation of the fjord matches that of the semidiurnal tides in the spring and fall of the year. Evidence of a semidiurnal internal resonance is sought by calculating the ratio of energy and the relative phase of the vertical current shear and the barotropic tide. It is possible to show a strong response in the fall coinciding with a phase shift of 180° , which is the signature of a resonance. Calculations prove the resonant mode to be the first harmonic in both the vertical and horizontal. Results based on springtime data also show a resonant response, although it is less clear owing to the effects of strong river run-off.

Exchange of deep water in Fortune Bay, Newfoundland

Brad de Young and Alex E. Hay

A seasonal cycle in the deep water of Fortune Bay, NFLD, is described. Cold (-1 to 1°C) Labrador Current Water flows in from the Saint-Pierre Channel, an extension of the Avalon Channel, in the summer. Warm (3 to 6°C) Modified Slope Water flows in from the Hermitage Channel in the winter. The warm water exchange in the winter is shown to be correlated with a seasonal shift in the wind stress. Light southwesterly summer winds shift to strong northeasterlies in the winter. Two possible mechanisms by which the wind can generate the Modified Slope Water inflow are put forward: a time-dependent upwelling model and a steady-state upwelling model. Cold water exchange in the summer period is found to be correlated with a seasonal variation in the Labrador Current. The transport of the Labrador Current in the Saint-Pierre Channel, in May 1982, is found to be $6.4 \times 10^4 \text{ m}^3 \text{ s}^{-1}$. Direct current measurements of the density current inflow are presented, together with an analytical discussion of the interaction between the inflow and the tide.

A model of low-frequency flow in the Canadian Arctic Archipelago

Sherman R. Waddell

A linearized one-dimensional barotropic model of the surface elevation and transport in the straits composing the Canadian Arctic Archipelago has been constructed using an electrical analogy. The model valid for periods longer than 12 h includes the effects of simple meteorological forcing. Readily available circuit analysis programs are used to evaluate the response of the region to a given forcing. The Canadian Arctic Archipelago comprises many bays and straits with complicated interconnections. In some areas, the interaction of several bays and straits can lead to significant resonant behaviour. The model is used to study the effects of such areas upon the overall flow within the Archipelago and upon the propagation of sea-level signals between the Arctic and Atlantic Oceans. Sensitivity studies have been made in an effort to isolate the effects of weakly connected regions, such as Hudson Bay, upon the overall flow. Where feasible, data sets have been compared with the model results.

Seasonal variations in surface transport through the Strait of Gibraltar

Myriam Bormans, Chris Garrett and Keith Thompson

A geostrophic interpretation of seasonal changes in sea-level difference across the Strait of Gibraltar suggests a reduction, from summer to winter, of about 12% in the surface transport. This interpretation is supported by the analysis of seasonal changes in the along-strait sea-level slope, assuming a frictional balance.

The fluctuation in surface transport is i) much larger than a barotropic signal that would be associated with the seasonal changes in a mass budget for the Mediterranean and ii) much less than would occur if a two-layer baroclinic flow were adjusting, to balance the salt budget for the Mediterranean on a seasonal time-scale.

We suggest that the reduction in winter inflow is a manifestation of the reduction in shear required to maintain a constant Froude number in the face of an increased density of the inflowing Atlantic water. This interpretation is shown to be reasonably consistent quantitatively if there is no change in the interfacial depth in the Strait, an assumption which we argue is consistent with Bryden and Stommel's (1983) overmixing solution even if the mixing in the Mediterranean varies seasonally.

The Strait of Belle Isle: Theory vs observations

Bechara Toulany, Brian Petrie and Chris Garrett

Low-frequency fluctuations in the flow through the Strait of Belle Isle are highly significant, being of the same order as the tidal streams ($0.5\text{--}1.0\text{ m s}^{-1}$).

Current meters, tide gauges and bottom pressure gauges were deployed across the Strait for 80 days from July to October, 1980, in order to study the detailed structure of the flow fluctuations. Cross-spectral analysis of the current data shows very high coherence in the long-strait current component throughout the whole cross-section. However, the near-surface currents are about 50% greater than currents 50 m below the surface, and lag by a few hours.

A theory of frictionally induced baroclinic adjustments is discussed, and an expression for the pressure fluctuations in the cross-section of the Strait is derived. A test of this theory has been carried out by comparing (i) δP_1 , the subsurface pressure difference across the Strait, and (ii) δP_2 , the difference between subsurface pressure and bottom pressure at one side of the cross-section. The two series are coherent, with a gain and phase that are consistent with the theory. A comparison of the ratio $\delta P_2 / \delta P_1$ allows us to obtain an estimate of the spin-down time. This is found to be of the order of 10 h.

Surface current measurements in southeast Dixon Entrance

J.R. Buckley and W.J. Robson

In February, 1983 we performed an experiment to measure surface currents in McIntyre Bay in southeastern Dixon Entrance. Measurements were made by following VHF transmitting oil-spill follower buoys with a boat and positioning the buoys with LORAN-C. On each of eight days, a group of four buoys was deployed in a square pattern. This pattern was positioned every half hour from dawn to dusk. Velocity, acceleration and spreading information was extracted from the position data. These values were correlated with tidal heights at Prince Rupert and Wiah Point and with wind velocities at Rose Spit and Langara Island.

Results showed that there was tidally dominated flow in the surface layer. Any large deviations from strictly tidal flow were well correlated with the wind; hence no significant mean flow could be determined.

The cross-channel flow at the entrance of Lancaster Sound

B.G. Sanderson and P.H. LeBlond

The cross-channel flow commonly observed near the entrance of Lancaster Sound is modelled assuming inviscid flow and the conservation of potential vorticity. Solutions for one- and two-layer models are considered. It is shown that the westward decrease in depth is sufficient to reduce the relative vorticity of an intrusive flow and to force it across and then out of the Sound. The flow reversal takes place at a distance similar to that observed.

Session 5C: Synoptic Meteorology and Climatology

Thursday 1400 - 1650

Arctic meteorology and climatology: Present problems and potential directions

Claude Labine

A review of Arctic meteorology and climatology is presented. The review concentrates briefly on the research that has been undertaken in the Canadian High Arctic. The main emphasis of the review is to present:

- 1) the major problems with the existing data gap
- 2) the present research activities
- 3) potential solutions to these problems

In discussing the potential solutions, the paper discusses the existing data requirements that are not being met at present, forecasts future research needs and proposes solutions that need to be attempted given the limited available financial resources.

On the motion and shape of migrant Arctic Highs

E. R. Reinelt

Arctic outbreak highs are generally understood to be surges of fresh cA air, mobile, elliptical domes of dense, dry air that have become detached from their parent source, the quasi-permanent continental polar anticyclone. Such outbreaks are usually most severe in the wake of the last member of a cyclone family, often a Pacific low that redeveloped and intensified in the lee of the Rocky Mountains.

The 200 migrant highs examined in this study followed for the most part well-established "storm tracks" through Alberta, Saskatchewan, and the U.S. Great Plains. A typical, elliptical high has a major axis about twice as long as its minor axis. Such systems move generally in a direction some 19° to the left of the major axis, along a southeasterly mean bearing of 140° , and at an average speed of 29 knots. Three types of high were identified, and classified according to markedly different contour configurations at levels beyond 850 mb.

Variability of the North Pacific Ocean-atmosphere heat exchanges

Gordon A. McBean

The net heat exchanges due to solar and long-wave radiation and the sensible and latent heat fluxes, as estimated from ship weather reports, are examined for the $20\text{--}60^\circ\text{N}$ region of the North Pacific Ocean. The computations are monthly averages for 5° squares for the period 1959–1979, with some earlier data. The mean annual cycle for each flux is shown. The variability of the fluxes from the long-term mean is examined. The magnitude of the interannual variability will be discussed in terms of: uncertainties in the data; association with El Niño events; and the spatial variability.

Estimating incoming solar radiation at sea

F. W. Dobson and S. D. Smith

The widely-used monthly short-wave radiation formula of Budyko (1974) is tested at Ocean Weather Station (OWS) P, and found to underestimate the measured incoming solar radiation by 26% on average, with the largest errors in summer. Similar results were obtained from tests with data from OWS A, I, J and K.

Models for estimating the hourly radiation as a function of solar elevation and reported cloud type and amount, including those of Lumb (1964), Lind and Katsaros (1982), a more detailed model with 24 cloud categories, and the daily-average model of Reed (1977), were evaluated on an hourly, daily, monthly and long-term basis in comparison with a model based only on cloud amount in oktas. The "okta" model performs as well as or better than the more complex models, and we conclude that, at least at high latitudes, the cloud type information does not help us to model solar radiation.

Sea surface temperature distribution in the tropics and its relationship to the incidence of tropical storms in oceans around the Americas

M. R. Morgan

This paper examines the differences in sea surface temperature distribution between the oceans of the Northern and Southern Hemispheres with particular reference to tropical latitudes. It will

show how these differences are associated with the location and intensity of the Inter-Tropical Front and the incidence of tropical storms that affect the climate of North America.

There is a strong sea surface temperature gradient across the Equator, during the Northern Hemisphere summer and fall, which facilitates the penetration of the Southeast Trades into northern oceans. These cool intrusions of latently unstable air become vigorously unstable as they progress northward over warmer water and the vorticity of the air stream increases. A much weaker sea surface temperature gradient exists in the Southern Hemisphere summer, which is less conducive to cross-equatorial airflow from north to south. Consequently, the ITF is vigorous in the North Atlantic and eastern North Pacific but rarely migrates south of the Equator. This accounts for tropical storms being a Northern Hemisphere phenomenon only, in the oceans around the Americas.

Normally, the SST gradient along the Pacific Coast of the Americas in the tropics is stronger than that in the Atlantic and this is reflected in the differences in length of the storm season and the frequency of storms. However, the occurrence of the warm El Niño current, at times, modifies the cross-equatorial gradient and is interrelated with tropical storm incidence in the Pacific.

The role of SST in tropical storm development in the Caribbean is less conclusive, since there is no cross-equatorial gradient there. Even so, there are SST features that may contribute to air-mass convergence and storm development.

The paper concludes that a strong equatorial SST gradient is the catalyst for tropical storm development in open ocean areas adjacent to North America and may be a contributory cause in the Caribbean.

Sea surface temperature distribution and its relationship to monsoon rainfall and line squall activity in SE Asian Waters

M. R. Morgan

SST data collection and analysis over the South China Sea were carried out routinely by the author during MONEX 78. The paper examines the changes in SST distribution during the NE Monsoon season and its relation to precipitation patterns over the South China Sea and the coastal areas of SE Asia. The probable contribution of SST in the formation of line squalls (SUMATRAS) in the Straits of Malacca will also be discussed.

The paper demonstrates the importance of SST distribution in the climate of SE Asia.

El Niño Southern Oscillation (ENSO) and the Indian monsoon rainfall – A brief update

M. L. Khandekar and V. R. Neralla

The concept of the Southern Oscillation was put forward by Sir Gilbert Walker more than fifty years ago to develop suitable predictors for seasonal forecasting of monsoon rainfall over India. In recent years, there has been a resurgence of interest in ENSO and its teleconnections with global climate and weather anomalies.

The temporal variations of ENSO and the Indian monsoon rainfall are re-examined in this study. Data for the sea surface temperatures (SST) over the equatorial eastern Pacific and a suitable Southern Oscillation index based on mean surface pressure difference over selected stations are used to represent the ENSO variations; while annual rainfall values for June to September suitably averaged over various subdivisions of India are used to represent the monsoon rainfall variations. Our analysis suggests a definite link between ENSO and the Indian monsoon.

A simple physical mechanism is proposed that may help establish a link between the Indian monsoon and some of the ENSO parameters, such as the SST in the equatorial eastern Pacific.

Canada's National Climate Data Archive

Mike Webb

The Canadian Climate Centre of DOE's Atmospheric Environment Service maintains for public use an archive of climate data and information in document, micrographic and digital form. This Poster Session will indicate information, service and product sources available from the Centre and how they can be obtained. Emphasis will be on recent publications including the new 1951-80 Climate Normals, on digitized data and support software ready to provide users with displays and analyses of station data, and on digitized marine weather data and exploitive software such as "MAST".

Session 5D: Continental Margin Studies Thursday 1340 - 1520

Time-series analysis of gravity anomalies and topography across the Nova Scotian continental margin

K.E. Loudon

Recent data, collected for the Gravity Map of Canada (1980) across the Nova Scotian margin, allow for a detailed look at gravity anomalies across an old, sediment-filled continental margin. As is typical of such margins, there exist lineated bands of free-air gravity highs coincident with the shelf edge, coupled with adjacent lows both inland on the shelf and offshore over the lower part of the slope, with a dominant wavelength of 200-300 km. However, within this overall pattern there exist significant variations in the amplitudes and shape of these anomalies from NE to SW along strike of the margin. A time-series analysis of 14 profiles each 400-km long was conducted to further quantify these observations. The resulting gravitational transfer functions show the effects of differing modes of compensation for different wavelengths. The long-wavelength anomaly is related to the regional compensation of the surface sedimentary load by an elastic plate that increases in thickness with age; while shorter wavelengths of 60-200 km give anomalously low values of the transfer function that cannot be fitted by the same simple analytical curves of plate compensation. A comparison with the results of recently developed thermo-mechanical models of passive margin evolution shows that these variations may be caused by the style of crustal thinning across the margin, which produce loads within the plate that are compensated differently than the surface topography is. If so, then the Nova Scotian data indicate that patterns of crustal thinning may vary quite rapidly along strike as a single margin sector is rifted.

A seismic base-event map for the continental margin around Newfoundland

A.C. Grant

Multichannel reflection seismic data from the continental margin around Newfoundland have been used to construct a subsurface "base-event" map. The map covers the Continental Shelf region from the western Grand Banks (excluding St Pierre Bank) to the Strait of Belle Isle, and the adjacent slope and rise, including Orphan Knoll, Flemish Cap and the Newfoundland Ridge. The map depicts the "regionally deepest mappable" seismic horizons; it approximates the base of the Cenozoic sedimentary sequence. In addition to providing a datum for showing the thickness

distribution of overlying Cenozoic deposits, it is a datum surface at which to map the underlying geology as indicated by seismic reflection character. A companion map presents estimated depths of the sedimentary basins defined at this level, and a combination of these data with the isopachs of Cenozoic deposits yields maps of total sediment thickness and depth to "basement".

The "base-event" in some areas may be viewed as "seismic basement" or "petroleum basement". Beneath much of the Continental Shelf the surface mapped may be best defined as a peneplain; over the sedimentary basins it is an angular unconformity on Cretaceous or older sediments. In Shelf areas this surface has been referred to as the Avalon Unconformity. Beneath the deeper parts of the Cenozoic basins this surface may trace a late Cretaceous carbonate horizon. Despite the disparate origins of the horizons composing this map, it provides an objective datum from which to assess regional geology at both deeper and shallower levels.

An investigation of the thermal and subsidence history of the Labrador Margin

Dale Issler

Extensional models have been successful in describing the first-order processes involved in the formation of passive continental margins. They predict stretching of the crust and subcrustal lithosphere during the rift phase followed by subsidence due to thermal contraction of the lithosphere. A finite-element model that considers non-uniform extension and allows for variable sediment properties is used to determine the thermal history of sediments in wells on the Labrador Shelf. The model assumes Airy isostasy and includes radiogenic heat production in the crust and sediments. Thermal conductivity within the sediments is allowed to vary as a function of lithology, temperature and compaction, and it is assumed that advective heat transport is negligible. The level of organic maturation is computed using appropriate time-temperature relations for the thermal alteration of organic matter.

Sediments are first backstripped to obtain the tectonic subsidence, which in turn is used to derive estimates for the stretching parameters, β and δ . These approximate values are then refined in the forward-modelling process. The model can be tested with crustal thickness estimates from seismic refraction experiments, corrected bottomhole temperatures and direct maturity measurements such as vitrinite reflectance.

Geophysical crustal studies off the southwest Greenland margin

Apostolos B. Stergiopoulos

Seismic refraction data were collected in the southern Labrador Sea off the southwest Greenland margin, from the Canadian Scientific Ship *Hudson* in the summer of 1979; airgun devices and explosive charges (dynamite) were utilized as energy sources and expendable sonobuoys as detectors to shoot five refraction lines in a direction roughly parallel to the Continental Shelf edge.

Among the main objectives of the cruise was to collect seismic information about the upper and lower crust and the upper mantle off the southwest Greenland margin and supplement this work with the collection of other useful geophysical data (magnetics, gravity and seismic reflection) to delineate subsurface structures.

This study is mainly concerned with the elaboration of the seismic data and the use of the seismic results along with other pieces of geophysical information to reveal the crustal structure of this continental margin.

All the available geophysical data were utilized to define a crustal model across the refraction lines, in a direction almost perpendicular to the margin.

The ocean-continent boundary proved to be difficult to locate. The most western of the five refraction lines was run in an area with a well-developed oceanic magnetic anomaly pattern and thus over true oceanic crust. In the region of the four eastern refraction lines, no correlatable oceanic magnetic anomalies have been identified and the seismic refraction studies revealed the presence of an attenuated crust of dubious nature. On the basis of the seismic wave velocities alone, the dubious crust may correspond to true oceanic crust or, equally well, to subsided and attenuated continental crust.

The average crustal thickness over a 200-km wide zone seawards of the foot of the continental slope that results from the modelling is 6.20 km. Mass balance calculations suggest that the model is very close to isostatic equilibrium if simple Airy-type compensation is assumed.

Other characteristics of the proposed model, its comparison to other relevant structural models from the Labrador side and its implications, will be discussed.

Iceberg scouring on Saglek Bank, Northern Labrador Shelf

B.J. Todd, C.F.M. Lewis and S.J. d'Appollonia

Abstract not available.

Session 5DD: Seismology and Deep Crustal Structure

Thursday 1550 – 1730

Preliminary gravity, magnetic, and refraction seismic results from the Abitibi greenstone belt, Québec

E.J. Schwarz, L. Laverdure, L. Losier, M. Bilkington, B. Keating and B.J. Crossley

The Abitibi greenstone belt is a large structure formed by metavolcanics, metasediments and granite intrusions. To investigate its deeper structure, gravity (Earth Physics Branch data), aeromagnetic (Geological Survey of Canada data), and refraction seismic data (in cooperation with COCRUST) are interpreted in an integrated way. The within-belt gravity data generally coincide with granite plutons and suggest a depth-to-bottom surface of 5 to 7 km. The regional low of -45 mgal may indicate a somewhat deeper MOHO with a slight dip East away from the Kapuskasing gravity high. Coloured magnetic anomaly maps and magnetic shadowgrams reveal a much finer structure much of which can be correlated with the surface geology. Average seismic P velocities are 6.3 km s^{-1} for the crust and 8.5 km s^{-1} for the upper mantle. The depth to the MOHO is 38 km in the central part of the belt, and a weak dip (2°) of the MOHO towards the east and south is indicated.

Interpretation of seismic refraction data from the Abitibi region of the Canadian Shield

D. Crossley, C. Parker, E. Poterlot and E.J. Schwarz

In 1982, COCRUST organised a refraction experiment in central Canada to examine the general crustal structure for three problems to a) determine the nature of the Ottawa graben, b) examine the Grenville front in western Québec and c) look at the Abitibi greenstone belt in Québec. For the third (Abitibi) portion, four large shots were fired into a line of recorders deployed from Val-d'Or in the south to 80 km north of Matagami. Two of these shots gave a partly reversed profile N-S and the other two were fan shots from the west (Matachewan) and east (Chibougamau).

We have modelled the data using ray tracing and synthetic seismograms to find a low velocity zone under the central portion of the belt that may coincide with a high-conductivity layer found from other MT studies. The in-line profile and fan-shot data do not at the moment agree on the Moho topography beneath the Abitibi, but we hope to present a consistent picture after further analysis.

The crust under the Canadian portion of the Williston Basin

Z. Hajnal

A two-dimensional technique for calculating synthetic seismograms was employed to analyse reversed and overlapping refraction profiles of COCRUST's 1977, 1979 and 1981 experiments from southern Saskatchewan and Western Manitoba. In the east, under the Superior tectonic Province a simple three-layer crust exists with a maximum 40-km thickness. In the Nelson Front region and in the Churchill Province the upper crust is complex showing both lateral and vertical velocity variations. The crustal thickness increases westwards from the margin of the Superior Province through the appearance of a 7.00 km s^{-1} lower crustal layer. A maximum thickness of 50 km is reached in the central portion of the Williston Basin. The upper mantle is also anomalous having a velocity of 8.00 km s^{-1} in the east increasing to 8.45 km s^{-1} under the Williston Basin. The behaviour of the crust appears contradictory to the rifted thermally-induced basin-forming process. The crustal thickness map of Western North America indicates a north-south-northeast trending anomaly that appears to wrap around the Archaean Superior Craton.

Update on Lithoprobe – A coordinated national geoscience project

Gordon F. West, M.J. Berry, R.M. Clowes, W.S. Fyfe, R.D. Hyndman, E.R. Kanasevich, J.C. McGlynn and C.J. Yorath

Lithoprobe is a major new project in Canadian earth sciences to study the interrelationship between the structure of the lithosphere and the surface geology, and thus to solve key geotectonic problems of significant interest to the university, government and industry-based geoscience communities. Phase I Lithoprobe now has been funded; preparation of a proposal for Phase 2 is in progress. The Lithoprobe program will be spearheaded by high-resolution multichannel seismic reflection technology, the only available geophysical method with adequate resolution to help unravel complex geological structures at depth. Seismic refraction experiments, other geophysical studies, geological studies and geochemical investigations will provide essential supporting data to complement the reflection results and enable integrated interpretations in selected transects to be obtained.

Phase I Lithoprobe includes three research components: (1) A Vibroseis deep reflection profile across southern Vancouver Island where preliminary studies and a major seismic refraction program have been completed. The study embodies a unique opportunity in Canada to solve a fundamental problem in global tectonics – the processes involved in, and structural manifestations at depth of, accreting terranes – and to delineate the geometry and characteristics of a young and actively subducting oceanic plate. (2) Seismic refraction and preliminary reflection studies on the Kapuskasing structural zone (KSZ) because it has recently been identified as a region of fundamental significance for understanding the nature and evolution of Archaean crust, within which resides a substantial proportion of the mineral resources of Canada. In particular, the recently

proposed model of KSZ as an upthrust, generally west dipping section through the continental crust requires verification. (3) Supporting geological, geochemical and other geophysical investigations in both these regions to enable integrated interpretations of geology and tectonics to be made.

Crustal electrical conductivity in the region of the Wopmay Orogen, N.W.T.

P.A. Camfield, D.H. Krentz, J.C. Gupta and J.A. Ostrowski

Earth Physics Branch studies of crustal electrical conductivity in the Wopmay region have three parts: audio-magnetotelluric profiling, magnetotelluric sounding, and magnetovariational profiling. Audio-magnetotelluric data (8–1000 Hz) were taken at 1-km intervals on a line 12 km long across the Wopmay Fault Zone near 65.7°N. They suggest that the Zone is 4 km wide, sub-vertical, and extends to at least the mid-crust. A magnetotelluric sounding (0.001–2000 s) at a point 8 km east of the fault scarp is consistent with an extremely resistive upper crust (resistivity greater than 100,000 Ω m) 12 km thick, overlying a conductive lower crust (200 Ω m or less). In the magnetovariational study, temporal variations of the geomagnetic field were recorded at eight sites along a profile 250 km long across the Orogen from near Echo Bay on Great Bear Lake to Itchen Lake. Vertical-to-horizontal transfer functions computed from these data in the period range of 60–1200 s show a minor anomaly at shorter periods near the allochthonous shelf margin mapped by Hoffman and colleagues at the eastern edge of the Hepburn metamorphic-plutonic belt. Similar observations over the exposed Precambrian in Saskatchewan and Manitoba detected a major anomaly apparently associated with enhanced electrical conductivity in former oceanic crust. The absence of a strong anomaly in the Wopmay area allows a preliminary conclusion to be drawn, viz. that the majority of such material was consumed during the various subductions.

Session 5E: Arctic Expeditions, CESAR, LOREX and FRAM: II

Thursday 1400 – 1710

Office of Naval Research programs: Present and future

G. Leonard Johnson

In 1984 the prime programmatic objective is a major field effort in the Marginal Ice Zone (MIZEX). The goal of this multi-national effort is to gain an understanding of the physical processes by which the ocean, ice and atmosphere interact in the region of the ice edge. Specifically, the program addresses: 1) the atmospheric processes (boundary-layer modification at the transition between open water and ice, and steering and generation of cyclones by baroclinicity induced by the ice margin); 2) oceanic processes (eddy generation along the fronts or ice edge by baroclinic or barotropic instabilities, wind-driven upwelling along the ice edge, fine or vertical structure generation by interweaving of polar and Atlantic water, and intermediate or bottom water formation in the Greenland Sea during winter); and 3) ice processes (the destruction of ice by melting in summer and advection into warmer waters, and enhanced ice production in winter due to frequent opening leads).

In the future we plan the following studies:

Winter 1985 APEX – Arctic Polynya Experiment to investigate heat fluxes, salt and ice generation in a polynya south of St Lawrence Island.

- Spring 1985 AIWEX – Arctic Internal Wave Experiment to investigate generative and dissipative mechanisms for the Arctic internal wave field; ice camp, 150–200 north of Prudhoe.
- Summer 1985 Sediment dynamics, Fram Strait.
- Winter 1986 Greenland Sea MIZ.
-

Scientific activity in Arctic Canada

George Hobson

Present scientific activity in the Canadian Arctic consists of acquiring relevant baseline data in all disciplines from archaeology to zoology. The period of putting out bush fires is past – some good science is being done. In 1984, as many as 200 different projects may be undertaken north of the mainland. The Polar Continental Shelf Project is reactive to all this activity in the provision of coordinated logistics. There is serious consideration being addressed to the occupation of an ice island calved in late 1982 from the Ward Hunt ice shelf. It is being tracked continuously while a scientific program is being planned. Investigation of the continental margin is of high priority.

Biological sampling program: CESAR Expedition

N.J. Prouse

A number of investigations relating to the organically derived material in the water column and the kind, number and distribution of organisms below the Arctic ice were carried out on the CESAR expedition. A large scavenging amphipod, *Erythenes gryllus*, was collected at the bottom (2000 m) with baited traps and preserved for analysis of Po^{210} and lipid content to compare with species captured in other areas. *Lycodes frigidus*, the glacial eel-pout, was also caught at this depth with a codjig; this represents the first recorded catch of this fish from the Arctic Canadian Basin. Plankton traps and net tows at different depths confirmed the limited vertical migration of zooplankton below the Arctic ice. Water samples taken every 50 m to the bottom indicate very low concentrations of particulate organic carbon and nitrogen but relatively high concentrations of dissolved organic carbon. The significance of these observations will be discussed in relation to other areas of the world's oceans.

The origin of the nutrient maximum in the Arctic Ocean

E. P. Jones and L. Anderson

Early studies from the T-3 Ice Island revealed maximum concentrations in phosphate, nitrate and silicate at a depth near 160 m. This feature was attributed to Bering Sea water having entered the Arctic Ocean through Bering Strait. More recently, measurements at the LOREX ice camp showed a silicate maximum at a slightly shallower depth, near 120 m. No new interpretation of this maximum was offered, though it was suggested that the nutrient maximum could involve other considerations other than simply that it was part of the Bering Sea water. We report results from the CESAR ice camp that show maximum concentrations for phosphate, nitrate and silicate also at 120 m. Measurements of alkalinity and total inorganic carbon at CESAR indicate that the nutrient maxima are a result of chemical processes occurring on the shelf regions of the Arctic Ocean and are not directly related to inflowing Bering Sea water.

F-11 and F-12 distributions in polar oceans

D.W.R. Wallace and R.M. Moore

Freon profiles collected in the Central Arctic Ocean during the CESAR project are presented. Measurable freon is present down to about 900 m in the Canada Basin while below this depth, the Arctic Ocean Deep Water has freon concentrations below our practical detection limit of 0.01 pM L^{-1} . The distributions are interpreted with the aid of 2 simple models that share the assumption that ventilation of the deep Arctic Ocean is principally by lateral or isopycnal processes. The models provide upper and lower bounds to the ventilation time-scales of the various layers of the water column and the results agree well with previous estimates based on other considerations. A residence time in the Arctic Ocean of about 30 years is estimated for the Atlantic Water at the CESAR location.

The Arctic Ocean profiles are compared with profiles collected from other polar regions, including the Greenland and Norwegian Seas, Baffin Bay, Jones Sound and Lancaster Sound. The penetration depth of the freons varies significantly from region to region. The physical reasons for this variation are examined.

Sellafield (Windscale) tracers in the Arctic Ocean

J.N. Smith, K.M. Ellis and P. Jones

The distributions of the radioactive tracers, Cs-134, Cs-137 and Sr-90 derived from the Sellafield (Windscale) fuel reprocessing plant on the West Coast of England, were determined in surface waters of the Norwegian Sea from analyses of sea water samples collected during the CSS *Hudson* cruise in 1982. Correlation of the spatial distribution of these tracers with their input function from the reprocessing plant provide information on water circulation processes in the Northeast Atlantic Ocean. Elevated levels of Cs-137 were detected in surface water at the FRAM III ice station in 1981, again due to inputs of Sellafield (Windscale) labelled water from the Norwegian Sea. An anomalously high Cs-137 activity measurement at a water depth of 1500 m at the FRAM III location is consistent with recent penetration of surface water to this depth. However, a Cs-137 activity profile measured at the CESAR ice station in 1983 does not indicate the presence of Sellafield (Windscale) labelled water at depths of the order of 1500 m.

Radiocarbon and water isotopes at CESAR

H. Gote Ostlund and Valery Lee

At the CESAR station, samples were collected for radiocarbon, tritium, helium-3 and oxygen-18. At time of writing, the measurements are still in process. Early results indicate that some bomb-produced C-14 has penetrated into the waters well below the halocline and temperature maximum. Tritium and O-18 seem to strongly suggest the presence of brine, presumably produced by freezing on the shelves. The data and some conclusions will be presented.

Regional oceanography around FRAM III

R. Perkin

The temperature and salinity fields surrounding the FRAM III ice station were surveyed to a depth of 1000 m. At the time, April 1981, the station was located north of a filament of Atlantic Water originating in the west Spitzbergen Current and apparently following the 1000-m isobath

of the Yermak Plateau. This filament could be traced farther east where it eventually rejoined the main core of Atlantic Water proceeding east along the north Spitzbergen Coast and the shelf break of the Barents Sea. Near 300-m depth, two isopycnal intrusive layers are found throughout the region with indications of double diffusion on their upper and lower surfaces. These features are thought to begin in the frontal zone of northern Fram Strait where contact between Arctic and Atlantic Waters may be increased by the production of eddies, leading to double diffusively driven intrusions.

CESAR radiopositioning evaluation

J.R. Weber and D.E. Wells

CESAR provided a unique opportunity to collect and evaluate radiopositioning data at high latitudes. Three kinds of radiopositioning data were collected during the CESAR field program: TRANSIT satellite navigation data (which provided the main source of reference positions for the CESAR camp); DECCA low-frequency navigation data, using the Polar Continental Shelf Project's DECCA chain, established along the north coast of Ellesmere Island, 500 km southeast of the CESAR camp; and OMEGA positions, using the Canadian Marconi 771 OMEGA receiver. The results of comparing both the DECCA and OMEGA with TRANSIT, taken as a standard, are presented.

Session 6A: Sea Ice and Icebergs

Friday 0900 - 1230

Ice forecasting requirements of the Gulf Beaufort Sea drilling system

F.J. Eley

New technology drilling systems, both floating and gravity-based have created a new set of hazardous ice specifications. This presentation will review the design ice capabilities of the conical drilling unit and its support system, some 1983 performance results, and their ice forecast requirements. The design of an ice forecast support system in light of this experience will be discussed. The design of forecast formats and communication techniques will be stressed. Utilization of a "front-line" weather and ice forecast facility will be discussed in detail. The anticipated ice forecast requirements for the mobile Arctic caisson will also be discussed briefly.

The discussion will be illustrated with photographs of the drilling vessels, ice-breaking support vessels and ice conditions, as well as some samples of data and forecast presentation material.

Labrador sea-ice dynamics as determined by Nimbus-7 SMMR data, March 1982

R.W. Gorman and M.A. Cameron

During March 1982 a joint project was undertaken by the Federal Government (AES, CCRS) and the Newfoundland Government to study the properties of the Labrador Sea pack-ice. The specific objective of the Atmospheric Environment Service and the Canada Centre for Remote Sensing was to study the microwave properties of ice as part of the RADARSAT program. This paper presents the results of the analysis of the microwave measurements obtained from the Nimbus-7 Scanning Multichannel Microwave Radiometer (SMMR) overflights on March 17 and 23, 1982 in comparison with data collected by the AES *Electra* SLAR and concurrent surface measurements made by RADARSAT personnel onboard the M.V. *Franklin*. Specific emphasis was placed on validating three Nimbus ice concentration algorithms. The two SLAR mosaics flown on March 17 and 23 were interpreted for ice concentration by an experienced ice forecaster at Ice Central. The mosaics were digitized and registered to the SMMR data. Detailed comparisons of the ice concentrations derived from the SLAR mosaics with each of the algo-

rithms were made. The prevailing weather conditions on March 17 were cloudy and warm, and on March 23 were clear and cool. Consequently, this experiment provided a good opportunity to assess the microwave properties of the sea ice as measured by the SMMR under varying environmental conditions. The results of this analysis provides information for developing a regional algorithm for the Labrador Sea.

Comparison of sea-ice algorithms using Nimbus-7 SMMR data

Anne E. Owens

The retrieval of sea-ice properties from passive microwave satellite data has been an ongoing effort since the launch of the ESMR onboard the Nimbus-5 spacecraft in 1972. The present operational satellite, Nimbus-7, carries a Scanning Multichannel Microwave Radiometer (SMMR), which has a 10-channel sensing capability. The SMMR brightness temperature data have proved useful in deriving sea-ice concentrations and extent, and discriminating ice types. Several algorithms have been tested, as part of this research effort, with the objective of defining a single "best" model.

This paper will present the results of a comparison of five algorithms, using SMMR data from March and October, 1979. The area of study is the Arctic Ocean, which contains two major ice types, first-year and multi-year, and open water. The effect of the presence of second-year ice will also be noted. Comparisons of the derived ice concentrations were made along two transects in the study area. A statistical correlation procedure was utilized as the means of comparison. The algorithm results were also compared to AES ice charts in order to evaluate their performance. This work has been done in conjunction with a NASA Goddard group in Maryland, who provided the ice concentration data from two of the algorithms.

A digital SLAR analysis of Mould Bay second-year ice

M.A. Cameron, R.W. Gorman and R.G. Onstott

In May 1983 the AES *Electra* made an overflight of Mould Bay in conjunction with the Mould Bay III experiment investigating second-year ice. The *Electra* imaged Mould Bay in three directions, directly down the bay, at a 90° angle, and a 45° angle using the Motorola AN/AP5-94E SLAR, imaging in both optical and digital formats. The purpose of this study was to investigate the utility of the digital SLAR system, and the manipulative procedures that may be applied to the digital data.

The digital data were analysed at the (RADARSAT) office in Ottawa using their Dipix image analysis system; to a lesser degree the CIAS system at CCRS was also utilized. Preliminary work involved a large amount of data manipulation. The results included the ability to differentiate distinctly between first- and second-year ice. The different look directions exposed many features on the ice surface that may have been missed had only one look direction been imaged. Interesting features identified include a potential history of the melt pattern of the ice during the previous summer, as well as many fractures within the ice. The stark appearance of the first-year ice compared to the second-year ice, and the enhancement capabilities of the digital procedures in highlighting ice features, showed promise. An attempt to correlate the data with scatterometer results and other ground-truth data collected at Mould Bay was also made.

Upwelling under a fast-ice cover

Edward B. Bennett

Theoretical considerations suggest that eastward flow in a zonal channel in the Northern Hemisphere is deflected to the north in the frictional boundary layer beneath a fast-ice cover, and that continuity requires upwelling along the south side. Observations in late winter (April) in Barrow Strait demonstrate the occurrence and consequences of such a process. Flow is generally eastward, with maximum speeds at mid-depth. Orientations of the net current vectors or major axes of the tidal ellipses show a northward deflection in both the under-ice and bottom boundary layers, with a compensatory southward deflection at mid-depth. The under-ice boundary layer at the south shore has a relatively high salinity and is several hundredths of a degree warmer than the freezing temperature, while in mid-channel the salinity is least and temperatures are at or slightly below freezing. The upwelling of relatively warm water slows local ice growth, with the result that level first-year ice is about 0.5 m thinner near the south shore than in mid-channel. The thinner ice has higher surface temperatures; hence upwelling under fast-ice has a signature in thermal imagery obtained by satellites.

Iceberg drift and dispersion at the junction of Lancaster Sound and Baffin Bay

B.G. Sanderson and P.H. LeBlond

Icebergs were tracked by radar as part of the 1978 Eastern Arctic Marine Environmental Study. The observed iceberg motion has a deterministic component on which are superimposed temporally and spatially fluctuating features of a more stochastic nature. Thus the icebergs are considered to be subjected to both advective and diffusive motions. Iceberg movement is assumed to be temporally stationary (but not homogeneous) in order to calculate such properties of their flow fields as mean motion, velocity gradients, and diffusion coefficients. The predictability of the iceberg motion is investigated for the various observed flow fields using a solution of the Lagrangian diffusion equation.

Eddies and tides from iceberg trajectories

Chris Garrett, Mark Hazen, Fouad Majaess and John Middleton

Results of a statistical analysis of iceberg trajectories on the Labrador Shelf are presented. Iceberg motions indicate the region to be highly turbulent, with Eulerian velocity integral time- and space scales of about 20 h and 25 km, a Lagrangian integral time-scale of about 14 h, and an eddy diffusivity $\approx 2 \times 10^3 \text{ m}^2 \text{ s}^{-1}$. Some dynamical interpretations of the results are discussed. We show how the effects of wind and tides on iceberg motion may also be extracted from the data, and discuss the nature of a statistically optimum scheme for the prediction of iceberg trajectories.

On damping inertial oscillations in time-dependent free-ice drift without employing empirical damping

Gordon E. Swaters

Air stress on sea ice is well known to be quadratic in wind speed. Traditionally the air stress is formulated as proportional to $A|A|$ where A is the wind velocity at some height. For the initial value problem in free-ice drift, this formulation predicts that the transport of ice and water will not converge to a steady-state solution, independent of the water stress formulation. McPhee (1978) has proposed an empirical damping term that is proportional to the component of the wind stress in the direction of the ice motion. It is shown that if the air stress is formulated as

being proportional to $(A - V)|A - V|$, where V is the ice velocity, the transport converges to its equilibrium value and, moreover, the lead term damping resulting from this formulation is formulated similarly to empirical damping term.

An experimental study to investigate the drift of a number of idealized iceberg models

K. Shirasawa and D.B. Muggerridge

Non-dimensional solutions for the equations of motion are introduced as an aid to understanding the movement of icebergs.

Laboratory experiments show that, during deceleration, spherical and cubical semi-immersed objects initially move under the action of a drag force that is proportional to the speed of the object, then enter a transition stage to a final stage where the drag force is proportional to the square of the speed of the object.

Frictional and form drag coefficients are obtained by postulating the relationship that the product of the initial speed and the time constant for any one object is a constant.

This approach to understanding the mechanism of the motion of semi-immersed objects applies in the motion of real icebergs during deceleration after the change of such external forces as wind, current and towing.

The approach may lead to a prediction method that does not require the use of such factors as the drag coefficient, and the underwater areas of icebergs, which are difficult and expensive to measure.

Session 6B: Coastal Oceanography IV:

Stratification and Mixing

Friday 0900 – 1020

Predictions of the summertime extent of vertically well-mixed areas in the Gulf of Maine

John W. Loder and David A. Greenberg

The roles of tidal and wind mixing in the maintenance of vertically well-mixed hydrographic conditions in parts of the Gulf of Maine throughout the summer heating season are assessed using a numerical tidal model, climatological wind stress information, and semi-empirical criteria for the availability of turbulent energy. The predicted extent of well-mixed areas from Simpson and Hunter's (1974) tidal mixing criterion is compared with the predictions of alternative tidal mixing criteria, based on a near-surface energy partition and bottom Ekman layer thickness. Existing observations of frontal positions in the Gulf do not appear adequate for the determination of the relative accuracies of these criteria. The influence of wind mixing is discussed using a version of Simpson and Hunter's (1974) criterion re-formulated to include a fixed fraction of the atmospheric energy transferred downward across the 10-m level above the sea surface. It is suggested that wind-derived turbulence, as well as tidally-generated turbulence, contributes significantly to the maintenance of well-mixed areas.

The influence of lake morphometry upon thermal stratification and the depth of the summer thermocline

E. Gorham and F.M. Boyce

Among the important physical characteristics of a lake are whether it stratifies seasonally and, if so, the depth to which mixing is limited by the stratification. It is generally known that sufficiently shallow lakes tend to remain isothermal throughout the year and that the depth of the thermocline in stratified lakes correlates positively with the surface area of the lake. Data from lakes in

several different regions of the temperate zone of the Northern Hemisphere are examined in this paper. The observations show that whether a lake stratifies or not depends on both the maximum depth of the lake and its surface area, whereas the depth of the thermocline depends primarily upon its surface area or cross-basin length. A modification of the scaling arguments presented by Spigel and Imberger (1980) suggests a theoretical basis for this behaviour. These arguments account for the mixing powered by the fundamental internal seiche in addition to the surface stirring caused by wind stress. The effects of the earth's rotation, the shape of the basin, the optical properties of the water column, and the turbulence generated by bottom friction are discussed.

Internal waves on Georges Bank

R.F. Marsden

Data from a section of eleven current meters oriented across isobaths at three locations on Georges Bank were examined. On the Bank, the M_2 tidal currents were barotropic and in close agreement with the Greenberg (1983) numerical model of the Gulf of Maine. On the slope, the M_2 tidal current contained 70° phase shifts for 35-m depth changes in the vertical. The results from the model were used to separate currents that were due to the internal and surface tides. An examination of the baroclinic currents indicated that the downward propagating characteristic dominated and that the baroclinic current amplitude decreased near the projected beam axis. The heat and salt fluxes off the Bank were calculated. The depth-averaged heat flux due to the mean currents was statistically zero while the depth-averaged mean salt flux on the slope, although non-zero, was directed opposite to that expected from upwelling. The eddy fluxes were significant on the slope and were in a direction consistent with a transport of scalar properties onto the bank. The maximum eddy flux contribution occurred near the internal wave beam while the eddy flux contribution from the bottom current meters was negligible. The results suggest that internal waves play a significant role in determining the balance of scalar properties on offshore banks.

Optimal sampling and stratification in the Gulf of St Lawrence

J.-P. Charut

Optimal stratified sampling was simulated from vertical profiles of physical parameters collected during summer in the Gulf of St Lawrence. Stratum boundaries were optimally defined for each experimental station and adjusted for all stations in order to delimit the different layers of this stratified structure in this region. The optimal allocation of the sampling units within each stratum was performed by computer for one or several ecological variables. Other sampling strategies were simulated from the same data and compared in terms of their accuracy and precision. The advantages and limitations of such sampling strategies in coastal waters are discussed.

Physical oceanography of the St Lawrence Estuary

Mohammed I. El-Sabh

Since February 1973, a network of more than 100 oceanographic stations distributed on 17 transects was occupied during the years 1973-1975. In addition, weekly measurements of surface salinity and temperature were taken at Rimouski Harbour, at both high and low tides, during the years 1976-1980. All these data, together with the long-term freshwater discharge for the period 1949-1981, were used to describe the tidal, seasonal and annual variability, in addition to mean conditions, in the Estuary. In this regard, some conclusions of general interest are as follows:

(1) All three types of estuarine mixing exist in the St Lawrence Estuary: the well-mixed, at the head of the estuary; the moderately-mixed, in the section below the head; and the stratified, in the lower part. (2) Both advection and diffusion contribute importantly to the upstream salt flux in the upper part while advective processes account for more than 99% of the upstream salt transfer in the lower part. (3) A series of long-period eddies with alternating rotational senses along the estuary accompanied by transverse currents between any two eddies have been observed in the lower part. The dimension of each eddy is in the order of the estuary width (46 km). (4) A distinct subsurface temperature minimum below 0°C can be observed in the 50–60 m depth range associated with salinities around ~32.5‰ in winter months. The layer is then isolated during spring, summer and fall by both warmer and fresher waters at the surface. Bottom waters (>200 m) typically have temperatures of 3–4°C and salinities of ~34‰ throughout the year. (5) During the period of high river discharge, differences in surface salinity as high as 17‰ were found in the coastal region during the same tidal cycle. (6) Large lateral heterogeneity in water properties and currents has been confirmed. (7) Spectral analysis of the long-term freshwater data shows a dominant peak near the 75-day period, in addition to seasonal and interannual variations. (8) Because of the presence of internal tides, vertical oscillations of up to 80 m of the intermediate layer are common in the area near the Saguenay entrance.

Session 6BB: Deep-Sea Oceanography I Friday 1050 – 1230

Drifter spectra and diffusivities

John F. Middleton

The relationships between Eulerian energy and drifter (or Lagrangian) diffusivities and frequency spectra are explored in detail using the mixed Euler-Lagrange analysis of Middleton (1983) and Corrsin's (1959) hypothesis. Principal results found are: 1) Eulerian power-law spectra k^{-3} may be identified in L frequency space by a corresponding ω^{-3} power-law. 2) The diffusivity K may be well approximated by the function $qv^2T_E/(q^2 + \alpha^2)^{1/2}$ where $q \approx 0.47$, v^2 is the mean-square velocity, T_E is an Eulerian integral time-scale and $T_a = T_E/\alpha$, an advective time-scale. These results are discussed in detail and their relative insensitivity to the details of spectral shape suggests their applicability to mid-ocean drifter and diffusion studies.

Observations and a model of turbulence in an internal wave field

Jim Moum

Measurements of velocity microstructure were made in the western North Pacific Ocean from 23 to 42°N in May/June, 1982. A cold core ring centred at 34°N effectively defines the northern boundary of a region distinguished by a strong thermocline at about 400–700 m depth. In this region the Brunt-Väisälä frequency, N , has maxima (calculated over 50-m depth intervals) of > 3 cph. Above the thermocline, N has minima of < 2 cph and decreases monotonically below the thermocline to 2 cph at 1000 m. An averaged profile of the turbulent kinetic energy dissipation, ϵ , calculated from the velocity microstructure data, exhibits both a strong local minimum corresponding to the minimum in N above the thermocline, and a maximum in the thermocline. An estimate is made of the fraction of the water column that is turbulent (over discrete depth intervals) based on a threshold value of ϵ and this corresponds roughly in shape to the profile of ϵ .

With the assumption that the primary source of the turbulent energy is the internal wave field, a theory based on Garrett and Munk's internal wave dynamics and a random superposition of wave shears is proposed to model the *distribution* of the turbulence.

Horizontal coherence of mixed-layer turbulence

N.S. Oakey

During a cruise in late November, 1982, measurements of the horizontal coherence of velocity microstructure were obtained using OCTUPROBE 2. The instrument profiled vertically from the surface to about 75 m with a horizontal linear array of three shear probes with spacings up to 1.20 m. Each microstructure velocity sensor was a "lift probe" that measures one component of the vertical shear of horizontal velocity relative to the profiler OCTUPROBE. It is sensitive to vertical scales from about 1 to 0.02 m. During each profile there is considerable vertical variability in the details of the structure for one sensor, and horizontal variability both in detail and intensity of the signal between the sensors. The data were spectrally analysed in segments corresponding to 1 to 2 m of vertical profile to examine the vertical variability. The coherence between the signals from sensors separated at different horizontal spacings was used as an indicator of horizontal variability. The results of these studies will be discussed.

Observations of inertial oscillations and mixed-layer deepening in the Western Mediterranean

J. Moen

Results are presented from a mixed-layer experiment (MILEX 82) conducted in the central Balearic Sea to the west of Sardinia during the autumn of 1982. The mixed-layer and thermocline structures were monitored for a 40-day period of high winds by means of thermistor chains and current meters taut-moored with nylon rope and surface floats. Wind velocity, barometric pressure, air temperature and sea-surface temperature were recorded by instruments mounted on the surface floats of two of the six moorings.

The data are characterized by strong inertial oscillations that occurred in both the mixed layer and thermocline throughout the entire measurement period. Vertical phase changes in the oscillations, most striking between the 40- and 60-m VACM records, are shown to vary between 0° and 180°. Associated with these appear to be periods of mixing caused by shear instability within the thermocline.

It is suggested that the large amplitude and persistent vertical inertial oscillations observed are generated in the Golfe du Lyon, 300 km to the northwest, where the wind-stress curl associated with the Mistral is known to be extremely high (of order 10^{-5} dynes cm^{-3}).

The relative importance of surface cooling and turbulent mixing in deepening the mixed layer during MILEX 82 is discussed.

Eddies in the Pacific North Equatorial Current

K.A. Thomson, W.J. Emery and D. Krauel

Observations of eddies in recent XBT surveys in the Pacific North Equatorial Current are discussed and compared with previous observations. A time series of four AXBT surveys in the region 13–16°N, 157–154°W, from 30 January to 16 April 1981 show a very active field of meso-scale variability. Three cyclonic eddies are observed moving westward at estimated speeds of

11 cm s^{-1} , superimposed upon a general warming of the subsurface waters, indicative of a southward displacement of the North Equatorial Countercurrent - North Equatorial Current divergence zone. A single SXBT section at 165°W in November 1982 shows a similar cyclonic eddy at 13°N . A multiship SXBT survey conducted at the same time at $4-11^\circ\text{N}$ reveals a northward meander of subsurface isotherms of the same scale as the above features, suggesting a generation mechanism. The relatively high resolution of these XBT surveys shows a complex ring-like structure that has not been observed in this region before.

Session 6C: Mesoscale Meteorology

Friday 0900 - 1210

Diurnal variation of valley flows in the Alberta Foothills*P. Gourlay, R.P. Angle and S.K. Sakiyama*

The preliminary step in assessing the environmental risk of a sour gas pipeline was to investigate the meteorological characteristics of a two-valley system in the Rocky Mountain Foothills of Alberta. A month-long intensive field measurement program was conducted in September 1982. A summary of surface wind speed, wind direction and air temperature measurements at four locations across each valley is reported. Both valleys support nocturnal (katabatic) flows and weaker up-valley (anabatic) flows. The mechanical turbulence produced by the drainage flow, and enhanced by the valley geometry, leads to much larger dilutions than would be experienced in stable conditions over flat terrain. In the event of a release of pollutants near ground level, rapid dispersion is possible and the likelihood of high concentrations at ground level is greatly reduced.

Vertical structure of mountain valley flows in Alberta*S.K. Sakiyama, R.P. Angle and P. Gourlay*

During clear sky periods in September 1982, field studies were conducted to determine the diurnal behaviour of the vertical wind and temperature structures within two Alberta Foothill valleys. In these studies a tethered balloon, minisonde and acoustic sounder were used. The study demonstrated that both valleys exhibit nocturnal drainage (katabatic) and daytime up-valley (anabatic) flows. Drainage flow depth, wind speed maxima, and temperature inversion evolution will be discussed along with their relation to valley geometry and the mechanisms that produce these features. Evidence of a large-scale, thermally induced circulation cell resulting from the juxtaposition of the Rockies and the Prairies will also be discussed.

The usefulness of supplemental upper-air sites to increase spatial and temporal resolutions*G.S. Strong and R.K.W. Wong*

The usefulness of supplementing existing upper-air networks with one or more sounding sites during field research experiments is examined. Questions to be addressed include: To what extent, both in the horizontal and vertical, does local orographic forcing affect a sounding? Do strong gradients of surface radiation significantly affect local sounding thermodynamics?

The study uses special sounding data obtained at Cranbrook, B.C. during March, 1983. This additional sounding site was operated in support of a study to investigate the potential for seeding orographic clouds to increase snowpack on the east slopes of the Rockies. While much of the

mountain snowfall results from the passage of synoptic-scale systems, local topography results in large variations in snowfall amounts. The Cranbrook soundings were necessary because these orographic influences on local environmental thermodynamics were unknown. This paper employs various statistical tests on data interpolated for Cranbrook from the existing synoptic network, and those obtained from the mobile test site. The utility of the single additional site in this case is then discussed.

Observational studies of sea breezes in the Lower Fraser Valley, B.C.: Preliminary results

Douw G. Steyn

Recent studies of total oxidant episodes in the Greater Vancouver Regional District have shown that these episodes are closely associated with the occurrence of sea breezes in the region. In order to further our knowledge of the local flow regimes associated with these episodes, an observational study of the sea-breeze phenomenon is being mounted to provide validation data for a numerical modelling exercise.

Preliminary results from the first season's field work will be presented. The results will include atmospheric profiles through the sea breeze at various locations within the region under a variety of controlling synoptic conditions. Within the context of the present data set, the importance of antecedent synoptic conditions will be indicated and the vertical scale and strength will be estimated.

Research plans for future field seasons will be outlined.

Field-dependent estimation: A key to mesoscale prediction

H. Jean Thiébaux and Paul R. Julian

The paper will discuss field-dependent estimation schemes and their relation to the goals of mesoscale prediction. It will compare the accuracy of predictions obtained with adaptive algorithms that incorporate current or proximal information about an observed field into the *structure of the prediction algorithm* with the accuracy of predictions obtained from classical statistical objective analysis techniques. Standard analysis techniques are based on assumptions of the stationarity of the stochastic properties of field values. We show that a direct, alternative approach provides far greater accuracy – especially for extreme states whose accurate prediction is most essential.

The prediction algorithms described here have important implications for mesoscale observing network specifications, in addition to their direct use in day-1 forecasting and limited area now-casting. Their roles in the determination of network designs *vis-à-vis* the time- and space scales of analysis goals will be discussed.

Mesoscale forecasting with the RPN finite-element model

Robert Benoit and Pierre Koclas

The Canadian finite-element regional model (Staniforth and Daley, 1979) has recently been equipped with a normal mode initialization, a semi-Lagrangian moisture advection scheme and a sophisticated boundary-layer procedure (Preprints, 6th NWP Conference, 1983).

The grid is chosen here to resolve the coarser part of the meso-beta scales; the mean vertical spacing is 60 mb, with a lesser spacing in the boundary layer. The investigation covers the short space/time- (3 h) scales performance of the model during the first 12 h of integration with the SESAME 1979 cases.

The formation of multiple frontal structures as a forcing mechanism for rain bands in extratropical cyclones

Han-Ru Cho

Using Hoskin's semi-geostrophic frontogenesis models it is shown that atmospheric development in the presence of non-uniformities in pre-existing baroclinic fields may frequently be expected to lead to multiple frontal structures with a spacing of 100 km or greater. In general, the condition on the amplitude of the temperature non-uniformities is that the temperature gradient must be significantly altered. This mechanism is suggested as a possible forcing for the formation of rain bands in mid-latitude cyclones.

On the dynamics of mid-latitude synoptic systems with strong cumulus convection

J. Mailhot and M.K. Yau

The effects of cumulus ensembles on extratropical synoptic-scale systems with strong convective activities, like the explosive East Coast winter storms, are examined. Using scale analysis, it is shown that the latent heat release by clouds increases the large-scale vertical motion significantly. This in turn induces a large divergent wind component. It is through a non-geostrophic mechanism that cloud heating influences the large-scale temperature and vorticity fields. In addition, the recycling rate effect due to the lifetime of the clouds also contributes to the large-scale vorticity. Results from a linear model of baroclinic instability incorporating these effects will be presented.

Session 6D: Marine Sediment Geochemistry and Paleo-Oceanography

Friday 0900 - 1230

Trace metal geochemistry of Eastern Canadian estuarine and coastal sediments

D.H. Loring and R.T.T. Rantala

The levels, distribution, and chemical partition of Zn, Cu, Pb, Cd, Co, Ni, Cr, V, Hg, As and Se have been determined in the marine sediments of the Gulf of St Lawrence including the St Lawrence Estuary and the Saguenay Fjord, the Bay of Fundy and Baffin Bay.

Trace metal concentrations in these areas vary regionally and with sediment texture. They are for the most part near or at natural levels relative to their source materials and to other marine sediments. Local anthropogenic accumulations of heavy metals, however, occur in the Saguenay Fjord (Hg, Pb, As), the upper St Lawrence Estuary (Zn, Cu, Pb), the lower St. Lawrence Estuary (Hg), Baie des Chaleurs (Cd, Pb, Zn), southern Gulf of St Lawrence, and the Bay of Fundy (Zn) as a result of industrial and urban metal discharges to the marine environment.

Chemical partition of the total metal concentrations into their weakly bound (non-detrital) and lattice bound (detrital) metal contributions allow certain deductions to be made as to the source and pathways by which the metals have been incorporated into the sediments. The data indicate that the entry and deposition of fine-grained clastic grains of Zn, Cu, Pb, Co, Ni, Cr and V-bearing minerals (sulphides, oxides, and silicates) have made the largest contribution (61-99%) to

the total metal concentrations in the sediments. The abundance and distribution of the smaller but geochemically significant non-detrital metal fraction is also controlled by the deposition of fine-grained material. The highest concentrations of non-detrital metals occur in the fine-grained sediments deposited closest to the outflow of the natural and anthropogenic dissolved and particulate matter from the St Lawrence and Saguenay Rivers. Fine-grained organic matter appears to be the main carrier of Hg, Zn, Cr and Pb in the upper St Lawrence Estuary and Saguenay Fjord sediments, whereas soluble iron oxide grain coatings, adsorbed and exchange positions, and carbonates appear to be the main sites for the weakly-bound metals elsewhere in the sediments.

Compositional changes of the particulate matter during estuarine mixing, St Lawrence Estuary

B. d'Anglejan and M. Lucotte

The evidence for changes in the chemical and mineralogical composition of the particulate suspended matter in the St Lawrence Estuary in the early stage of estuarine mixing is presented. These changes are determined by 1) physical processes, namely modifications in particle size by flocculation, erosion of exposed early Quaternary marine deposits and particle exchanges with local mudflats; 2) input of organic detritus from these flats; and 3) chemical transformations. Interactions between these processes may explain the large compositional variations observed from season to season and from year to year. Fluctuations in organic content and in the relative abundance of amorphous silica are discussed. Local sources and size sorting both contribute to an increase in the chlorite-to-illite ratio observed in the turbidity maximum. The relative abundance of the labile and detrital fraction of particulate iron as a function of salinity, and the effects of iron colloid aggregation on the adsorption of phosphorus and other elements are examined.

Biologically available iron in estuaries: The effect of particle geochemistry

A. G. Lewis

The ionic states of iron are available to organisms. Because of the low solubility of the ferric ion in oxic marine and estuarine environments, the equilibrium with particulate and colloidal iron appears to play a major role in controlling the supply of available metal to phytoplankton. Particulate iron, when ingested by planktonic and benthic animals, may also form an important source if the metal can be mobilized by digestive processes. The interaction of ionic, colloidal and particulate iron in rivers is strongly affected by increasing salinity in estuaries. Extraction of particulate metal may occur or flocculation may take place if humic materials are present. These processes will affect the supply of iron available to organisms in estuarine regions.

The relationship between geochemical profiles and sedimentological variability in the Southern Nares Abyssal Plain during the Quaternary

D. E. Buckley, R. E. Cranston and G. Vilks

The Southern Nares Abyssal Plain (22°30' to 23°30'N and 63° to 64°30'W) is an area of flat sea floor with a bathymetric variation between 5810 and 5860 m. According to seismic survey results, there is limited variability in sediment type ranging from mostly acoustically well-stratified to a few areas of acoustically transparent. Sediment thickness over basement volcanics ranges from 0.5- to 1.0-s. reflection time.

A series of piston cores taken from this area in 1982 contained fine-grained clays (mean grain size $\leq 2 \mu\text{m}$) and scattered laminations of fine-grained silt. Most of the cores appear to have sampled a sequence of distal turbidites, but one core consists almost entirely of brown clay. There is little variation in the dominant clay mineral types in any of the cores (mica \gg kaolinite $>$ chlorite/smectite).

In general, only the upper 1 m of cores contains several species of preserved benthic foraminifera. Between 15- and 100-cm depth in one core the average $\delta^{18}\text{O}$ value in the tests of *P. wullesdorfi* was measured as 3.098 to 0.534‰, which is 0.4‰ higher than the average Holocene value of this species from the North Atlantic at 4600-m water depth. This higher isotopic value in our sample may be due to colder bottom water (1.01°C potential temperature). Cocolith biostratigraphy is incomplete due to poor fossil preservation but maximum ages of 200,000 and 400,000 years have been determined at depths within the cores that indicate the average rates of sedimentation range between 1 and 3 cm (1000 a)⁻¹.

Maximum rates of sedimentation (10 cm (1000 a)⁻¹) occur in the Holocene section in the upper metre of one core. This section also contains the most highly reduced sediments as indicated by the depletion of nitrate and the addition of Mn and Fe in pore water samples collected from closely spaced sample intervals. Also the reducible Mn and Fe extracts from sediments in this zone are at a minimum. The degree of chemical reduction appears to be related to the rates of sedimentation, with high rates of sedimentation leading to reduction while low rates of sedimentation result in preservation of the oxidized sediments.

The use of Pb-210 geochronology and sub-bottom profiling to study sedimentation in the Kitimat Fjord system

R. W. Macdonald, D. M. Macdonald and B. D. Bornhold

Pb-210 profiles for five cores in Douglas Channel and Kitimat Arm are interpreted using a constant rate-of-supply model. Surface mixing and slumping events are examined. Sub-bottom profiling guides the choice of three coring sites and provides an independent estimate of average sedimentation rates.

Kinetics and capacity of metal and radionuclide binding by bacteria in sediments

Paul E. Kepkay

Sediments association with freshwater ferromanganese concretions in Lake Charlotte, Nova Scotia, contained microscopic precipitates of manganese and iron. These precipitates were dispersed throughout the sediment and were found to be as rich in nickel, cobalt and copper as deep-sea concretions. The development of the precipitates appeared to be associated with the bacterial oxidation of manganese.

Results from the deployment of in situ dialysis probes or "peepers" demonstrated that bacterial manganese oxidation and nickel binding were closely associated and were approximately five times greater than the capacity for abiotic binding (expressed in terms of adsorption or distribution coefficients). In contrast, the microbial enhancement of copper and iron binding was far less pronounced owing to organic-metal interactions in competition with manganese oxidation. This interaction between metals and dissolved organics tended to keep more copper and iron in solution and acted against the tendency of oxidative processes to bring the metals out of solution.

The binding of americium-241 and cesium-137, two significant components of medium- and long-lived radioactive waste, appeared to be closely associated with the fate of specific trace metals. The binding of americium-241 appeared to be governed by manganese oxidation, whereas the binding of cesium-137 was more closely associated with the fate of copper.

North Atlantic benthic paleocirculation

E.A. Boyle

Numerous studies have established that Atlantic deep ocean circulation patterns have changed significantly over the last several thousand years. The quantitative extent of the change is documented by time-slice studies of $\delta^{13}\text{C}$ and Cd/Ca in benthic foraminifera; these quantitative indicators are supported qualitatively by studies of benthic foraminiferal faunal changes. These studies have shared a common qualitative conclusion: The flux of nutrient-depleted North Atlantic Deep Water has been significantly lower during cold climate episodes such as the last glacial maximum. These studies differ over the quantitative extent of the reduction, with estimates ranging from 25% to just short of 100%. Some of these discrepancies are likely to be due to the real variability between the circulation histories at various core locations; others may be due to the insufficient attention to bioturbation blurring of sediment records, shortcomings of techniques, or conceptual errors.

In this presentation, the basic types of evidence for changes in North Atlantic circulation are critically reviewed and uncertainties in our knowledge of past circulation are estimated.

Early diagenesis in hemipelagic sediments at 21°N on the East Pacific Rise

Tom F. Pederson

Sediments collected by box-coring 8 km west of the active hydrothermal vent field at 21°N show a classic chemical stratigraphy with 8 cm of chocolate-brown oxide-rich clay grading vertically through a thin cream-coloured transition zone to olive-green clay at depth. Pore water nutrient and metal profiles are consistent with the colour zonation and associated redox conditions: NO_3^- is totally depleted below the cream-coloured horizon and dissolved Mn increases sharply in the brown-cream transition zone 8–10 cm deep, ~10 cm higher in the core than a similar rise in the pore water Fe concentration.

Solid phase Mn is highly enriched (>1%) in surface sediments, decreasing sharply to <0.1% at depths below 8 cm. A decrease of ~0.5% Mn in the upper 4 cm of the core is *not* accompanied by a concurrent increase in pore water manganese, suggesting that the sedimentary Mn profile is not a steady-state, solely diagenetic feature. Rather, the distribution apparently reflects a relatively recent increase in the flux of particulate Mn to the sediments in the area, which may be related to temporal variations in the rate and extent of proximal hydrothermal activity. Ni, Co and especially Mo are also enriched in surface sediments. The Mo concentration decreases very sharply from ~18 to 2 ppm in the upper 4 cm and is associated with a similar surface enrichment and rapid decrease in pore water Mo (~0.18 to 0.10 $\mu\text{mol L}^{-1}$ in the top 4 cm). The contrast with the Mn chemistry indicates that the Mo distribution is independent of the oxide phase. The data suggest instead that the molybdenum distribution in these sediments is controlled by a labile phase that releases the element to solution very near the sediment-water interface.

DSDP Leg 85: Equatorial Pacific-wide seismic reflectors as indicators of major Middle and Late Miocene paleo-oceanographic events

Larry A. Mayer and John A. Barron

DSDP Leg 85 used the newly developed hydraulic piston corer (HPC) and rotary drilling to collect a series of Upper Eocene to Quaternary reference sections across the high productivity region of the central and eastern equatorial Pacific. The combination of relatively undisturbed HPC samples and nearly continuous core recovery make these sites invaluable for high-resolution stratigraphic and paleo-oceanographic studies. These sites were also the first DSDP sites to be surveyed with a high-resolution water gun seismic system providing the potential for a new insight into equatorial Pacific acoustic stratigraphy. In particular, a N-S transect along approximately 133°W tying together Sites 573, 574 and 575 reveals several distinct and laterally continuous acoustic units that are thickest near the Equator and thin to the north. Seismic modeling based on shipboard physical property measurements reveals that changes in seismic character are associated with distinct variations in sediment saturated bulk density (SBD). SBD variations are, in turn, correlated with changes in per cent calcium carbonate, thus implying ultimate paleo-oceanographic control of the acoustic properties. The most prominent acoustic boundary correlates with a major change in the nature of carbonate deposition (dissolution) at the end of the middle Miocene. Sediments older than middle Miocene are characterized by relatively constant high carbonate values while younger material shows large amplitude, short wavelength fluctuations between high and low carbonate percentages. Quantitative sedimentological and biostratigraphic analyses reveal that the time of this transition (12–11 Ma) is also characterized by: 1) a decrease in siliceous sedimentation in the mid-latitude North Atlantic; 2) an increase in siliceous sedimentation in the North Pacific; 3) a widespread hiatus (NH₄) associated with severe carbonate dissolution; 4) a dramatic increase and then decline (leading to extinction) in the abundance of the cool-water diatom *D. hustedii* in the equatorial Pacific; and 5) pronounced increases in provincialism between middle- and low-latitude forams, calcareous nannofossils, silicoflagellates, and diatoms. These changes indicate increased cooling of equatorial Pacific surface waters between 12 and 11.5 Ma probably the result of increased production of NADW. Enhanced polar cooling at 11.3 Ma contributed to steepened latitudinal thermal gradients and warming of tropical surface waters. The ability to acoustically trace, over large areas of the equatorial Pacific, this major paleo-oceanographic event presents, for the first time, the opportunity to apply seismic stratigraphic techniques to equatorial Pacific paleo-oceanographic programs.

Session 6E: Theory, Modelling, General Geophysics and Navigation

Friday 0900 – 1230

Heat and mass transfer associated with exceptionally thick sedimentary piles

V.A. Saul

Geochemical balance calculations, stratigraphic measurements, and isostatic principles all indicate that exceptionally thick deposits of sediment should be dominantly shale.

In quantitative studies of heat and mass transport associated with such sediment loading, the unusual temperature variation of shale properties (stemming from its clay component) must be included, but this has not generally been done.

Paleogeographic reconstructions, and continental margin studies, suggest that extensive shale basins existed over the axis of the future mid-Atlantic ridge long before its initial activity. At least

in its embryonic stages the ridge would have been a zone of mantle-shale thermal, mechanical and chemical interaction. Numerical modelling of this interaction provides constraints on the possible nature and characteristic times of the process. A testable global tectonic model equating ridges with exotic terranes can be built on these concepts. A particular feature of the model is that it yields a quantitative explanation of continental area vs age plots.

The "Prism Effect" of layered media

D.J. Hearn and E.S. Krebs

When velocity dispersion is included in a calculation of seismic ray paths in layered media, the Earth can act as a prism in that different frequencies will follow spatially different ray paths. At the boundary between two materials with different phase velocities and quality factors, an incident ray consisting of a band of frequencies will be refracted into the second medium as a fan of rays because each frequency component has a different angle of refraction. Assuming a standard, logarithmic dispersion relation and reasonable models for the velocity and Q contrasts, the difference in refraction angle between 1 and 100 Hz can be as much as 9° . This difference in refraction angle is zero for normal incidence and increases with increasing angle of incidence, up to the critical angle. Low frequencies are refracted at a greater angle than higher frequencies.

The prism effect has consequences for tracing ray paths between seismic sources and receivers in horizontally layered media. In order to arrive at the same receiver, each frequency contained in the source wave-form must have a different take-off angle, and will follow a spatially different path from source to receiver. Assuming that the linear superposition of these various frequencies arriving at the same receiver still applies, the resultant wave-form could be potentially altered by the prism effect. In particular, for a fixed source-receiver offset, the total distance travelled by the low frequencies in the pulse is greater than the distance travelled by the higher frequencies. Since the low frequencies also have lower velocities owing to dispersion, the overall travel-time of the low frequencies ought to be increased even more than they are by velocity dispersion alone. In addition, there will be increased attenuation of the low frequencies since they travel a greater distance. Closer examination of the ray paths shows that the low frequencies actually travel a shorter distance in all but the deepest layer, which is most commonly the layer with the least velocity dispersion. Therefore the low-frequency travel-times are not significantly increased relative to the higher frequencies, and the prism effect is generally not observable in the pulse wave-form detected by the receiver, despite the large angular difference in refraction angle and thus in the take-off angle.

A structural representation of the magnetotelluric impedance tensor

E.C. Yee and K.V. Paulson

A canonical decomposition of the impedance tensor is described that yields eight independent scalar parameters, each of which has a simple physical interpretation as a function of frequency. There are two polarization parameters for the magnetic (input) field and two for the electric (output) field as well as four transfer-function parameters (two moduli and two phases) that characterize the Earth's complex resistivity. This decomposition provides a principal coordinate system without any a priori assumptions about the dimensionality of the basic structure and is more applicable to the analysis of 3-D structures than the conventional method as described by Vozoff (1972, *Geophys.* 37:98).

Eggers's (1982, *Geophys.* 47:1204) eigenstate formulation of the magnetotelluric impedance tensor may be related to the canonical decomposition. The two approaches diverge because Eggers falsely assumes that the electric and magnetic fields are orthogonal, independent of the resistivity structure.

A Mueller 4×4 real matrix representation of the impedance tensor exhibits certain structural features that are not readily discernible in the conventional form. The constraint equations associated with this representation can be used to test for departures from a vertical plane-wave assumption.

Length of day and atmospheric pressure dependence of absolute gravity

M.A. Jedy

Changes in the absolute determination of gravity by A. Sakuma at the Bureau International des Poids et Mesures (BIPM) in Sèvres (near Paris), France over a period of four years (August 1967–July 1971) are analysed in terms of their correlations with changes in other environmental variables such as local atmospheric pressure, River Seine water level, latitude and Earth rotation rate. The present study demonstrates a significant correlation with atmospheric pressure ($-0.7 \pm 0.5 \mu\text{Gal mb}^{-1}$) ($1 \mu\text{Gal} = 10^{-8} \text{ m s}^{-2}$) and with length of day variation ($-10 \pm 5 \mu\text{Gal ms}^{-1}$, where the error bounds are 2σ units). In both cases the correlation significance is estimated by a variance-ratio F test where the actually published standard errors and deduced covariances have been taken into account. The same test indicates the non-correlation with latitude variation (due to polar motion) and with River Seine water level changes. A detailed analysis of the gravity dependence with length of day is made using spectral analysis, the variance-ratio F test and χ^2 confidence intervals. The semi-annual constituent in length of day proves to be the cause of the observed correlation with gravity, as previously determined by R. Lecolazet in a different frequency band. Explanations in terms of liquid core theory are not satisfactory as shown by Hinderer (1980). An alternative in which the correlations are attributed to imbalances in global atmospheric gravitational attraction is preferred.

Inversion of cosmogenic nuclide data from meteorites

Steven J. Pearce and R. Don Russell

The long-accepted conclusion that the galactic cosmic ray flux has been "fairly" constant over the past billion years or so is based upon both weak inferences and self-inconsistent interpretation. For example, the well-known exposure age discrepancy between the analyses based on ^{40}K and those of the narrower window isotopes (i.e. ^{10}Be , ^{26}Al , and ^{36}Cl) has yet to be properly reconciled. Recent work by Schaeffer et al. (1981) on space erosion rates for irons suggests that only a variation in the galactic cosmic ray flux yields the satisfactory explanation. A reformulation of this problem within the Backus-Gilbert framework of geophysical inversion (1967, 1968, 1970) allows for an unprecedented restriction of model space to reasonable, mutually consistent solutions, as compared with any previous analysis. Further, the lack of any independent exposure age determination presents an inherent non-linearity. But, it can be shown that a single model for both the cosmic ray flux and the exposure ages, consistent with the observations and associated errors, can be derived under several fundamental criteria.

Geomagnetic reversals - Flicker noise or chaos?

D. Crossley and O. Jensen

We contrast two interesting ideas, both recently promoted in separate areas of geophysics, in the problem of geomagnetic excursions of the main field. The first is that the reversals are evidence of a flicker-noise (or $1/f$ spectrum) excitation of a basis steady two-state deterministic physical dynamo mechanism in the Earth's core. The pertinent property of this kind of excitation is that it contains correlations from very short to very long intervals. This model was applied to the Chandler wobble problem by Jensen and Mansinha (1983). An alternative possibility is that the reversals are merely the pseudo-random consequences of the behaviour of a perfectly deterministic non-linear process. This behaviour (loosely called "chaos") appears when the trajectory is integrated forward in time and is completely hidden analytically in the governing equations. On this model the reversals do not require any external forcing from the core conditions, but are in-built once the regenerative mechanism begins.

We are doing numerical simulations of the two processes described to find whether any differences exist in a synthetic reversal sequence as the paleomagnetist might find from field data.

Coastal Geophysics: Gravity measurements in Mahone Bay, N.S. with a shipborne seagravimeter

B.D. Loncarevic and J.M. Woodside

Conventional offshore geophysical surveys must keep a safe distance from the coastal zone. This zone may be several tens of kilometres wide, depending on the nature of the coastline and the state of navigational charting. To extend the coverage through this zone and to carry out gravity surveys to within a few kilometres of the shoreline requires a small, shallow draft and maneuverable ship, a precise positioning system, reliable hydrographic charts and a quick-response seagravimeter capable of obtaining meaningful measurements over short-length survey lines. A prototype survey of an inshore bay was carried out in April 1983 onboard CSS *Maxwell* (35-m length, 275-t displacement) using a KSS-30 seagravimeter and a SYLEDIS positioning system with an accuracy of better than 5 m and a repeatability of the order of 1 m. The RMS accuracy of our survey is about 1.5 mGal. This figure can be greatly improved by taking into account the time delay in the instrument and the variations of tidal height of the bay.

First Canadian experiences with the Macrometer GPS positioning system

H.D. Valliant, D.E. Wells and D. McArthur

A field trial with the MACROMETER GPS positioning system was made in the vicinity of Ottawa, Canada, during July and August 1983, using two V-1000 single frequency receivers. Despite persistent hardware problems 26 observations were made on a variety of baselines, ranging from 30 m to 65 km. Reduction of the data using Macrometrics' software showed an agreement with conventional values on the short baselines (30 m and 2200 m) of 4 and 9 mm, respectively. On longer baselines from 13 to 65 km the standard deviation of a single observation ranged from 0.3 to 3.0 ppm of the baseline length in all three coordinates. Latitudes and longitudes on the longer baselines also agree with currently available geodetic values to within a few ppm of the baseline

length. Height differences appear to agree reasonably well with estimated geoid heights. Agreement is generally within the error limits of established data. An improved definition of the geodetic network is required before a more definitive comparison can be made. To this end a readjustment of the network is currently in progress at the Geodetic Survey of Canada.

The Ottawa Macrometer Experiment: An independent analysis

G. Beutler, R.B. Langley, H.D. Valliant, P. Vanicek and D.E. Wells

The data obtained from the Ottawa test of the MACROMETER V-1000 GPS receivers (described in the preceding paper in this session) were independently processed at the University of New Brunswick. The impetus for this analysis was two-fold: 1) to corroborate the results obtained by the Earth Physics Branch using Macrometrics' "black-box" software and 2) to develop an independent Canadian capability to process MACROMETER (and other types of) GPS observations.

A computer software package was developed to process double-differenced phases from single or multiple observing sessions with the capability of estimating both receiver and satellite coordinates. For the 30-m and 2-km baseline data of the Ottawa test, the software yielded baseline components agreeing with the mean of those obtained with Macrometrics' software to within 2 and 4 mm in all three components for the 30-m and 2-km baselines, respectively. The corresponding agreement with terrestrial measurements of the baselines was 3 and 15 mm, respectively. Somewhat larger differences were found on the longer baselines.

Session 7AB: Deep-Sea Oceanography II Friday 1330 - 1610

Gas exchange during deep water renewal

R. Allyn Clarke

During the winter of 1976, the renewal of Labrador Sea Water through deep convective processes to depths greater than 2,000 m was observed. The deep mixed layers so produced were only 93% saturated by oxygen throughout their depth range even though such waters remain in contact with the atmosphere for periods greater than a week. A simple deepening mixed-layer model driven by cooling and evaporation at the air/sea interface demonstrates that this degree of undersaturation is compatible with the range of exchange rates for oxygen across air/water interfaces as determined in laboratory and field observations. This undersaturation of oxygen in deep mixed layers is also seen in measurements taken during the winter of 1982 in the Norwegian-Greenland Sea. Here the same model is used to investigate whether the effect is greater when deep convection is associated with sea-ice formation.

This undersaturation of oxygen during the formation of deep water types is important to geochemists who have traditionally extrapolated their nutrient and oxygen distributors back to saturation in order to determine the various nutrient concentrations that a water mass might have had when first formed. Also, since CO₂ and oxygen have similar exchange rates, one should expect a similar undersaturation of deep water in CO₂ and this has considerable bearing on models that seek to use the deep oceans as a large sink for excess atmospheric CO₂.

Overflow through Denmark Strait

C.K. Ross

Measurements taken in Denmark Strait show that the cold, dense "overflow water" is always present but varies considerably in magnitude. The time-averaged volume flux of water colder than 2°C is computed to be $2.9 \times 10^6 \text{ m}^3 \text{ s}^{-1}$. The temperature/salinity characteristics of this "overflow water" are dominated by Arctic Intermediate Water and Norwegian Sea Deep Water. It is estimated that the volume flux of Norwegian Sea Deep Water is $0.5 \times 10^6 \text{ m}^3 \text{ s}^{-1}$. The currents at any point within the overflow are dominated by variability at periods of less than 2 days, which have been shown to be due to baroclinic instability in the overflow current. The total overflow is shown to be dominated by variability at longer periods that may be due to atmospheric forcing.

Current-meter records from the North Atlantic Current

J.R.N. Lazier

Between November 1982 and August 1983 sixteen current meters were moored across the North Atlantic Current or Polar Front in association with temperature and salinity surveys. The meters were suspended at 250, 1300, 2500 and 3500 m on four moorings 55 km apart, in a straight line lying 130°T, centred at 51°17'N, 44°50'W, approximately perpendicular to and across the mean position of the front. The results show the array was well-placed. Both the mean and fluctuating velocities past the southern moorings were more energetic than those past the northern moorings indicating the front stayed fairly close to the expected position. The records at each site are highly correlated and show a strong barotropic component of 0.05 to 0.08 m s^{-1} near the core of the current. Also near the front the baroclinic component of the flow increases in strength relative to the barotropic component. At the northern mooring away from the front there is little shear through the water column. The most energetic variability has a period of about 60 days and a wavelength of 120 km suggested by a satellite photo. The transport is estimated to be $45 \times 10^6 \text{ m}^3 \text{ s}^{-1}$, which is within 20% of previous estimates.

Mixing and the *T*, *S* characteristics of the water in Hudson Strait

K.F. Drinkwater

Results from a hydrographic cruise to Hudson Strait in August-September 1982 are presented. Mixing, as indicated by the lack of, or a reduction in, the vertical density gradient, was observed at the eastern entrance to Hudson Strait and between Resolution Island and Baffin Island, both areas identified as tidally well-mixed by Griffiths et al. (1981) from a numerical model of the M_2 tides and using the h/u^3 criteria. Stratification was observed in the northeastern corner of Ungava Bay, a region also suggested by Griffiths et al. (1980, *Deep-Sea Res.* 28: 865) as tidally well-mixed. It is suggested that the stratification is an effect of high river run-off into Ungava Bay that was not explicitly taken into account in the model. Water that flows out of Hudson Strait through Grey Strait is well-mixed and can be seen on the Northern Labrador Shelf. Continuous traces of surface fluorescence were recorded by connecting the ship's intake to a Turner fluorometer. The highest readings were found near the mixed regions, consistent with findings in other tidally energetic areas. This suggests that such mixing may be important to the biology of the Strait.

Oceanic thermal structure in the Canadian Western Arctic

Humphrey Melling, R.A. Lake, D.R. Topham and D.B. Fissel

Recent hydrographic data (1981–1982) from the western Canadian Arctic Archipelago and adjacent areas of the Arctic Ocean are interpreted from the viewpoint of thermal energy transfer. Within the Archipelago, a warmer halocline and a cooler Atlantic layer than in the Arctic Ocean are identified. The warmer halocline is a consequence of the continued diffusion of heat from underlying Atlantic Water without a significant compensating downward penetration from the surface of cold ($\leq -1.5^{\circ}\text{C}$) sea water with salinity increased consequent to ice growth. The cooler Atlantic layer is primarily attributable to an enhanced cooling of these waters in a narrow band over the continental slope and shelf of the southern Beaufort Sea prior to their inflow into the Archipelago. The significance of these findings for regional and Arctic oceanography is discussed.

Is potential vorticity conserved in the Gulf Stream?

Dave Hebert

Seasat measurements of sea surface elevation across the Gulf Stream show a relaxation at the edge of the Gulf Stream. A simple calculation of this departure from Stommel's simple two-layer model suggests that the relaxation could be due to an interfacial Ekman layer. Another possible explanation for the sea surface elevation is that there exists a more complicated density structure in which potential vorticity is conserved. A three-layer model with constant potential vorticity, geostrophically balanced, and no friction is studied. The prediction of sea surface elevation by this three-layer model is compared to the sea surface elevation measured across the Gulf Stream by Seasat. The extension of this three-layer model to a continuously stratified model is also discussed.

Mapping the local structure of the Gulf Stream near 60° W

R.M. Hendry

Detailed surveys of temperature, salinity and dissolved oxygen were carried out in the Gulf Stream near 60° W and 40° N during May and September 1983 in support of a combined current-meter and hydrographic study of the local-scale structure and variability of currents and water properties in the Stream. The resulting maps of properties allow a discussion of the horizontal variation of temperature and salinity correlations across the Stream and the vertical variation of spatial patterns in the fields over a region 300 km in diameter. Subsurface features in the maps can be compared with remotely-sensed sea surface patterns.

Session 7D: Geophysical Heat Flow

Friday 1330 – 1550

Heat flow studies in the Sohm Abyssal Plain, Western North Atlantic Ocean

M. Burgess

In June 1980, geothermal investigations were carried out by the Earth Physics Branch of Energy, Mines and Resources, in the Sohm Abyssal Plain, Western North Atlantic Ocean. The geothermal programme formed part of a major oceanographic expedition organized by the Bedford Institute of Oceanography on board the CSS *Hudson*, to study the nature of abyssal plain sediments and their suitability for hosting implanted containers of nuclear waste. To determine the

small-scale variability of the sediments, a 10 km × 10 km flat study area in water depths over 5300 m was selected in the southern Sohm Abyssal Plain. The investigations of the thermal characteristics of the sediments focused on measurements of thermal conductivity and temperature gradients. Five heat flow stations, for a total of 6 gradiometer probe penetrations to depths of over 5 m in the sea-bottom, were successfully occupied. In all, 450 thermal conductivity measurements were made on retrieved core samples at an average spacing of 15 cm using the transient needle probe technique.

Thermal conductivities corrected to sea-bottom water temperatures and pressures ranged from 0.74 to 2.12 W m⁻¹ K⁻¹ and averaged 1.06 W m⁻¹ K⁻¹. High conductivities encountered at the base (10–12 m) of many piston cores correspond to a coarse sediment layer deposited by a major turbidity flow from the Grand Banks. The occasional high conductivities encountered throughout a core appear to correlate with the base of turbidite sequences.

Sediment temperature gradients measured with the 7 thermistor sensor gradiometer probe range from 35.0 to 68.4 mK m⁻¹ and average 54.4 mK m⁻¹. Temperature-depth profiles show a departure from linearity, in general, concave downwards. The non-linearity cannot be accounted for by a variation in conductivity and suggests that perturbations to the thermal regime, such as the circulation of interstitial waters, changes in bottom water temperature and variable currents at the sea floor, may exist.

Heat flow through Old Ocean floor – Results from the Sohm Abyssal Plain, Northwest Atlantic

D.O. Wallace, K.E. Loudon and R. Courtney

The plate model and the half-space model are two classifications of theoretical models that have been proposed to explain the variations of surface heat flow and basement depth as a function of age. The heat fluxes predicted by these models are the same for an oceanic lithosphere younger than 120 Ma; beyond this point the results diverge by up to 10%. With Dalhousie's recently acquired heat flow package we set out to determine temperature gradients and in situ thermal conductivity values for a section of Old Ocean floor (164 Ma). The area of interest was on the Sohm Abyssal Plain and was predicted by the plate model as having a zero-depth anomaly. A 4-m violin-bow type sensor string with 9 thermistors was used in determining a mean temperature gradient of 48.8 ± 2.5 mK m⁻¹. Needle probe conductivities on two 10-m piston cores from the area provided a mean corrected conductivity of 1.06 ± 0.15 W m⁻¹ K⁻¹. These values yield a heat flow estimate of 52 ± 3 mW m⁻², which is about 20% higher than that predicted by either of the models. Our estimates do, however, correlate well with the data of Davis et al. (1984) for sites south of Bermuda of ages between 115 and 152 Ma. Reducing the plate thickness by 20% in the plate model of Parsons and Sclater (1977) would provide heat flow estimates that better reflect the observed data. We intend to return in May 1984 to resample this site and to obtain data for sites of younger ages.

Heat flow variations with depth in Alberta

J.A. Majorowicz, F.W. Jones, H.L. Lam and A.M. Jessop

Estimated average heat flow values for the Mesozoic and Cenozoic formations (Q_1) are compared with average heat flow values for the Paleozoic formations below the erosional unconformity (Q_2) in the Alberta part of the western Canadian sedimentary basin. Significant heat flow differences exist for these two intervals and the map of $\Delta Q = Q_1 - Q_2$ shows that Q_2 is generally greater than

Q_1 in the eastern and southeastern parts of Alberta, while in the northern part of the province Q_2 is generally less than Q_1 . The regional variations of ΔQ are large, with a standard deviation of 26 mW m^{-2} and an average value of -13.5 mW m^{-2} . A regional trend of ΔQ correlates with topographic relief and the hydraulic head variations in the basin. It seems probable that there is a continuous heat flow increase with depth in water recharge areas and a continuous decrease in heat flow with depth in the low relief water discharge areas.

Heat flow in Alberta and its significance for the occurrence of hydrocarbons

J.A. Majorowicz, M. Rahman and F.W. Jones

Detailed heat flow studies in the Alberta part of the western Canadian sedimentary basin show that the hydrodynamically controlled geothermal pattern and the depth/temperature distribution of the Mississippian and Devonian oil and gas pools are related. Cooling below the Rocky Mountain Foothills and the deep part of the basin caused by gravity-imposed downward water movement results in low geothermal gradient values and deep burial of the oil generation "window". An increase in the geothermal gradients in the shallower eastern part of the basin caused by rising fluid flow brings the oil generation window closer to the surface. It can be shown that the geothermal conditions during the time of maximum burial of the sediments, which was the most important time for oil and dry gas generation, were not very different from the present ones. This means that when burial and erosional history are known, the present heat flow data can be used to study hydrocarbon generation and the conditions for preservation of the oil and gas pools.

Studies of the paleogeothermal field and its relation to the present heat flow pattern in southern Alberta

M. Rahman, J.A. Majorowicz and F.W. Jones

Correlation studies of thermal maturation and hydrocarbon generation are important in oil exploration. If the sedimentary basin history is known, Lopatin's method can be used to calculate a Time-Temperature-Index (TTI) when the geothermal gradient is known. This can be done by a numerical integration method (McKenzie, 1978). The index provides an estimate of the degree of maturation of organic material. By using Waple's relation (1980) between vitrinite reflectance (R_0) and TTI, then R_0 can be calculated and compared with measured values. The thermal history can thus be reconstructed if the erosional-burial history and maturation level of the organic material are known. For southern Alberta, current heat flow information is available from the University of Alberta. In our study, a program has been developed in which R_0 can be calculated for any number of steps of erosion, uplift or times of no tectonism. Using this, different erosional and heat flow history models have been used to calculate R_0 in southern Alberta, and from these a best model can be sought.

McKENZIE, D. 1978. Some remarks on the development of sedimentary basins. *Earth Planet. Sci. Lett.* **40**: 25-32.

WAPLES, D.W. 1980. Time and temperature in petroleum formation: Application of Lopatin's method to petroleum exploration. *Am. Assoc. Pet. Geol. Bull.* **64**: 916-926.

Geothermal and geophysical investigation of the distribution of permafrost and gas hydrates in the Mackenzie Delta and Beaufort Sea

A.S. Judge, A.E. Taylor, I.P. Norquay and W.E. Bawden

In the past decade, through the cooperation of industry and some government agencies, temperature measurements in 45 deep wells drilled for hydrocarbon exploration and in 100 shallow holes both onshore and offshore have outlined the regional distribution and thermal characteristics of permafrost in the Mackenzie Delta, Tuktoyaktuk Peninsula and Continental Shelf areas of the Beaufort Sea. This broad outline has been further defined through a detailed analysis of the permafrost base as exhibited in the geophysical well-logs of the 175 exploratory wells drilled in the region to date. The entire data set reveals very wide variations in the spatial distribution of permafrost both onshore and offshore. In the offshore the permafrost thickness ranges from almost 700 m on the Beaufort Shelf north of the central Mackenzie Delta to near-zero or zero in the western Beaufort. The onshore thickness ranges from 700 m in the northern Mackenzie Delta to less than 150 m in both the southern and younger western areas of the Delta. Indications of the presence of gas hydrate are encountered in about 20% of the wells that are generally associated with and adjacent to the areas of thickest permafrost both onshore and offshore.

Temperatures in each well, after the removal of the thermal disturbance of drilling, have been determined to depths of 4 km using a combination of precise logging, bottom-hole temperatures and drill-stem test temperatures. Temperatures gradients below the base of the permafrost characteristically range from 20 to 40 mK m⁻¹ throughout the region. The variation of temperature with depth both within and below the permafrost horizons has been used to characterize the permafrost and to mathematically model its time of origin and history. Onshore temperature gradients through the thick largely continuously frozen permafrost column indicate quasi-equilibrium with present conditions. In contrast, the thick permafrost of the offshore is almost isothermal and the frozen section is discontinuous both vertically and spatially in response to the gradual submergence of the Beaufort Shelf over the past 20,000 years. The presence of extensive shallow gas deposits and high pressure ground-water offshore is attributed to the gradual decomposition of gas hydrates beneath the permafrost horizons providing further confirmation of the warming trends. Contiguity of the permafrost distribution and history onshore and offshore is shown by the existence onshore of a region of thick, warm permafrost similar to that found offshore and newly emergent in the past 1000 years. The results of the thermal modelling will be compared and contrasted with conventional wisdom on the Quaternary history of the Beaufort/Mackenzie region.

Session 7E: Magnetics

Friday 1330 – 1630

Direct geophysical evidence for displacement along Nares Strait from low-level aeromagnetic data

Peter Hood, Margaret Bower, C.D. Hardwick and D.J. Teskey

A low-level (305-m) aeromagnetic reconnaissance of the Nares Strait between Greenland and Ellesmere Island has been carried out as part of the cooperative project between the Geological Survey of Canada and the National Aeronautical Establishment. In the Kane Basin, the resultant stacked profiles clearly show a disruption in the trend of a band of 500-gamma amplitude anomalies (and the concomitant lows) that extend from the Bache Peninsula on Ellesmere Island towards the southern side of the Humboldt Glacier on Greenland. The disruption occurs about

60 km due east of Bache Peninsula and there appears to be an offset of the anomalies of approximately 25 km in a sinistral sense. At the northern end of Kane Basin the short wavelength components of the aeromagnetic profiles abruptly disappear indicating that there is a sediment-filled faulted basin at the entrance to Kennedy Channel that probably extends under Washington Land.

At the northern end of Nares Strait, a line of isolated anomalies some 200 gammas or so in amplitude extends from Judge Daly Promontory along Robeson Channel to the Arctic Ocean for a distance of 107 km. A quantitative interpretation of the data indicates that the elongated anomaly is due to an axial dyke or, more probably, a swarm of closely-spaced dykes. These line up with the prominent fault zone on the Judge Daly Promontory mapped by Christie (1964) and others. Mayr and de Vries (1982) tentatively estimated the sinistral displacement along the Judge Daly fault zone to be 19 km. Volcanic fragments with an olivine-rich basaltic composition have been found in the Tertiary rocks along the fault system and the aeromagnetic survey evidence also indicates that the dyke system extends across the Judge Daly Promontory. Thus it is concluded that the dyke system has been intruded into an existing fault system that extends a distance of at least 200 km along and parallel to the axis of Nares Strait.

Thus collectively, the low-level aeromagnetic data obtained in Nares Strait itself indicates that at least 20 km of sinistral strike-slip displacement has occurred.

New aeromagnetic data from the High Arctic and Norwegian-Greenland Sea

L.C. Kovacs and G.E. Vink

Data were collected in October, 1983 over previously unsurveyed areas of the High Arctic and Norwegian-Greenland Sea. The areas investigated were: 1) the Nansen Ridge offset between 60 and 70°E, 2) the Kolbeinsey Ridge-Jan Mayen Island region between 70 and 72°N, 3) the Makarov Basin-Marvin Spur region north of Ellesmere Island, and 4) the Nares Strait and nearby continental regions of Ellesmere Island and Greenland.

The Nansen Ridge offset is found to consist of two fracture zones of about 30 and 55 km of apparent dextral offset, rather than the smooth bend usually seen in most magnetic and bathymetric charts.

The Kolbeinsey Ridge results show the ridge following the earthquake data for the region. A fracture zone having about 35 km of dextral offset appears at 70°50'N, 14°00'W on the ridge crest.

The Makarov Basin shows only occasionally linear, moderate amplitude magnetic features, with the only truly linear anomaly being associated with Marvin Spur. This suggests the Makarov region is more closely tied to Alpha Ridge, as has been recently suggested by Sweeney, rather than the oceanic origin we had previously hypothesized.

The Nares Strait results (collected at 10,000 ft to avoid topography) show significant differences in aeromagnetic character across the Strait. On the Greenland side, and over Ellesmere Island south of 79°N the anomalies have moderate amplitudes and very short wavelengths (< 10 km), while north of 79°N the magnetic anomalies over Ellesmere Island abruptly change to very long wavelengths and low amplitudes.

Advances in the magnetic anomaly mapping program at the Geological Survey of Canada

D.J. Teskey, S.D. Dods and P.J. Hood

The one:one million mapping program of the Geological Survey of Canada has now been almost completed for the mainland areas of the Canadian Shield and the Appalachian Province in Canada. The associated data bank includes the flight-line data, digitized at the contour intercepts on the original one inch:one mile (or 1:50,000) sheets and the gridded data (812.8 m) in the Lambert Conformal projection using the standard parallels of latitude and longitude for Canada (49° N, 77° N, 92° W) and using the standard parallels for each individual International Map of the World (IMW) sheet. These have proven to be quite versatile for such image enhancement techniques as the Magnetic Shadowgrams and Stereo Shadowgrams, for compilation at a smaller scale (i.e. one:five million) where the gridded data can be used directly, and for recompilation at larger scales from the original digitized flight-line data. A program has now been commenced to publish a series of 1:250,000 colour Magnetic Anomaly Maps, an example of which has been produced for an area in Northwestern Ontario.

Uplift studies and the nature of remanent magnetization in the contact zone of some Precambrian dykes

E.J. Schwarz, K.L. Buchan, A. Cazavant and G. Salvat

Remanent magnetization has been studied in the contact zone of several Precambrian diabase dykes of varying ages from the Northwest Territories and Québec. In some cases the magnetic overprinting in the contact zone is clearly of thermal origin. Such results are useful in establishing the ambient temperature of the country rock at the time of dyke emplacement and hence the amount of uplift since dyke intrusion. An Indin dyke (2.1 Ga) in Yellowknife, N.W.T. yields a depth of burial of 7 ± 2 km. The only other available uplift estimate for a dyke of this age is $6\frac{1}{2} \pm 2$ km, obtained for a 2.15-Ga dyke in Munro Township, Ontario.

For other dykes, however, it is shown that overprinting in the contact zone is chemical in nature. Although such results are often of no use in estimating uplift, in some cases an upper limit for the amount of uplift can be established.

The paleomagnetic record of the Appalachians

E. Tanczyk, J.L. Roy and P. Lapointe

The present study synthesizes paleomagnetic results from the Paleozoic of North America, revealing important features of the tectonic history of the Appalachians. The far-reaching effects of the Hercynian Orogeny (Permo-Carboniferous) are apparent, since its magnetic signature can be detected on both sides of the Appalachian structural front. Appalachian rocks usually carry multi-remanences composed of the initial remanence acquired during rock formation, and later remanences produced during subsequent tectonic events. In some instances the initial remanence may have been erased and replaced by one of orogenic age. Many poles are believed to be signatures of orogenic episodes of Hercynian or Acadian (Devonian) age. Thus pole ages and rock unit ages can by no means be equated. Hypotheses based on the assumption of the contemporaneity of pole and rock unit ages are unsubstantiated, unless it is proven conclusively that poles of the same age are being compared. Only by recognizing the signatures particular to specific tectonic events is it possible to reconstruct, on the basis of the paleomagnetic record, the regional extent of orogenic episodes, and to further our knowledge about Appalachian tectonics throughout the Paleozoic.

New paleomagnetic data from Carboniferous redbeds and volcanics from central New Brunswick

Maurice K.-Seguin, A. Singh and L. Fyffe

Kent and Opdyke (1979), Scotese et al. (1979) and Lefort and Van der Voo (1981) argued on the basis of paleomagnetic data from Devonian, Carboniferous and Permian lithological units from eastern North America, for the presence of a sinistral megashear along faults within and parallel to the Caledonian chains that occurred during the Carboniferous. This same left-lateral motion was used as a paleomagnetic constraint on the assembly of the Old Red Continent (Van der Voo, 1983). Recent paleomagnetic studies in the northern Appalachians by Seguin et al. (1982a, b) cast some doubt on the models advanced by Kent and Opdyke (1979) and Scotese et al. (1979). The geologic evidence suggests that only a small amount of dextral (and not lateral) slip occurred, mainly on faults parallel with pre-Acadian paleogeographic realms (Bradley, 1983). The purpose of this paleomagnetic study is to test the validity of the proposed left-lateral motion at one of the sites of its presumed emplacement in central New Brunswick. Six sites (≈ 80 oriented specimens) consisting of Carboniferous redbeds and volcanics were collected on both sides of the Fredericton Fault and other faults parallel to it. After AF and thermal cleaning, the mean direction of magnetization is approximately $145, +25$; the fold test is positive. The corresponding paleopole is $135^\circ\text{E}, 35^\circ\text{N}$ and the paleolatitude 13°N . The paleopole positions and paleolatitudes are not significantly different on either side of the main fault and no left-lateral motion is detected. As no such motion has yet been detected in southern New Brunswick and in Nova Scotia, it is possible but unlikely that it took place in northern New Brunswick or in the western Gaspé peninsula.

BRADLEY, 1983. *J. Geol.* **91**: 381-400.

KENT AND OPDYKE, 1979. *Earth Planet. Sci. Lett.* **44**: 365-372.

SCOTESE ET AL., 1979. *J. Geol.* **89**: 537-550.

SEGUIN, 1982a. *EOS*, **63**: 913.

SEGUIN, 1982b. 1982 Fredericton meeting of IGCP Project 27.

VAN DER VOÛ, 1983. *Tectonophysics*, **91**: 271-283.

Paleomagnetic results from the Port-Daniel diabase sills and Middle Ordovician metasediments of the Mictaw Group, Gaspé

Maurice K.-Seguin, E. Gahé and G. De Broucker

Five sites (50 oriented samples) were collected on sills and metasediments of the Port-Daniel region, southern Gaspé Peninsula. The sills are composed of diabases and the sediments of the Mictaw Group of greywackes. The Mictaw Group is in faulted contact with the older (Cambrian or Eocambrian) Maquereau Group. Two phases of folding affected the diabase sills and the Mictaw Group sediments. Both alternating field and thermal cleaning techniques were used to determine the direction of magnetization. The mean direction obtained after cleaning is $170, +50$ for the sills and $150, +55$ for the sediments *in situ*. After a double tilt correction, the mean values are $239, +28$ and $210, +56$, respectively. The baked contact test of the sills on the metasediments is positive and so is the fold test for the sills. The paleolatitude (15°N) obtained from the Mictaw Group is comparable with that of other Ordovician poles from the stable North American continent but the paleopole is substantially different. The positive fold test of the sills indicates that the magnetization is pre-tectonic, i.e. older than Late Ordovician. The magnetization of the sediments may be related to the time interval between their formation and the first phase of deformation (Late Ordovician) or else to a later metamorphic event (Acadian Orogeny of Late Devonian age).

Paleomagnetism of the Ottawa Islands of the circum-Ungava belt

K.L. Buchan and W.R.A. Baragar

The komatiite basalts of the Ottawa Islands of eastern Hudson Bay dip gently to the west. They are on strike with, and are thought to form a continuation of, similar steeply-dipping units at Cape Smith 150 km to the northeast. Before a tilt correction is applied the dominant magnetization of the Ottawa Islands ($D = 207.6^\circ$, $I = 61.9^\circ$, $K = 128$, $\alpha_{95} = 3.7^\circ$) is similar to the uncorrected direction reported for Cape Smith. This negative fold test implies that the remanence at each location was acquired after folding, probably during uplift following the Hudsonian orogeny.

A second stable component directed to the west with a shallow inclination is superimposed on the dominant component at a number of sites. Magnetic and polished-thin section studies have not conclusively established its age relative to that of the dominant magnetization.

Dix-Neuvième Congrès Annuel

Le Centre de Montréal de la Société canadienne de météorologie et d'océanographie et l'Université du Québec à Montréal (UQAM) seront les hôtes du dix-neuvième Congrès annuel de la SCMO, congrès qui se tiendra à l'UQAM du 12 au 14 juin 1985. Le congrès a pour thème *La modélisation en météorologie et en océanographie*.

À la suite du congrès de la SCMO, l'American Meteorological Society tiendra deux congrès à Montréal: le Septième congrès sur la prévision numérique du temps du 17 au 20 juin, et le Deuxième congrès international sur les services météorologiques à l'aviation du 19 au 21 juin.

Nineteenth Annual Congress

The Montréal Centre of the Canadian Meteorological and Oceanographic Society and l'Université du Québec à Montréal (UQAM) will host the Nineteenth Annual CMOS Congress, which will be held at UQAM from June 12 to 14, 1985. The theme is *Modeling in Meteorology and Oceanography*.

Back to back with the CMOS congress, the American Meteorological Society will hold two conferences in Montréal the following week: the Seventh Conference on Numerical Weather Prediction from June 17 to 20, and the Second International Conference on Aviation Weather Systems from June 19 to 21.

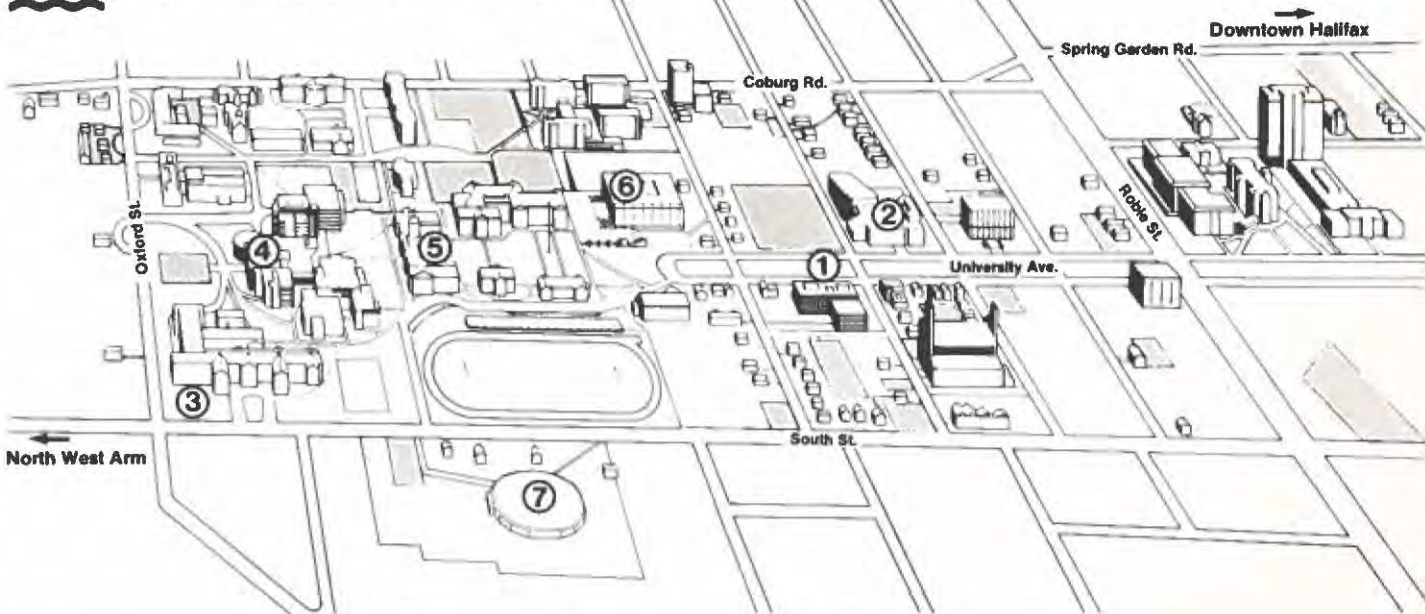
CGU/CSEG Joint Meeting

The Canadian Geophysical Union will meet jointly with the Canadian Society for Exploration Geophysics from May 7 to 10, 1985 at the Calgary Convention Centre, Calgary, Alberta.



HALIFAX '84

JOINT ANNUAL MEETING



① **STUDENT UNION BUILDING**
Registration: Monday, May 28
Green Room

② **DALHOUSIE ARTS CENTRE**
Rebecca Cohn Auditorium
Plenary Session

③ **SHIRREFF HALL**

④ **LIFE SCIENCES CENTRE**

⑤ **ARTS & ADMINISTRATION**

⑥ **KILLAM LIBRARY**

⑦ **DALPLEX**

■ **PARKING**



Canadian Meteorological and Oceanographic Society
 La Société Canadienne de Météorologie et d'Océanographie
 Canadian Geophysical Union
 Union Canadienne de Géophysique



HALIFAX '84



JOINT ANNUAL MEETING
 RÉUNION ANNUELLE CONJOINTE

MAY 29-JUNE 1, 1984 DALHOUSIE UNIVERSITY